Program in Molecular

and Translational Medicine

DIMET

(XXVII cycle, year 2013-2014)

University of Milano-Bicocca

Department of Biotechnologies and Biosciences

Functional characterization and targeting of CRLF2 gene alerations in pediatric High Risk Acute Lymphoblastic Leukemia

Angela Maria Savino **Matr. 716165**

PhD Coordinator: Prof. Andrea Biondi

Tutor: Prof. Andrea Biondi

Co-Tutors: Dr. Giovann Cazzaniga

Dott.ssa Chiara Palmi

TABLE OF CONTENTS

Chapter 1

General introduction

Acute lymphoblastic leukemia

Leukemias are the most frequent cancers in childhood. Acute leukemia is a malignant (clonal) disease of the bone marrow in which hematopoietic precursor cells over-proliferate replacing normal marrow elements, resulting in a marked decrease in the production of mature functional blood cells and accumulation of leukemic blasts in primary and secondary hematopoietic sites such as liver, spleen, lymph nodes and thymus (1). Depending on the lineage of origin of the malignant cell population (blasts), the disease is defined as Acute Myeloid Leukemia (AML), with involvement of uncommitted precursor of myeloid lineage, or Acute Lymphoblastic Leukemia (ALL), with involvement of the lymphoid lineage. The latter is more frequent among pediatric patients and accounts for 80% of all *de novo* leukemia cases during childhood. ALL derives from B- or T- lymphocyte progenitors, which are blocked in their maturation. Arrest of lymphoblasts in early developmental stages is caused by altered genetic expression, often as result of genomic alterations including chromosomal translocations.

Newly diagnosed ALL bone marrow or peripheral blood specimens are routinely processed for cytomorphology, cytochemestry, immunophenotypic, cytogenetic and molecular characterization. Immunophenotyping at diagnosis is tested by flow cytometry using a panel of lymphoid specific Cluster of Differentiation (CD) markers.

Approximately 85% of diagnosed ALL cases are a result of the expansion of B-cell precursors (BCP-ALL). It is possible to

further sub-classify the BCP-ALL in early pre-B cell or pro-B, common, pre-B cell, and B-cell ALL, according to the corresponding CD expressed by the leukemic cells (2). The differentiative stages of B- cell leukemia development, identified on the basis of the expressed antigens on the blast, are listed below:

- Early pre-B (or Pro-B): CD19+ CD10- HLA-DR+ CD7- SmIg-
- CALL (common): CD19+ CD10+ HLA-DR+ CD7- SmIg-
- Pre-B: CD19+ CD10+ HLA-DR+ CD7- SmIg+ (κ- e λ-)
- B: CD19+ CD10+/- HLA-DR+ CD7- SmIg+ (κ+ o λ+)

Fifteen per cent of ALL cases have a T cell origin. T-ALL is thought to arise from malignant thymocytes, corresponding to defined stages of intrathymic T-cell differentiation. Different maturation states of T lymphoblasts define the subtypes:

- Pre-T ot Early T: CD1-CD2+/- cyCD3+CD3-CD7+
- Intermediate T: CD1+CD2+ cyCD3+CD3+CD7+
- Mature T: CD1-CD2+ cyCD3-/+CD3+CD7+

Genetic subtypes in ALL

Genetic abnormalities, such as aneuploidy, chromosome translocations, and/or deletions, but also point mutations, occur very frequently in ALL and are present in 80% of the patients.

These alterations are important indicators of prognosis and they could be divided into two groups: numerical and structural abnormalities (3).

The numerical chromosome abnormalities are very common in pediatric ALL and are investigated through evaluation of blasts DNA content. The ratio between DNA content of leukemic blasts and normal cells, defined as DNA Index, is a reliable method to evaluate the aneuploidy and is evaluated routinely in all new diagnosed patients. Unitary DNA Index indicates a cell population with chromosomal diploid arrangement. DNA Index values greater than 1,16 corresponding to a number of chromosomes ≥50 are used to define hyperdiploidy of the blasts population. DNA Index value below 1 reveals hypodiploidy of blasts population. Hyperdiploidy is associated with favorable prognosis whereas hypodiploidy is linked to unfavorable prognosis (4). The structural chromosome aberrations can be found through cytogenetic analysis, such as karyotyping and Fluorescence In Situ Hybridization (FISH), or through molecular screening (PCR detection of recurrent break-point regions). This cytogenetic characterization is commonly performed at diagnosis and several subtypes of leukemia can be distinguished based on cytogenetic analysis (Figure 1). Many translocations generate fusion genes, having in some cases a negative prognostic impact (2).

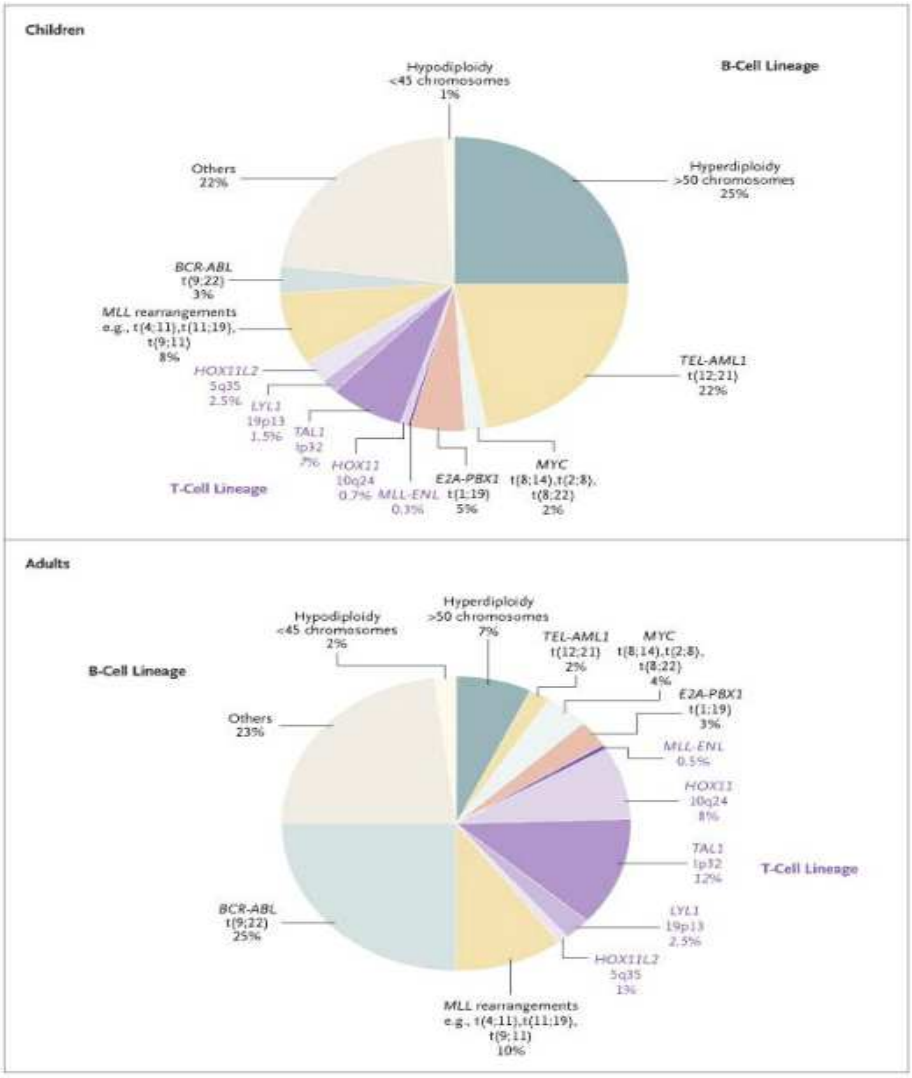

Figure 1*: Estimated frequency of ALL genotypes in children and adult. T-ALL exclusive lesions are indicated in violet* (2).

In the last years, a rapid progress has been made in high-throughput genomic technologies, not limiting the genetic analysis to cytogenetic but allowing more in depth studies. This has led to a very complex and heterogeneous picture of ALL genetics. Several groups have used high-resolution single

nucleotide polymorphism (SNP) arrays of diagnostic ALL samples and detected recurrent genetic aberrations.
Often these were small genetic lesions, mostly deletions but also chromosomal translocations were detected. With increasing numbers of studies performed, it becomes clearer which cellular pathways are the targets of DNA copy number aberrations (CNA). Most often aberrations were observed in master regulators of lymphoid development, such as *PAX5*, *EBF* and *IKZF1*. Other targets include regulators of the cell cycle (*CDKN2A/B*), tumor suppressor genes (*PTEN, BF1, RB1*) and regulators of apoptosis (*BTG1*) (5-10).

Genetic aberrations in B-ALL

Among B-ALL the most common prognostic important structural aberrations are:

The t(12;21)(p13;q22), resulting in *ETV6/RUNX1* gene rearrangement, fuses *ETV6* gene, which encodes an ETS family transcription factor, and *RUNX1* gene, which encodes a transcription factor with a DNA binding domain. The translocation t(12;21) is the most frequent structural aberration in childhood ALL and is found in around 20-25% of the cases. It is associated with favorable outcome.

The translocation t(1;19)(q23;p13) fuses the *TCF3(E2A)* gene on 19p13 to the homeobox (HOX) gene *PBX1* on 1q23 and can occur in a balanced or un-balanced form. E2A transcription

factor plays a role in lymphocyte development and as the translocation impairs one copy it is like to contribute to leukemogenesis. HOX family genes are known for their role in leukemogenesis and as PBX1 can alter the HOX regulated programs, it may contribute to malignant transformation of blasts (11).
This aberration is found in 5% of patients, it is more frequent in pre-B subtype ALL and seems not to have prognostic impact.

The translocation t(9;22)(q34;q11) generates the BCR/ABL fusion protein. It is the result of the fusion of the BCR signaling protein to the tyrosine kinase ABL1 causing constitutive active kinase activity. The BCR/ABL fusion protein acts as an oncoprotein by activating several signaling pathways an interacting with other transforming elements such as RAS, which contribute to the malignant transformation of the blast cells. The size of the BCR fragment included in the fusion protein differs because of splicing of different breakpoints in *BCR* locus. Three distinct protein products have been described: their difference in structure influences the biological and clinical phenotypes of the leukemia. The translocations occurs in 2-3% of children with ALL, frequency increases with patients' age, and is associated with a very poor prognosis.

The translocation t(17;19) (*E2A-HLF*) occurs in around 1% of ALL patients. Like the t(1;19) rearrangement, t(17;19) contains the E2A transcription factor which plays a crucial role in

lymphocyte development (11). The fusion protein has been shown to be sufficient to immortalize lymphocyte precursors (12) and to up-regulate the anti-apoptotic protein Survivin (13). Both mechanisms could explain the resistance to treatment observed in patients positive for this translocation.

Rearrangements of the *MLL* gene at 11q23 are found in 80% of infants (ALL patients younger than 1 year of age), in 2% of older children and in 7% of adults. *MLL* rearrangements involve about 50 different partner genes: t(4;11)(q21;q23) is the most common one. These rearrangements can occur in AML and ALL and some cases show both lymphocytic and monocytic involvement, which triggered the naming of *mixed-lineage-leukemia (MLL)* for the gene on 11q23. MLL is a DNA binding protein that is involved in hematopoiesis through the regulation of *HOX*-family genes and was shown to be a leukemia initiating event (14). The *MLL* prognosis is poor in infant patients, but better in older children (15).

Intrachromosomal amplification of 21q. The amplification has been associated with an adverse prognosis. The amplification of 21q is found in 2% of children patients (16).

In 60% of pre-B ALL cases, a loss of genes that regulate B-lymphoid development is observed and it was shown in experimental models that this leads to an acceleration of leukemogenesis (8,17,18) and thus these aberrations could also contribute in human leukemogenesis. The most frequent

deletion in this group was found in the *IKFZ1* gene. It encodes the transcription factor Ikaros and was deleted in 76.2% of childhood BCR-ABL ALL and in 90.9% of adult BCR-ABL ALL cases. Further, *PAX5*, located on chromosome 9p, was frequently deleted (in 51% of samples), mostly occurring in cases also carrying the *IKZF1* deletion (8). Also located on chromosome 9p are the cell cycle regulators *CDKN2A* and *B*, which were frequently deleted and the whole 9p chromosome arm was lost in many cases. Overall, the average number of aberrations is limited to around six per case at diagnosis, demonstrating that there is no general chromosomal instability in ALL. On the other hand, the number of aberrations differs significantly between different subgroups of ALL (8). MLL-rearranged leukemias carried up to one CNA, indicating that only a limited number of lesions are necessary for leukemia initiation. In BCR-ABL and TEL-AML1 rearranged leukemias more than 6 CNAs were found, suggesting that disruption of multiple pathways is required for leukemia initiation and progression.

Genetic aberrations in T-ALL:

There are also some structural abnormalities in T-ALL, but since these leukemias are less frequent, they have been less studied. Generally, T-ALL patients have a worse outcome than BCP ALL (7,19,20). In about 40% of T-ALL cases, the identified translocation involve the TCR gene. The oncogenic potential

and the prognostic meaning depend on the partner gene (21). The translocation t(1;14)(p33;q11) juxtaposes *TAL1* gene localized on chromosome 1p33,to TCRα (14q11) leading to *TAL1* overexpression.

TAL1 activation may also due to different deletions on Chromosome 1. Seven different deletions of more than 90 kb have been described. This deletion juxtaposes the 5' portion of *TAL1* gene with *SIL*, leading to *TAL1* overexpression. The frequency of the translocation and deletions involving *TAL1* is about 30% in T-ALL. This suggest the existence of other mechanisms as *TAL1* gene resulted overexpressed in more than 60% on T-ALL cases (22). The translocations originating fusion genes are less frequent in T-ALL than in BCP-ALL. The t(10;11)(p12;q14),leading to *PICALM* e *MLLT10* genes fusion and MLL gene rearrangement, in particular t(11;19) translocation, leading to *MLL-ENL* fusion are diffused only in 5-10% of patients. Finally, the amplification of 9q34 portion, leading to *NUP214-ABL1* fusion gene, is found in 4% of patients. More than 50% of patients have activating mutations of *NOTCH1* gene and the 70% of cases present the deletion of 9p21 region involving the oncosuppressor gene *CDKN2A/B* (23).

Risk factors and treatment response

In childhood ALL, a limited number of significant risk factors have been described with different clinical and biological

characteristics that are used for prognosis and adaptation of the treatment. From the end of eighties, in Italy, ALL patients are stratified according to guidelines of study protocols (named AIEOP ALL 88, 91, 95, 2000, R2006 and 2009) in collaboration with BFM (Berlin-Frankfurt-Munster) study group.

In the ALL 2009 protocol actually in use, numerous clinical and biological prognostic factors are used to stratify patients in risk classes, which are submitted to distinct therapeutic approaches. The risk classes are based on clinical features, such as age, White Blood Cells Count (WBC), and leukemic cells biological features, such as immunophenotype, karyotype, chromosomal abnormalities and response to initial therapy (Table 1), (24).

Factors commonly used for risk stratification		
Factor	**Favorable**	**Adverse**
Age (years)	1-9	<1 or ≥10
Leukocyte count ($\times 10^9$/L)	<50	>50
Immunophenotype	B-cell precursor	T-cell
Genotype	Hyperdiploidy>50 chromosomes, TEL-AML1 (ETV6-RUNX1)	Hypodiploidy<44 chromosomes, BCR-ABL1, MLL-AF4
MRD after induction	<0.01%	≥1%

***Table 1**: Risk factors in childhood ALL* (1).

Another leukemic prognostic factor, the *clearance,* is monitored by Minimal Residual Disease (MRD) evaluation. MRD is the name given to small numbers of leukemic cells that remain in the patient during treatment or after treatment when the patient is in remission (in the absence of signs of disease) and their quantification is a powerful method to follow the disease regression over treatment time.

In detail, MRD monitoring is a quantification of residual leukemic blasts in the bone marrow and peripheral blood of patients measured either by quantitative PCR of clone specific Immunoglobulin (Ig) and T-cell receptor (TCR) rearrangements and/or by flow cytometry of surface markers (25-28). Multi-parameter flow cytometry uses the atypical expression of leukemia associated surface proteins to distinguish between normal and malignant cells. For example, CD10 is often expressed at a higher level in precursor B-ALL than in normal B precursor cells. For detection of MRD, proteins that are aberrantly co-expressed on ALL cells, such as CD58 or CD9 for precursor-B ALL will be very useful to clearly distinguish a small population of blasts over the background of normal regenerating lymphoid cells. Other aberrantly expressed markers are cross-lineage expression of T-cell and myeloid cell markers including CD7, CD13 and CD33 (21). From a molecular point of view, the junctional regions of Ig and TCR gene rearrangements are suitable PCR targets as they represent unique sequences, which are created through deletions and random insertions of nucleotides during the rearrangement process of B- and T-cell receptors. Leukemic blasts, stalled in their maturation process have undergone the rearrangement process as normal lymphocytes, but often not until the complete V-D-J rearrangement. Unlike in healthy blood, where it is possible to detect multiclonal rearrangements, reflecting the diversity of B- and T-cells, leukemic blasts are more homogeneous and allow detecting strong signals of

monoclonal rearrangements. Extensive studies have established the time points and cut offs for MRD levels that are most suitable to distinguish between patients with a high risk or low risk to relapse with their disease. The AIEOP ALL protocol distinguishes three risk groups: High, Medium and Standard Risk. The patients are placed in one of the three groups, according to prednisone response at 7 day, complete bone marrow remission at 33 days, MRD at days 33 and 78 and to the presence of *BCR/ABL* or *MLL/AF4* transcripts. Patients with MRD negative at 33 and 78 days, evaluated with at least two markers, are classified as Standard Risk (SR). Patients not classified as SR and MRD < 10^3 at 78 days are considered as Intermediate risk (IR). Patients with persisting MRD levels above the determined cut off (10-3 leukemic cells per one normal cell) after 78 days of chemotherapy, at the beginning of consolidation phase, have a high risk of relapse (MRD-HR, Figure 3 left panel). These patients, as well as few additional cases identified based on cytogenetic risk criteria (cases with the translocations t(9;22) or t(4;11), see below and Table1) will qualify for more intensive treatment after this time point. All the above described factors are used to stratify patients into different treatment groups and optimize their individual treatment. Thereby patients with unfavorable factors receive more intense chemotherapy, whereas those with “good prognosis” receive less or modified versions of the intensive treatment elements

New prognostic markers in ALL

Over the last decades therapies of pediatric ALL patients have led to improvement of remission induction and long-term survival presently achieving cure rates of over 80% (2). However a relapse incidence (20%) involving all three risk groups shows the limitation of current prognostic factors and emphasizes the need to identify new molecular prognosis factors which will allow to early recognize patients with high risk of relapse and to modify the protocol risk groups.

Recently some research groups (29) (30) identified a new player in childhood leukemia: *CRLF2* (Cytokine Receptor like Factor 2). The presence of *CRLF2* overexpression and rearrangements in ALL, suggest a possible role for *CRLF2* signaling pathway in lymphoid malignancy and seem to identify high-risk patients not recognized by current high-risk parameters.

Physiological role of CRLF2 in B cells

Cytokines and their receptors play an important role in cell survival, proliferation, and differentiation during hematopoiesis (31). Cytokine receptors share common extra-cellular domain structural features and homologies in the primary amino acid sequence. In 2000, Pandey and colleagues reported the isolation of a new Type I cytokine receptor subunit (32). Later on Tonozuka and colleagues and Zhang et. al, identified this

novel type I cytokine receptor based on homology searches, in cDNA libraries of human T lymphocytes and dendritic cells respectively (33,34). Thus the newly discovered cytokine receptor has common characteristics of type I cytokine receptor family members and was termed *CRLF2*, which stands for cytokine receptor-like factor 2 (33). *CRLF2* gene is localized at the end of the *petit* arm of the chromosome X or Y (ChrX-1,314,890-1,331,616; ChrY-1,264,890-1,281,616; ENSG00000205755) in the Pseudoautosomal Region 1 (PAR1) (29). Binding and cross-linking experiments demonstrated that this protein is the receptor for a recently described interleukin 7 (IL-7)-like factor, Thymic Stromal Lymphopoietin (TSLP). Most of type I cytokine receptor systems, require at least two distinct receptor chains for high affinity binding with the ligands and subsequent signal transduction. The heterodimeric complex formed by the CRLF2 subunit and IL-7Rα was demonstrated to be a functional receptor for TSLP. CRLF2 itself has low affinity for TSLP but in combination with IL-7Rα generates high affinity binding for TSLP, called TSLP-R, which triggers signaling transduction (He R. *et al.*, 2010). TSLP ligand is produced by epithelial cells in order to activate dendritic cells, and is involved in inflammation and allergic responses (35). Moreover, this cytokine mediates also B-cell precursor proliferation and survival (36). Demehri et al showed that endogenously overexpressed or exogenous TSLP supplemented during neonatal hematopoiesis results in drastic expansion of peripheral pre- and immature B cells, thus causing B-cell

lymphoproliferative disorders. (37). The binding of TSLP to its receptor mainly activate signaling networks involving several key proteins, namely Janus kinases (JAK) 1, 2, and 3, and STAT proteins, mainly STAT5a/b (38).

Overview of JAK-STAT signaling pathway

The Janus kinase (JAK)/ Signal Transducer and Activator of Transcription (STAT) pathway has a central role in the signaling of cytokines by regulating cell proliferation, survival, differentiation and immune response. This pathway begins by the binding of cytokine to its cognate receptor, which basally is completely inactive. Cytokine binding induces a conformational change that either reorients a preformed dimer (ref 3-6 vainchenker) or induces receptor dimerization/oligomerization (39). As a consequence, JAKs prebound to the receptor's cytoplasmatic region, become activated, leading to cross-phosphorylation and receptor tyrosine phosphorylation, thus creating binding sites for cytoplasmic proteins such as the STAT proteins, which becomes substrates of JAKs (40). Phosphorylation leads to STAT homodimerization and translocation to the nucleus, where they act as transcription factors prompting cell proliferation, survival and differentiation.

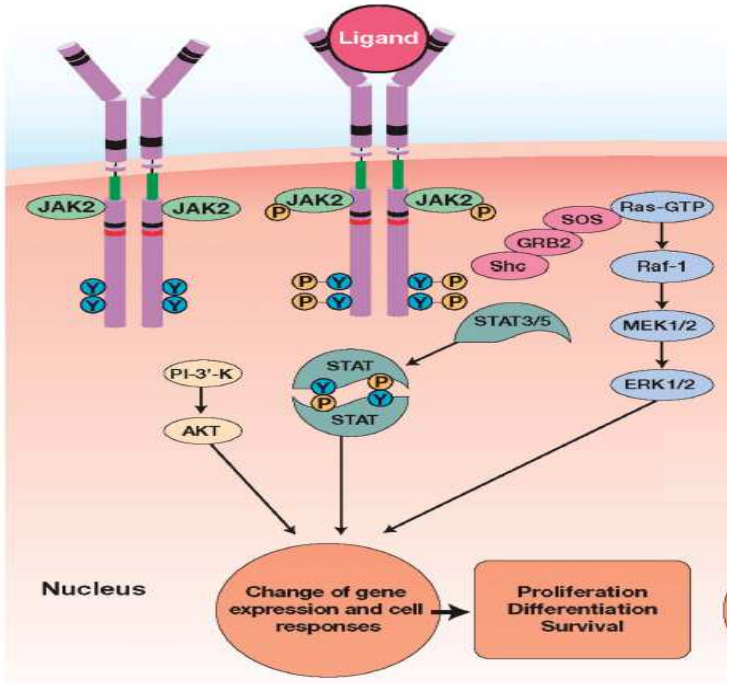

Figure 2: JAK/STAT signaling cascade. *The binding of a ligand to its receptor induces a conformational change in the preformed dimer, leading to tyrosine phosphorylation and cross-activation of JAKs, which phosphorylate intracellular receptor tyrosine residues (Y-P). Various adaptor proteins become substrates of JAKs, triggering signaling cascades. Cytokine receptors are linked to the STAT, Ras–MAPK, and phosphatidylinositol-3'-kinase (PI3K)–AKT pathways, which converge at the nucleus and regulate gene expression.*

Main actors of JAK/STAT pathway and their aberrancies in leukemia

<u>JAK kinases and STAT transcription factors</u>

The JAK family of non-receptor tyrosine kinases comprises four members: JAK1, JAK2, JAK3, and TYK2, all of which signal

aberrantly in different malignant contexts. The JAKs are crucial modulators of signal transduction pathways. They associate with the cytoplasmic tails of cytokine receptors, and ligand-induced reorientation of receptor places the JAKs in adequate proximity for transphosphorylation of the partner JAK. In JAK2, this occurs at residues Y1007 and Y1008 (41). The JAK family of kinases contains a C-terminal kinase domain (JH1) adjacent to a pseudokinase domain (JH2).

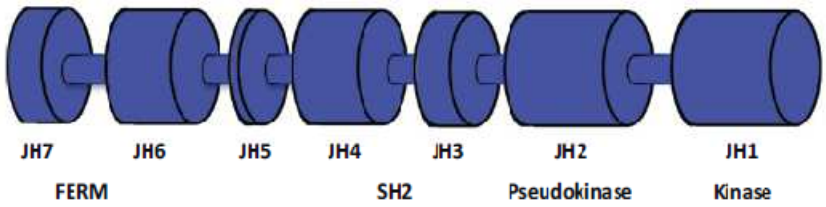

Figure 3: JAK2 structure: *JAK2 has seven domains (JH7–JH1) including a FERM domain (cytokine receptor interaction), a SH2 domain (recruitment of interacting proteins), a psuedokinase domain, and a kinase domain.*

It is predicted that this JH2 domain acts as an autoinhibitory domain because its loss renders the protein constitutively active (42). Recent purification of the JH2 domain led to the observation that it may have catalytic activity, even though the study demonstrated that this domain has only 10% activity compared to the JH1 domain when assessed in vitro (43). In fact, in vitro kinase studies have revealed that the purified JH2 domain can phosphorylate itself on S523 and Y570 as a way of negatively regulating the protein. Mutation of the predicted catalytic lysine in the JH2 domain resulted in loss of activity and in increased downstream STAT activation (44). Additional

functional studies are needed to show if this domain can serve as a kinase in physiological and pathophysiological states. The JH2 domain adopts a typical protein kinase fold with an activation loop that cannot be phosphorylated and with varied residues in sites critical for canonical kinase function. Successful crystallization of the entire JAK2 kinase will provide more definitive evidence to finally elucidate the complete structure of the protein. To date, only the JH1 domain of JAK2 and JAK3 and the JH2 domain of JAK2 have been individually crystallized (45-47). Phosphorylation of JAK2 is integral for its regulation. JAK2 is phosphorylated on many sites, and it has been shown that phosphorylation of different residues within JAK2 can negatively or positively regulate JAK kinase activity. Phosphorylation at Y221, Y637, Y813, Y868, Y966, Y972, Y1007, and Y1008 enhances JAK2 activity, whereas phosphorylation of S523, Y119, Y317, Y570, and Y912 favors an inactive conformation (Figure 5) (48-52).

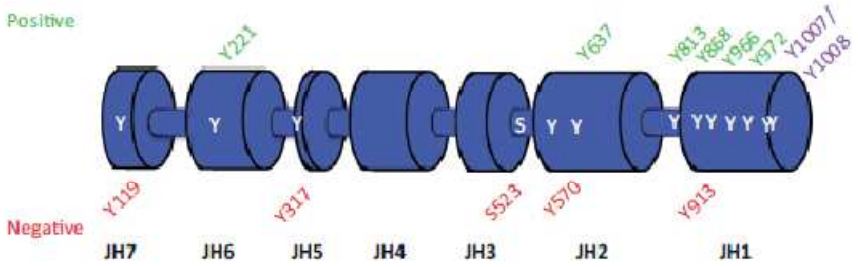

Figure 4 : Phosphorylation sites identified for JAK2*. Green residues indicate that phosphorylation is required for optimal activation of the kinase activity of JAK2. Red residues indicate that phosphorylation results in negative regulation of JAK2 activity. Y1007 and Y1008 are indicated in purple and are the activation loop*

residues that must be phosphorylated for activity of the kinase. Abbreviations: JH1–7, JAK homology domains 1–7 (adapted from Lafave,2012 (53).

Phosphorylation of residues on cytokine receptors by activated JAKs results in the generation of docking sites for downstream signaling mediators that contain Src homology 2 (SH2) domains, including the STAT family of transcription factors. The STAT family comprises seven members STAT1,2,3,4,5A,5B and 6. They are phosphorylated by JAKs and dissociate from the receptor to form homo and heterodimers with other STAT proteins. The STATs then translocate to the nucleus, bind to STAT DNA-binding sequences, and activate cytokine-dependent transcription factors, gene related to proliferation, cell growth and division, programmed cell death, cell specialization and differentiation.

In addition, it has been shown that JAK2 itself is able to translocate to the nucleus and directly phosphorylate Y41 on histone H3, resulting in disruption of heterochromatin protein 1 alpha (HP1a)-mediated epigenetic repression and ultimately in the activation of leukemic transcription factors (54). This novel mechanism may be important in explaining how JAK2 regulates the transcription of downstream targets, and recent work has suggested that this leads to a feed- forward loop by which JAK2 activity can enhance JAK2 transcription (55).

JAK /STAT negative regulators

The JAK/STAT pathway is negatively regulated by several types of proteins acting on the degradation of JAKs and STAT proteins (SOCS, PIAS), on JAKs or receptor phosphorylation (LNK, phosphatase), or on the degradation of the cytokine receptors (Casitas B-cell lymphoma (CBL)). Genes coding for most of these proteins can be considered tumor suppressor genes, and their inactivation (mutations, silencing) potentiates JAK/STAT signaling when mutations of JAK are present. However, some of these molecules may also have the opposite effect. For example, SOCS proteins modulate signaling by binding to JAK kinase thus inactivating it and their overexpression can be observed in some malignancies, allowing, for example, for resistance to the antiproliferative effect of interferons (56). LNK, also called SH2B3, is a member of the SH2B family, an adaptor protein family that does not possess any enzymatic activity. This family contains two other members (57) and has an important role in hematopoiesis by negatively regulating JAK2 activation through its SH2 domain (58,59).

In murine models, the knockout of LNK leads to myeloproliferation associated with myelofibrosis (MF) (60). In humans, rare mutations in LNK have been found in patients with essential thrombocytopenia (ET) and primary myelofibrosis (PMF) without other mutations in signaling molecules (61). LNK mutations lead to loss of regulatory functions and consequently

to increased JAK2/STAT signaling. LNK mutations have also been described during disease progression to AML (62).

Disregulation of JAK-STAT pathway

A number of genetic lesions in hematopoietic disorders cause hyperactivation of the JAK-STAT pathway and thereby mimic the survival and proliferation signals from constitutively active cytokine receptors. Genetic lesions that activate this pathway occur at three different levels: cytokine receptor chains themselves (e.g.CRLF2 and IL/Rα); activating mutations of JAKs or deletion of inhibitory molecules (e.g. SH2B3) that regulate JAK activity; oncogenic tyrosine kinase, that can target STAT5 (e.g. ABL1) (63).

<u>CRLF2 chromosomal rearrangements leading to its overexpression</u>

The first report about the involvement of *CRLF2* overexpression in leukemia came from two groups in 2009 (29,30). Russell and colleagues used FISH analysis on leukemic cells of BCP-ALL patients and identified chromosomal abnormalities involving this gene. The overexpression of *CRLF2* gene arises from a translocation juxtaposing *CRLF2* to the Immunoglobulin Heavy Chain (*IGH@*) locus of chromosome 14 or from an interstitial deletion of the pseudoautosomal region 1 (PAR1) (29,30).

The *IGH@* is a locus involved in several common translocations and rearrangements involving *IGH@* locus have been identified as a new cytogenetic subgroup in BCP-ALL, occurring predominantly among older children and young adults. Translocation of *CRLF2* with the *IGH@* locus leads to expression of *CRLF2* via *IGH@* enhancer elements as the entire CRLF2 gene has relocated to the chromosome 14 (Figure 5) (29).

.

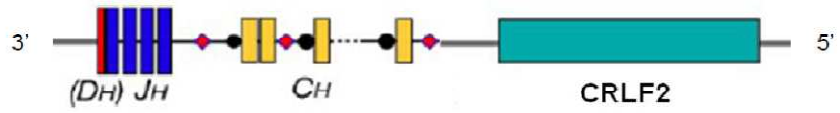

Figure 5*: translocation t(X;14) t(Y;14). The enhancer regions of the locus are colored in pink (adapted from (64)).*

The PAR1 deletion is an intra-chromosomal deletion of Xp22.3 or Yp11.3 that seems to be the result of aberrant use of recombinant signals (Figure 7).

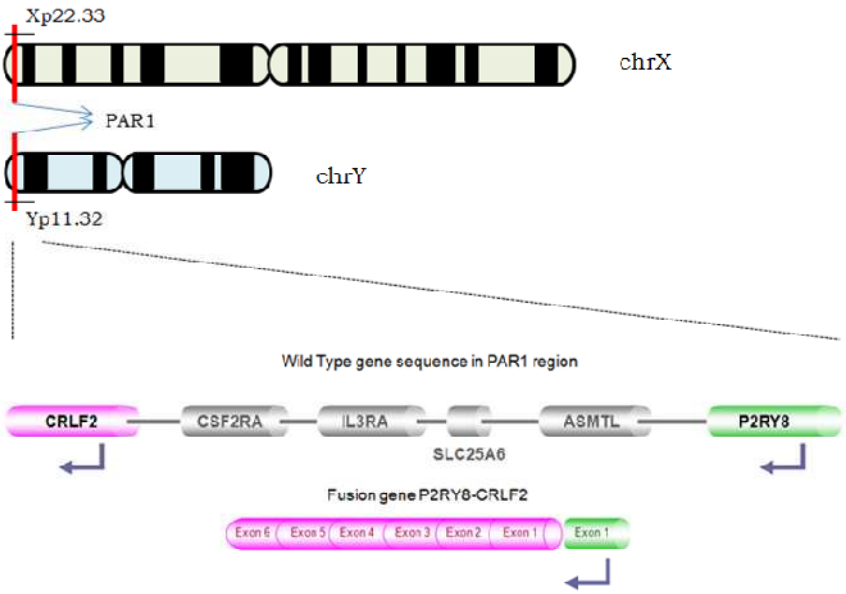

Figure 6. P2RY8-CRLF2 fusion gene. *The idiograms of X and Y chromosomes show the location of the PAR1 region. Breakpoint locations are marked with red arrows. PAR1 deletion juxtaposes the first non-coding exon of P2RY8 gene (in green) to the first coding exon of CRLF2 (in pink), resulting in high expression of chimeric transcripts, P2RY8-CRLF2 fusion gene.*

The region of the PAR1 deletion involved at least five genes (*P2RY8*, *ASMTL, SLC25A6, IL3RA* and *CSF2RA*). The deletion juxtaposes the first non-coding exon of *P2RY8* gene to the first exon of *CRLF2*. *P2RY8* encodes a purigenic receptor (P2Y, G-protein coupled, 8) that is expressed at high levels in many tissues, including leukemic cells. A single case of rearrangement of *P2RY8* to *SOX5* has been reported in primary splenic follicular lymphoma (65). *CRLF2* expression from this chimeric locus is driven by the constitutively active *P2RY8* promoter resulting in high expression of chimeric transcripts, *P2RY8-CRLF2*.

The frequency of translocations and deletions involving *CRLF2* that lead to *CRLF2* overexpression seems to be dependent on the cohort of samples studied. In unselected B-progenitor ALL cases, PAR1 deletions are more common than *CRLF2* translocations (approximately 2:1). In contrast, the *IGH@-CRLF2* alteration is much more frequent than PAR1 deletions in a cohort composed of high-risk B-precursor ALL (10).

CRLF2 activating mutations

Recently, it has been reported that aberrant expression or activating mutations of a heterodimeric receptor components, may induce homodimer formation. Sequencing of *CRLF2* in childhood B-ALL specimens, including over-expressing cases, identified in some cases a point mutation changing the phenylalanine 232 to cysteine. This mutation was also detected in several adult B-ALL patients that showed overexpression of *CRLF2*. The *CRLF2* Phe232 residue is near the junction of the extracellular and trans-membrane domains. Mutations that introduce cysteine residues in this region of other receptors can activate signal transduction through intermolecular disulfide-bonded dimers. To confirm that *CRLF2* Phe232Cys promotes constitutive dimerization, Yoda and colleagues performed immunoblots in BaF3 cells expressing wild type (WT) *CRLF2* or *CRLF2* Phe232Cys. Under non-reducing conditions, the molecular weight of *CRLF2* Phe232Cys band, but not the WT band, was doubled, consistent with constitutive dimerization

through the cysteine residues. Moreover, it has been demonstrated that, CRLF2 may signal independently of TSLP as a homodimer when harboring the F232C mutation inducing a strong costitutive Stat5 phosphorylation. Anyway, cells expressing CRLF2 Phe232Cys are still sensitive to enzymatic JAK inhibitors arguing that JAKs are involved in signaling even when CRLF2 is mutated (66).

It is reasonable to hypothesize that *CRLF2* Phe232Cys could also interact with unknown partners to create a mutant heterodimer, leading to activation of signal transduction in absence of TSLP.

JAK mutations and their cooperation with CRLF2 alterations:

In 2005, an acquired mutation in exon 14 of JAK2, V617F was found in 90% of patients with the classical non BCR-ABL myeloroliferative disorder (MPN) polycythemia vera (PV) and 50% of those with essential thrombocythemia (ET) and primary MF (PMF). The JAK2V617F mutation is located in the pseudokinase domain. Structural modeling predicts that F617 is involved in stacking interactions with the aromatic residues F594 and F595, which probably stabilize the JAK2 V617F protein (43). Bandaranayake et al. proposed a bimodal activation mechanism by JAK2 V617F: (i) loss of JH2 catalytic activity and (ii) gain of a stimulatory JH1 interaction (45). V617F is a gain of function mutation, which requires activation of cytokine receptors such as G-CSFR, EPOR and MPL/TPOR.

This includes the activation of STATs, PI3K and MAP/ERK pathways respectively. The choice of activated STATs may largely depend of the receptor type, for example, essentially STAT5 for EPO-R and STAT3, STAT5 and STAT1 for MPL. In *in vitro* experiments, the EPO independence induced by JAK2 V617F required both STAT5 and PI3K activation (67) (68). However, JAK2 V617F can also induce the canonical pathways of these receptors in absence of cytokine.

Although JAK2 mutations are most common in MPN patients, recent genetic and functional studies have implicated dysregulated JAK–STAT signaling in patients with ALL. Izraeli and colleagues first identified JAK2 mutations in Down syndrome-associated ALL (69). Flex et al. identified somatic activating JAK1 mutations in patients with ALL and suggested that these mutations are associated with adverse outcomes similar to the presence of the BCR– ABL1 translocation (70).

A deletion in pseudokinase domain of JAK2 called JAK2ΔIREED including R683 was initially discovered in a patient with DS and BCP-ALL (71). Expression of JAK2ΔIREED in Ba/F3 cells induced constitutive activation of JAK/STAT pathway and growth factor-independent cell proliferation (71).

Subsequently JAK2R683 mutations were found in about 20% of Down syndrome patients with ALL. These JAK2 mutants are associated with CRLF2 rearrangements leading to overexpression of this receptor (30). Mullighan and colleagues showed coimmunoprecipitation of human CRLF2 and phosphorylated mutant JAK2, suggesting that these proteins

physically interact. (30). Consequently, JAK gain-of-function mutants do not confer a transformed phenotype in the absence of a compatible cytokine receptor. This situation would be analogous to JAK2 interaction with cytokine receptors in myeloproliferative neoplasms (MPN), in which MPN associated with JAK2 mutants requires expression and interaction with a cytokine receptor to induce transforming signals (58). To test this idea, several groups expressed CRLF2 and JAK2 Arg683 mutants in combination and alone in BaF3 cells, and determined the ability of these proteins to transform cells to cytokine independence. The combination of WT CRLF2 and WT JAK2 provided a growth advantage versus JAK2 alone, and JAK2 Arg683 mutation alone was insufficient to confer IL-3 independence (66,72). Cells overexpressing CRLF2 and expressing JAK2 Arg683 mutants had constitutively phosphorylated JAK2 and induced activation of transforming signals in the presence or absence of IL-7R (72) (Figure 7). The reason why most JAK2 Arg683 mutations are not transforming in absence of CRLF2 overexpression is still unclear (72).

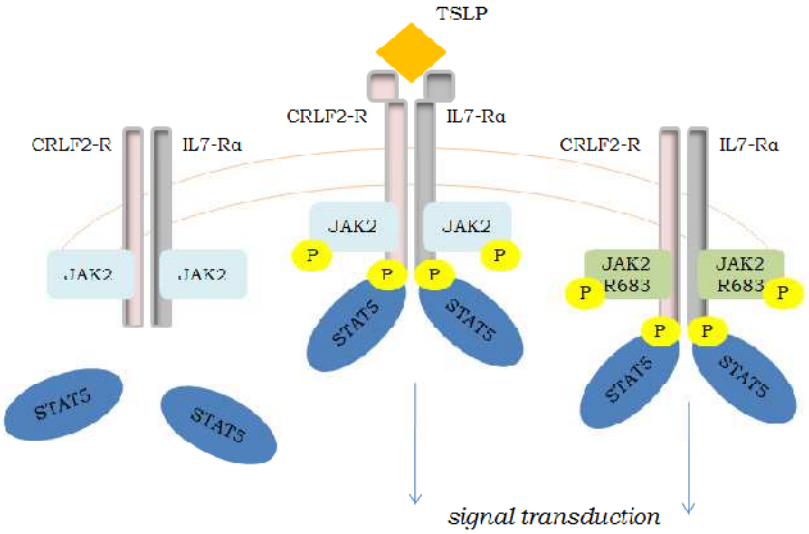

Figure 7. JAK2 and the gain of function mutant JAK2 R683. *In absence of the ligand TSLP there is no signal transduction. When TSLP binds the CRLF2/IL7-Rα receptor, JAK2 is activated through phosphorylation, and can recruit STAT5 to allow signal transduction. In presence of JAK2 R683 and CRLF2 overexpression, the signal transduction can be performed even in absence of TSLP ligand.*

As described above, also *CRLF2* point mutation are able to trigger the signal trough JAK2 independently from cytokine binding (Figure 8)

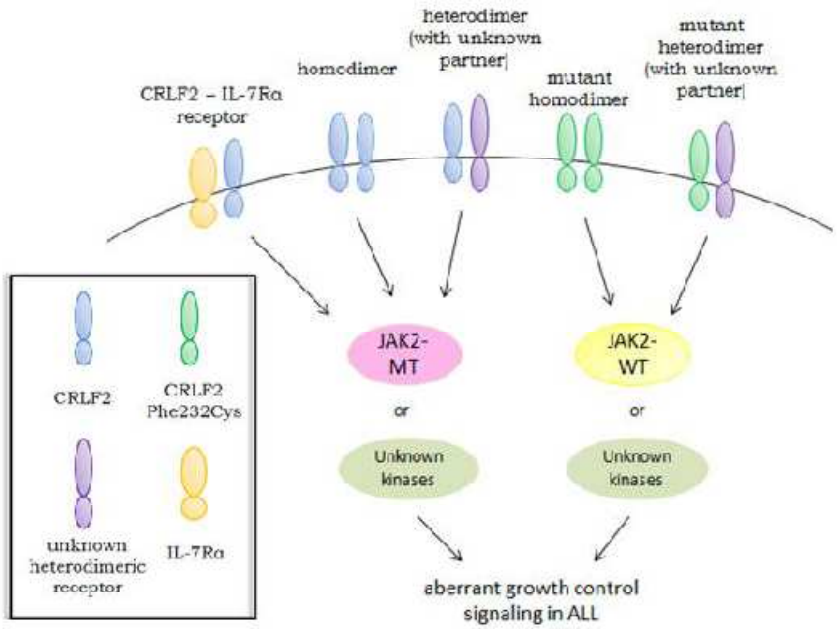

Figure 8. Aberrant CRLF2/JAK2 signaling in ALL. *Overexpression of CRLF2 may lead to aberrant signaling through homodimeric or heterodimeric receptor configurations of wild type (blue) or mutated (green) CRLF2 protein and IL-7Rα or an unknown partner receptor (violet), via action of mutant (pink) or wild-type (yellow) JAK2 or other unknown kinases, as indicated.*

IL7R function and alterations

The over expression of CRLF2 can be associated with mutations in other genes such as *IL7Rα* (73). CRLF2 dimerizes with IL-7Rα to form the receptor for TSLP. The IL-7Rα is a component of both the IL-7 and TSLP receptors and this suggests that the activation of these two receptors may trigger a common signaling pathway.

Human IL-7 and TSLP use two different but complementary mechanisms to regulate peripheral T cell homeostasis. IL-7 has a potent and direct effect on T cells activation and displays a limited effect on DCs, whereas TSLP predominantly acts on DCs and has a moderate direct effect on T cells (74). A dominant role of TSLP in human B-lymphoid development has been highlighted by a recent study showing that CRLF2 and not IL7R signaling induces proliferation of human fetal liver-derived multi-lineage progenitors, pro-B and pre-B cells. The authors observed that human CD34+CD38-HSCs display a short wave of precursor B-cell expansion with IL7, followed by extended CRLF2 signaling that increases the absolute numbers of mature human B cells (75).

Both receptors activate the transcription factor STAT5 (Signal Transducer And Activator of Transcription 5), but they use two distinct mechanisms of activation. Signaling from the IL-7 receptor is known to involve JAK1 and JAK3 whereas intracellular signaling by the TSLP receptor is poorly characterized, and involves JAK2 (Janus Kinase 2) activation through phosphorylation.

Somatic gain-of-function IL7Rα exon 6 mutations have been found in B and T-ALL.

In most cases, these mutations introduce an unpaired cysteine in the extracellular juxtamembrane-transmembrane region and promote dimerization of the receptor, inducing constitutive JAK1 activation. In B-ALL these mutations are sometimes associated

with an overexpression of CRLF2 forming a functional, spontaneously activated receptor for TSLP (76).

STAT alterations

Although constitutive STAT activation is very frequent in hematological malignancies, very few mutations in STAT genes have been described yet. Mutation in the STAT6 DNA-binding domain have been found in primary mediastinal B-cell lymphoma which may lead to a loss-of-function (77). However the oncogenic properties of these mutants remain to be determined.
Like for some solid tumors, recurrent activating mutations of STAT3 have been found in large granular lymphocytic leukemia (78). No recurrent mutations in STAT1, STAT3 and STAT5 have been found yet in other hematological malignancies.

CRLF2 and Ph-like ALL

Recent reports described a subgroup of B-ALL patients with a gene expression signature similar to Philadelphia positive ALL (Ph+), carrying the typical the translocation t(9;22) encoding for BCR/ABL1 fusion gene (79-81). Although the gene expression profile of this new patient subgroup was able to classify them together with Ph+ ALL, this novel group of patients was actually negative for the fusion gene BCR/ABL1, therefore they were defined as Ph-like or BCR/ABL1-like. They account for 15% of

BCP-ALL and had a particular poor prognosis (6,79,81,82). These patients share multiple genetic and biological functions with Ph+ALL patients. Deletions or mutations of the lymphoid transcription factor gene IKZF1 (encoding Ikaros), for example, are a hallmark of both BCR– ABL1–positive ALL and Ph-like ALL (7). To further characterize the full spectrum of kinase-activating genetic alterations in Ph-like ALL, Roberts et al performed a detailed genomic analysis of 1725 children, adolescents, and young adults with precursor B-cell ALL (83).
CRLF2 rearrangement and JAK mutations are found in approximately 50% of Ph-like cases (84), identified in a group of patients with JAK- associated fusion leading to hyperactivation of JAK/STAT pathway and the majority of the remaining cases is characterized by activation of ABL1-associated signaling pathways (85). Among these newly identified genetic abnormalities, EBF1-PDGFRB or NUP214-ABL1 fusion responded to known TKIs, while BCR-JAK2 responded to JAK2 inhibitor in preclinical studies (85,86). These findings, including recent case-reports translated in the clinic, open the possibility to include Phlike-ALL either into the current approach of combination of chemotherapy and TKI inhibitors or into new protocols using JAK2 inhibitors.

CRLF2 and Down Syndrome

Down Syndrome (DS) is one of the most common genetic disorders (87). Children with DS have a dramatically 20-150

increased risk for acute myeloid and lymphoid leukemias (ML-DS and DS-ALL, respectively) (88,89,Vyas, 2007 #664,90). Leukemia, especially DS-ALL, is the third cause of death in children with DS after congenital heart disease and respiratory infections (91,92). Interestingly the risk for common cancers is *lower* in DS (88,93). Thus, the association between DS and childhood leukemias suggests that constitutional trisomy 21 (cT21) is leukemogenic. In case of ALL, DS is associated with higher risk than non-DS, and DS-ALL is a clinical and biological distinct subset from non-DS ALL patients (94). DS-ALLs are almost exclusively of B cell precursor immunophenotype and, unlike the myeloid leukemias in DS, there are no infant leukemias. The genetic profile of DS-ALL differs from non-DS ALLs. The more common cytogenetic subtypes of childhood ALL, especially the good prognosis hyperdiploid (HD) and ETV6/RUNX1, are less common in DS comprising only 17% compared with 55% in non-DS ALL (30,95).

CRLF2 alterations have an incidence of 55% in these patients and they seem to occur exclusively in cases in which recurring ALL-associated chromosomal translocations are absent.

Several groups have reported the presence of somatic activating mutations in the Janus kinase *JAK2* in approximately 20% of DSALLs (69,72,96).

Targeting of JAK/STAT pathway

As described above, STAT proteins are constitutively activated in the majority of hematological malignancies. However, only in a minority of them it could be demonstrated that JAK/STAT signaling is directly altered, such as in BCR-ABL–negative MPN, a subset of T- and B-ALL, very rare AML, Hodgkin lymphoma, B-cell mediastinal lymphoma, and multiple myeloma. The discovery of JAK2 mutants linked to MPNs prompted the development of JAK2 inhibitors as targeted therapy for MPNs. Several JAK2 inhibitors are being tested in clinical trials for primary and secondary myelofybrosis (MF) in patients positive or negative for JAK2 mutations (97-99).

Ruxolitinib has recently been approved by the Food and Drug Administration for treatment of intermediate- or high-risk MF, and the Committee for Medicinal Products for Human Use of the European Medicines Agency recently recommended the approval of Ruxolitinib for the treatment of MF-related splenomegaly or symptoms. Because none of the present compounds discriminate between wild-type and mutated JAK2, as a consequence of efficacy and their mechanism of action, JAK2 inhibitors may induce significant levels of anemia and thrombocytopenia, which is considered a toxic effect and can lead to treatment interruption. Additionally, it is unknown whether these inhibitors can target heterodimers such as JAK1/JAK2 and JAK2/TYK2, which may participate in G-CSF or TPO signaling.

Treatment of patients with MF with Ruxolitinib has a modest impact in reducing JAK2 allele burden and decreasing marrow fibrosis. Strikingly, and particularly in Ruxolitinib treatment, two important positive effects of JAK2 inhibitors are the substantial and rapid reduction of spleen size and decrease in constitutional symptoms (99,100,Tefferi, 2012 #675,101-103).

These effects are exerted both by JAK1/JAK2 inhibitors such as Ruxolitinib and by other JAK2-specific inhibitors, as the SAR302503 (TG101348). For constitutional symptoms, inhibitors might prove beneficial in preventing the cytokine storm present in MF (99). In contrast, the molecular basis for the spleen-reducing effects of JAK2 inhibitors remains unexplained. Several evidences in literature shows the employment of JAK inhibitors to target JAK/STAT pathway also in ALL. Maude et al. (80) showed the efficacy of JAK1/2 inhibitors, in *in vivo* xenograft models of Ph-like B-ALL and in a subset of T-ALL, ETP-ALL, in which the hyperactivation of JAK/STAT pathway is a common feature (104). However, the development of new resistance mechanisms to JAK inhibitors is growing and impairing their efficacy thus emphasizing the need for novel approaches (105).

Clearly, the understanding of the players involved in JAK2 signaling network and how the mutants exactly interact with the cytokine receptors, will be important for future therapeutic improvement. It is possible that the combination of JAK2 inhibitors with inhibitors of downstream targets of STAT5 including BCL2/BCL-XL (ABT-737) might be more effective

(106). Certainly, it may be important to directly target STAT5 and STAT3. Recently, it was shown that a molecule already developed, Pimozide, was capable of inhibiting STAT5 activation in BCR-ABL cell lines (107). Furthermore, a promising approach may be represented by the combination of JAK inhibitors with epigenetic therapy. Inhibitors of histone deacetylase 6, which is involved in deacetylation of HSP90, are attractive because acetylated HSP90 can no longer associate with JAK2 and this leads to JAK2 degradation via ubiquitination (108). This effect takes on great importance in hematological diseases characterized by JAK2 mutations leading to its hyperactivation, such as MF. A recent phase II clinical trial demonstrates the efficacy of a pan-histone deacetylase inhibitor, in inducing a hematological response in most patients with PV and some patients with MF (109). This introduces the concept of specifically targeting mutant JAKs for degradation, especially in the case of mutants of JAK2 as JAK2 V617F that are resistant toJAK inhibitors. Moreover, HSP90 inhibitors are extremely efficient in murine models of MPNs including those driven with JAK2 inhibitor-resistant mutants (108) (110).

JAK inhibitors and such combined therapeutic strategies might be extended in the future to other subsets of ALL with dysregulation of the JAK/STAT signaling and eventually to therapy-refractory malignancies.

For DS-ALL patients for example, the great diffusion of CRLF2 rearrangements leading to hyperactivation of JAK/STAT signaling, suggests that therapeutically targeting this pathway

could be of potential benefit. Moreover, the poor outcome of DS-ALL compared with ALL in children without DS increases the urgent need for safer therapies. The high fatality rate for these patients is not only because of enhanced toxicity of chemotherapy but also primarily because of intrinsic resistant of DS-ALL to therapy. Hence, ALL is a major and fatal problem of DS children and deciphering its biology is urgently needed for rational effective therapy.

Novel therapeutic approaches

Role of Hystone deacetylase inhibitors in treatment of cancer and non-cancer diseases

Acetylation and deacetylation of histones help to regulate gene expression with remodeling of chromatin, allowing the binding of transcription factors. The acetylation of histones is regulated by two classes of enzymes: histone acetyltransferases and histone deacetylases (HDACs) (111) (112). Whereas the base pair sequence of DNA provides the fundamental code for proteins, posttranslational modification of proteins plays a major role in the control of gene transcription. HDACi's were initially studied for their ability to increase gene expression. Today, the increasing number of orally active, synthetic HDACi's are primarily developed to treat cancer by modulating the gene expression of pro- apoptotic genes that have been suppressed in malignant cells (112,Marks, 2003 #687). The development of

HDACi's for treatment of cancer is based on de-repression of genes that participate in endogenous proapoptotic pathways and bring about a selective death of malignant cells while sparing healthy cells. With hyperacetylation of nuclear histones, chromatin unravels and transcription factors can now bind to DNA and initiate the synthesis of RNA coding for proapoptotic genes. By use of this mechanism, HDACi's would avoid the toxic effects of many chemotherapeutic drugs. Presently, HDAC inhibitors are used to treat patients with advanced solid and hematological tumors (113) (i.e. the HDAC inhibitor Suberoylanilide hydroxamic acid was approved for the treatment of cutaneous T-cell lymphoma). In general, HDAC inhibition selectively alters the transcription of few of the expressed genes (approximately 2% to 10% of expressed genes are increased or decreased in their rate of transcription) (114-117). Knowing the concentration of a particular HDACi for inducing apoptotic cell death in primary tumor cells *in vitro* is often not possible, and the success of any HDACi in the treatment of humans with cancer is thus measured by a reduction in the tumor burden. Moreover, at concentrations lower than those used for antitumor effects, HDAC inhibitors can modulate inflammation primarily by reducing cytokine production as well as immune responses (118-122). Indeed, it has been reported that Suberoylanilide hydroxamic acid can suppress acute graft versus host disease afterallergenic bone marrow transplantation, in part, by reducing proinflammatory cytokine production (121) (123).

HDAC inhibitors have also been shown to reduce in mouse models the severity of inflammatory bowel disease (124) and of other inflammatory and immune-mediated diseases such as lupus (120,122,125). Thus, inhibitors of HDAC represent a new class of therapeutic options for these diseases. The attractive aspect of HDACi's is that they are orally active, and low concentrations are effective in reducing inflammation in humans (126) and animal models (127). One unifying property of all HDAC inhibitors is the reduction in cytokine production as well as inhibition of cytokine signaling.

Givinostat (ITF2357) and treatment of a wide spectrum of diseases

Among the new synthetic HDAC inhibitors, the class I/II orally active Givinostat (ITF2357) is widely used for a broad spectrum of diseases. As demonstrated by Leoni et al., Givinostat is effective in reducing inflammatory cytokines *in vitro* and *in vivo* models (128) having a potential and important role in treatment of chronic inflammatory and degenerative diseases. The molecular mechanisms of action related to anti-inflammatory properties are broad. Because HDACi's increase gene expression, one possible mechanism of action is the induction of genes that are themselves inhibitors of inflammation: transforming growth factor (TGF)-β, IL-10 or IL-1 receptor antagonist. Moreover, Givinostat, as many other HDAC inhibitors has the property to increase the acetylation of non-

histonic proteins such as transcription factors. STAT3, for example, suppresses inflammatory cytokines such as INFγ and IL-17. Activationof STAT-3 can take place by acetylation, and it has been reported that Givinostat induces acetylation of STAT-3 in dendritic cells at concentrations that are achievable in humans (129). Givinostat has also an effect in reducing chemokine receptors such as CXCR4 in PBMCs of healty donors (130), thus impairing the response to inflammation. Moreover, Givinostat is prove to be protective on cartilage catabolism in a mouse model of non-autoimmune inflammatory arthritis induced by Streptococcus pyogenes cell walls (131) and provides benefits in treatment of GvHD after allogeneic bone marrow transplantation, probably due to decreased cytokine production (129). In oncology, the activity of Givinostat was studied on multiple myeloma and acute myelogenous leukemia cells. In particular, in these tumors, Givinostat induced hyperacetylation of histone H3, H4 and tubulin and caused apoptosis at an IC50 of 0.2 µM *in vitro* (132). *In vivo* in mice models, Givinostat, at a dose of 10 mg/kg, significantly prolonged survival of severe combined immunodeficient mice inoculated with acute myelogenous leukemia cells and inhibited the production of growth and angiogenic factors by bone marrow stromal cells, in particular IL-6 and VEGF (132). These results suggest that part of the mechanism of action of HDACi's in these diseases may be due to a reduction in cytokine production, since these hematopoietic malignancies are driven by IL-1β and IL-6 as growth factors (52,133-135).

In addition, Givinostat down-modulated the IL-6 receptor α transcript and protein in KMS18 myeloma cell lines and freshly isolated patient cells (136). The decrease in the IL-6 receptor expression was accompanied by decreased signaling, as measured by STAT-3 phosphorylation. These data support the previous studies that ITF2357 inhibits cytokine-mediated myeloma cell growth and survival.

A phase II, multiple-dose clinical trial in 19 patients with relapsed or progressive multiple myeloma was carried out but Givinostat showed a modest clinical benefit (137). It appears that the optimal use of HDACi's in multiple myeloma would be in smoldering myeloma, where the combination of IL-1β blockade by Givinostat plus Dexamethasone significantly delays or even prevents the progression to full-blown multiple myeloma (133). Givinostat exerts efficacy also in myeloproliferative disorders. The efficacy of Givinostat in 12 patients with polycythemia vera (PV) and in 16 patients with myelofibrosis, bearing the JAK2V617F mutation, has been reported (109). Givinostat was well tolerated and could induce hematological response in most PV patients alone or in combination with hydroxycarbamide, expecially in patients unresponsive to hydroxycarbamide monotherapy (138). *In vitro*, the clonogenic activity of JAK2 (V617F) mutated cells was reduced by low concentrations of 1–10 nmol/L of Givinostat, which is 100- to 250-fold lower than concentrations that are traditionally required to inhibit the growth of tumor cells lacking this mutation. By Western blotting, Givinostat resulted in the

disappearance of total and phosphorylated pSTAT5 and pSTAT3 (139). Furthermore, Calzada et al demonstrated that Givinostat was able to modulate the hematopoietic transcription factor NFE2 and C-MYB in JAK2 (V617F) subset *in vitro* and to synergize with Hydroxyurea to efficiently kill JAK2 (V617F) cell lines (140).

Together, these studies provide evidence that, in some hematopoietic disorders, the efficacy of HDACi's is in part due to a reduction in either cytokine production or cytokine signaling. Clinically, acute myelogenous leukemia, polycythemia vera and multiple myeloma are associated with markers of systemic inflammation such as recurrent fevers. The low concentrations effective *in vitro* and *in vivo* also support the concept that the cytokine-reducing properties of HDACi's contribute to controlling disease activity rather than direct tumor cell death. To accomplish tumor cell death, Dexamethasone or another proapoptotic regimen is required. To date, efficacy of Givinostat in lymphoblastic leukemia have not been jet investigated even if other HDAC inhibitors have been already demonstrated to be effective alone or in combination with proteasome inhibitors (Bortezomib) in *in vitro* and *in vivo* models of ALL (141).

Xenografts and Genetic Mouse Models to Study High-Risk Leukemias

Genetic engineered mouse models mimic known genetic aberrations and allow investigating their importance for the

biology of the tumor. In the field of leukemia, only a few models could be established. There is a model for BCR-ABL ALL, where the transduction of *arf*-null murine bone marrow progenitors with BCR-ABL was enough to induce lymphoblastic leukemia. These leukemias were highly tumorigenic in serial transplantations and resistant to imatinib in presence of cytokines (142).

There are also models for MLL-AF9 leukemias, which result in myeloid, but not lymphoid leukemias in mice (143,144). Other models cover T-cell lymphomas, B-lymphomas, CML and AML (145,146), illustrating the variety of tumors that can be modeled but also showing the lack of a representative model for high-risk B-ALL. A general disadvantage of genetic models is that they investigate single genetic aberrations and not the full genetic complexity. Therefore, they represent only a minor fraction of patients. In future, it will be a challenge as it is time consuming, but necessary to generate more genetic mouse models for the characterization of relevant genetic aberrations and their role in tumorigenesis and drug resistance.

For preclinical drug testing, xenografts have been more widely used. In that approach, primary patient material is transplanted into immunodeficient mice and is then recapitulating the original leukemia. The advantages of xenografts are – that the starting material is usually from advanced cancers, - that the tumors represent the original tumor in the patient, including the genetic complexity – and that you can test multiple drugs in different settings against the same set of cells or against different tumors

from different patients. Therefore, by using xenograft models all relevant patient groups can be modeled.

The recipient mice must be immunodeficient to allow the engraftment of human cells without developing an immune response against them. Progress in the development of humanized mouse models was advanced by the discovery of the severe combined immunodeficiency (scid) gene mutation, which occurs spontaneously on the CB17 strain background. The CB17-scid mouse was the first immunodeficient mouse model shown to engraft with human haematopoietic cells. The mutation involves *Prkdc*^{scid} (protein kinase, DNA activated, catalytic polypeptide) gene coding for an enzyme involved in rearrangement of Immunoglobulins loci and TCR genes. This mutation causes the block of lymphocyte maturation and the absence of mature B and T cells. These mice were shown to support the engraftment of some transplantable human haematological neoplasms, but tumour growth was limited by the high levels of host NK-cell activity (147). Another important advance in the development of humanized mice came from crossing mice with the scid mutation onto the non-obese diabetic (NOD) strain, which led to improved engraftment of human haematopoietic cells owing to decreased natural killer (NK)-cell activity and decreased innate immunity. A breakthrough in the effectiveness of humanized mice came from crossing immunodeficient mice homozygous for targeted mutations at the interleukin-2 receptor (IL-2R) γ-chain locus (Il2rg; also known as the common cytokine receptor γ-chain, γc,

part of the high affinity receptor for different cytokines IL-2, IL-4, IL-7, IL-9, IL-15 e IL-21, required for their cellular signaling) onto the NOD/LtSz-scid, NOD/Shi-scid, NOD-Rag1–/– (recombination-activating gene-1-deficient) and BALB/c-Rag2–/– strain backgrounds, also termed NSG. This resulted in mouse strains with a complete absence of NK-cell activity, further decreases in innate immunity and a greatly increased ability to support the engraftment of human hematopoietic cells and tissues (52,148,149).

Additional crosses have generated scid or Rag1–/– mice expressing transgenes or mutant alleles, to produce mouse models of human diseases for use in studying regenerative medicine.

For human leukemia studies, the NOD/SCID and NSG model is widely used. In this model, once engrafted in bone marrow or other hematopoietic organs, leukemia cells recapitulate the main characteristics of human leukemia as phenotype, cytomorfology, antigenic profile, clonality and caryotype (150,151). Blast growth and expansion in hematopoietic compartment of the mouse leads to the typical symptoms of the disease in the mouse (leukocytosis, splenomegaly, lethargy and anorexia) and finally to the death of the animal. In the last decades, the xenograft models have been employed for studying the leukemogenesis biological processes allowing the in vivo expansion of leukemic cells generating a powerful source of leukemic stem cells that could be used for further

transplantation and represent an important tool for efficacy studies of novel therapies.

REFERENCES

1. Pui CH, Jeha S. New therapeutic strategies for the treatment of acute lymphoblastic leukaemia. Nature reviews Drug discovery 2007;6(2):149-65.
2. Pui CH, Relling MV, Downing JR. Acute lymphoblastic leukemia. N Engl J Med 2004;350(15):1535-48.
3. Nordgren A. Hidden aberrations diagnosed by interphase fluorescence in situ hybridisation and spectral karyotyping in childhood acute lymphoblastic leukaemia. Leuk Lymphoma 2003;44(12):2039-53.
4. Kaspers GJ, Smets LA, Pieters R, Van Zantwijk CH, Van Wering ER, Veerman AJ. Favorable prognosis of hyperdiploid common acute lymphoblastic leukemia may be explained by sensitivity to antimetabolites and other drugs: results of an in vitro study. Blood 1995;85(3):751-6.
5. Mullighan CG, Downing JR. Global genomic characterization of acute lymphoblastic leukemia. Semin Hematol 2009;46(1):3-15.
6. Mullighan CG, Su X, Zhang J, Radtke I, Phillips LA, Miller CB, et al. Deletion of IKZF1 and prognosis in acute lymphoblastic leukemia. N Engl J Med 2009;360(5):470-80.
7. Mullighan CG, Miller CB, Radtke I, Phillips LA, Dalton J, Ma J, et al. BCR-ABL1 lymphoblastic leukaemia is characterized by the deletion of Ikaros. Nature 2008;453(7191):110-4.
8. Mullighan CG, Phillips LA, Su X, Ma J, Miller CB, Shurtleff SA, et al. Genomic analysis of the clonal origins of relapsed acute lymphoblastic leukemia. Science 2008;322(5906):1377-80.
9. Mullighan CG, Goorha S, Radtke I, Miller CB, Coustan-Smith E, Dalton JD, et al. Genome-wide analysis of genetic alterations in acute lymphoblastic leukaemia. Nature 2007;446(7137):758-64.
10. Harvey RC, Mullighan CG, Chen IM, Wharton W, Mikhail FM, Carroll AJ, et al. Rearrangement of CRLF2 is associated with mutation of JAK kinases, alteration of IKZF1, Hispanic/Latino ethnicity, and a poor outcome in pediatric B-progenitor acute lymphoblastic leukemia. Blood 2010;115(26):5312-21.
11. Armstrong SA, Look AT. Molecular genetics of acute lymphoblastic leukemia. J Clin Oncol 2005;23(26):6306-15.

12. de Boer J, Yeung J, Ellu J, Ramanujachar R, Bornhauser B, Solarska O, et al. The E2A-HLF oncogenic fusion protein acts through Lmo2 and Bcl-2 to immortalize hematopoietic progenitors. Leukemia 2011;25(2):321-30.
13. Okuya M, Kurosawa H, Kikuchi J, Furukawa Y, Matsui H, Aki D, et al. Up-regulation of survivin by the E2A-HLF chimera is indispensable for the survival of t(17;19)-positive leukemia cells. J Biol Chem 2010;285(3):1850-60.
14. Owens BM, Hawley RG. HOX and non-HOX homeobox genes in leukemic hematopoiesis. Stem cells 2002;20(5):364-79.
15. Pui CH, Chessells JM, Camitta B, Baruchel A, Biondi A, Boyett JM, et al. Clinical heterogeneity in childhood acute lymphoblastic leukemia with 11q23 rearrangements. Leukemia 2003;17(4):700-6.
16. Harewood L, Robinson H, Harris R, Al-Obaidi MJ, Jalali GR, Martineau M, et al. Amplification of AML1 on a duplicated chromosome 21 in acute lymphoblastic leukemia: a study of 20 cases. Leukemia 2003;17(3):547-53.
17. Hu Y, Liu Y, Pelletier S, Buchdunger E, Warmuth M, Fabbro D, et al. Requirement of Src kinases Lyn, Hck and Fgr for BCR-ABL1-induced B-lymphoblastic leukemia but not chronic myeloid leukemia. Nat Genet 2004;36(5):453-61.
18. Ross ME, Zhou X, Song G, Shurtleff SA, Girtman K, Williams WK, et al. Classification of pediatric acute lymphoblastic leukemia by gene expression profiling. Blood 2003;102(8):2951-9.
19. Meijerink JP, den Boer ML, Pieters R. New genetic abnormalities and treatment response in acute lymphoblastic leukemia. Semin Hematol 2009;46(1):16-23.
20. Harrison CJ, Haas O, Harbott J, Biondi A, Stanulla M, Trka J, et al. Detection of prognostically relevant genetic abnormalities in childhood B-cell precursor acute lymphoblastic leukaemia: recommendations from the Biology and Diagnosis Committee of the International Berlin-Frankfurt-Munster study group. Br J Haematol 2010;151(2):132-42.
21. Szczepanski T, van der Velden VH, van Dongen JJ. Flow-cytometric immunophenotyping of normal and malignant lymphocytes. Clinical chemistry and laboratory medicine : CCLM / FESCC 2006;44(7):775-96.
22. Harrison CJ. Acute lymphoblastic leukaemia. Best Practice & Research Clinical Haematology 2001;14(3):593-607.
23. Szczepanski T, Harrison CJ, van Dongen JJ. Genetic aberrations in paediatric acute leukaemias and implications for management of patients. Lancet Oncol 2010;11(9):880-9.

24. Basso G, Veltroni M, Valsecchi MG, Dworzak MN, Ratei R, Silvestri D, et al. Risk of relapse of childhood acute lymphoblastic leukemia is predicted by flow cytometric measurement of residual disease on day 15 bone marrow. J Clin Oncol 2009;27(31):5168-74.
25. van Dongen JJ, Seriu T, Panzer-Grumayer ER, Biondi A, Pongers-Willemse MJ, Corral L, et al. Prognostic value of minimal residual disease in acute lymphoblastic leukaemia in childhood. Lancet 1998;352(9142):1731-8.
26. Schrappe M. Evolution of BFM trials for childhood ALL. Annals of hematology 2004;83 Suppl 1:S121-3.
27. Flohr T, Schrauder A, Cazzaniga G, Panzer-Grumayer R, van der Velden V, Fischer S, et al. Minimal residual disease-directed risk stratification using real-time quantitative PCR analysis of immunoglobulin and T-cell receptor gene rearrangements in the international multicenter trial AIEOP-BFM ALL 2000 for childhood acute lymphoblastic leukemia. Leukemia 2008;22(4):771-82.
28. Ratei R, Basso G, Dworzak M, Gaipa G, Veltroni M, Rhein P, et al. Monitoring treatment response of childhood precursor B-cell acute lymphoblastic leukemia in the AIEOP-BFM-ALL 2000 protocol with multiparameter flow cytometry: predictive impact of early blast reduction on the remission status after induction. Leukemia 2009;23(3):528-34.
29. Russell LJ, Capasso M, Vater I, Akasaka T, Bernard OA, Calasanz MJ, et al. Deregulated expression of cytokine receptor gene, CRLF2, is involved in lymphoid transformation in B-cell precursor acute lymphoblastic leukemia. Blood 2009;114(13):2688-98.
30. Mullighan CG, Collins-Underwood JR, Phillips LA, Loudin MG, Liu W, Zhang J, et al. Rearrangement of CRLF2 in B-progenitor- and Down syndrome-associated acute lymphoblastic leukemia. Nat Genet 2009;41(11):1243-6.
31. Heim MH. The Jak-STAT pathway: cytokine signalling from the receptor to the nucleus. Journal of receptor and signal transduction research 1999;19(1-4):75-120.
32. Pandey A, Ozaki K, Baumann H, Levin SD, Puel A, Farr AG, et al. Cloning of a receptor subunit required for signaling by thymic stromal lymphopoietin. Nat Immunol 2000;1(1):59-64.
33. Tonozuka Y, Fujio K, Sugiyama T, Nosaka T, Hirai M, Kitamura T. Molecular cloning of a human novel type I cytokine receptor related to delta1/TSLPR. Cytogenet Cell Genet 2001;93(1-2):23-5.

34. Zhang W, Wang J, Wang Q, Chen G, Zhang J, Chen T, et al. Identification of a novel type I cytokine receptor CRL2 preferentially expressed by human dendritic cells and activated monocytes. Biochem Biophys Res Commun 2001;281(4):878-83.
35. Rochman Y, Leonard WJ. Thymic stromal lymphopoietin: a new cytokine in asthma. Current opinion in pharmacology 2008;8(3):249-54.
36. Roll JD, Reuther GW. CRLF2 and JAK2 in B-progenitor acute lymphoblastic leukemia: a novel association in oncogenesis. Cancer Res 2010;70(19):7347-52.
37. Demehri S, Liu Z, Lee J, Lin MH, Crosby SD, Roberts CJ, et al. Notch-deficient skin induces a lethal systemic B-lymphoproliferative disorder by secreting TSLP, a sentinel for epidermal integrity. PLoS Biol 2008;6(5):e123.
38. Tal N, Shochat C, Geron I, Bercovich D, Izraeli S. Interleukin 7 and thymic stromal lymphopoietin: from immunity to leukemia. Cellular and molecular life sciences : CMLS 2014;71(3):365-78.
39. Thomas C, Moraga I, Levin D, Krutzik PO, Podoplelova Y, Trejo A, et al. Structural linkage between ligand discrimination and receptor activation by type I interferons. Cell 2011;146(4):621-32.
40. Ihle JN. The Janus protein tyrosine kinase family and its role in cytokine signaling. Adv Immunol 1995;60:1-35.
41. Feng J, Witthuhn BA, Matsuda T, Kohlhuber F, Kerr IM, Ihle JN. Activation of Jak2 catalytic activity requires phosphorylation of Y1007 in the kinase activation loop. Mol Cell Biol 1997;17(5):2497-501.
42. Saharinen P, Takaluoma K, Silvennoinen O. Regulation of the Jak2 tyrosine kinase by its pseudokinase domain. Mol Cell Biol 2000;20(10):3387-95.
43. Gnanasambandan K, Magis A, Sayeski PP. The constitutive activation of Jak2-V617F is mediated by a pi stacking mechanism involving phenylalanines 595 and 617. Biochemistry 2010;49(46):9972-84.
44. Ungureanu D, Wu J, Pekkala T, Niranjan Y, Young C, Jensen ON, et al. The pseudokinase domain of JAK2 is a dual-specificity protein kinase that negatively regulates cytokine signaling. Nature structural & molecular biology 2011;18(9):971-6.
45. Bandaranayake RM, Ungureanu D, Shan Y, Shaw DE, Silvennoinen O, Hubbard SR. Crystal structures of the JAK2

pseudokinase domain and the pathogenic mutant V617F. Nature structural & molecular biology 2012;19(8):754-9.
46. Lucet IS, Fantino E, Styles M, Bamert R, Patel O, Broughton SE, et al. The structural basis of Janus kinase 2 inhibition by a potent and specific pan-Janus kinase inhibitor. Blood 2006;107(1):176-83.
47. Boggon TJ, Li Y, Manley PW, Eck MJ. Crystal structure of the Jak3 kinase domain in complex with a staurosporine analog. Blood 2005;106(3):996-1002.
48. Mazurkiewicz-Munoz AM, Argetsinger LS, Kouadio JL, Stensballe A, Jensen ON, Cline JM, et al. Phosphorylation of JAK2 at serine 523: a negative regulator of JAK2 that is stimulated by growth hormone and epidermal growth factor. Mol Cell Biol 2006;26(11):4052-62.
49. Robertson SA, Koleva RI, Argetsinger LS, Carter-Su C, Marto JA, Feener EP, et al. Regulation of Jak2 function by phosphorylation of Tyr317 and Tyr637 during cytokine signaling. Mol Cell Biol 2009;29(12):3367-78.
50. Feener EP, Rosario F, Dunn SL, Stancheva Z, Myers MG, Jr. Tyrosine phosphorylation of Jak2 in the JH2 domain inhibits cytokine signaling. Mol Cell Biol 2004;24(11):4968-78.
51. Argetsinger LS, Kouadio JL, Steen H, Stensballe A, Jensen ON, Carter-Su C. Autophosphorylation of JAK2 on tyrosines 221 and 570 regulates its activity. Mol Cell Biol 2004;24(11):4955-67.
52. Argetsinger LS, Stuckey JA, Robertson SA, Koleva RI, Cline JM, Marto JA, et al. Tyrosines 868, 966, and 972 in the kinase domain of JAK2 are autophosphorylated and required for maximal JAK2 kinase activity. Molecular endocrinology 2010;24(5):1062-76.
53. LaFave LM, Levine RL. JAK2 the future: therapeutic strategies for JAK-dependent malignancies. Trends in pharmacological sciences 2012;33(11):574-82.
54. Dawson MA, Bannister AJ, Gottgens B, Foster SD, Bartke T, Green AR, et al. JAK2 phosphorylates histone H3Y41 and excludes HP1alpha from chromatin. Nature 2009;461(7265):819-22.
55. Rui L, Emre NC, Kruhlak MJ, Chung HJ, Steidl C, Slack G, et al. Cooperative epigenetic modulation by cancer amplicon genes. Cancer Cell 2010;18(6):590-605.
56. Brender C, Lovato P, Sommer VH, Woetmann A, Mathiesen AM, Geisler C, et al. Constitutive SOCS-3 expression protects T-cell lymphoma against growth inhibition by IFNalpha. Leukemia 2005;19(2):209-13.

57. Rudd CE. Lnk adaptor: novel negative regulator of B cell lymphopoiesis. Science's STKE : signal transduction knowledge environment 2001;2001(85):pe1.
58. Lu X, Levine R, Tong W, Wernig G, Pikman Y, Zarnegar S, et al. Expression of a homodimeric type I cytokine receptor is required for JAK2V617F-mediated transformation. Proc Natl Acad Sci U S A 2005;102(52):18962-7.
59. Tong W, Lodish HF. Lnk inhibits Tpo-mpl signaling and Tpo-mediated megakaryocytopoiesis. J Exp Med 2004;200(5):569-80.
60. Velazquez L, Cheng AM, Fleming HE, Furlonger C, Vesely S, Bernstein A, et al. Cytokine signaling and hematopoietic homeostasis are disrupted in Lnk-deficient mice. J Exp Med 2002;195(12):1599-611.
61. Oh ST, Simonds EF, Jones C, Hale MB, Goltsev Y, Gibbs KD, Jr., et al. Novel mutations in the inhibitory adaptor protein LNK drive JAK-STAT signaling in patients with myeloproliferative neoplasms. Blood 2010;116(6):988-92.
62. Pardanani A, Lasho T, Finke C, Oh ST, Gotlib J, Tefferi A. LNK mutation studies in blast-phase myeloproliferative neoplasms, and in chronic-phase disease with TET2, IDH, JAK2 or MPL mutations. Leukemia 2010;24(10):1713-8.
63. Buchner M, Swaminathan S, Chen Z, Muschen M. Mechanisms of pre-B-cell receptor checkpoint control and its oncogenic subversion in acute lymphoblastic leukemia. Immunol Rev 2015;263(1):192-209.
64. Dyer MJ, Akasaka T, Capasso M, Dusanjh P, Lee YF, Karran EL, et al. Immunoglobulin heavy chain locus chromosomal translocations in B-cell precursor acute lymphoblastic leukemia: rare clinical curios or potent genetic drivers? Blood 2010;115(8):1490-9.
65. Storlazzi CT, Albano F, Lo Cunsolo C, Doglioni C, Guastadisegni MC, Impera L, et al. Upregulation of the SOX5 by promoter swapping with the P2RY8 gene in primary splenic follicular lymphoma. Leukemia 2007;21(10):2221-5.
66. Yoda A, Yoda Y, Chiaretti S, Bar-Natan M, Mani K, Rodig SJ, et al. Functional screening identifies CRLF2 in precursor B-cell acute lymphoblastic leukemia. Proc Natl Acad Sci U S A 2010;107(1):252-7.
67. Ugo V, Marzac C, Teyssandier I, Larbret F, Lecluse Y, Debili N, et al. Multiple signaling pathways are involved in erythropoietin-independent differentiation of erythroid progenitors in polycythemia vera. Exp Hematol 2004;32(2):179-87.

68. Garcon L, Rivat C, James C, Lacout C, Camara-Clayette V, Ugo V, et al. Constitutive activation of STAT5 and Bcl-xL overexpression can induce endogenous erythroid colony formation in human primary cells. Blood 2006;108(5):1551-4.
69. Bercovich D, Ganmore I, Scott LM, Wainreb G, Birger Y, Elimelech A, et al. Mutations of JAK2 in acute lymphoblastic leukaemias associated with Down's syndrome. Lancet 2008;372(9648):1484-92.
70. Flex E, Petrangeli V, Stella L, Chiaretti S, Hornakova T, Knoops L, et al. Somatically acquired JAK1 mutations in adult acute lymphoblastic leukemia. J Exp Med 2008;205(4):751-8.
71. Malinge S, Ben-Abdelali R, Settegrana C, Radford-Weiss I, Debre M, Beldjord K, et al. Novel activating JAK2 mutation in a patient with Down syndrome and B-cell precursor acute lymphoblastic leukemia. Blood 2007;109(5):2202-4.
72. Mullighan CG, Zhang J, Harvey RC, Collins-Underwood JR, Schulman BA, Phillips LA, et al. JAK mutations in high-risk childhood acute lymphoblastic leukemia. Proc Natl Acad Sci U S A 2009;106(23):9414-8.
73. Chen IM, Harvey RC, Mullighan CG, Gastier-Foster J, Wharton W, Kang H, et al. Outcome modeling with CRLF2, IKZF1, JAK, and minimal residual disease in pediatric acute lymphoblastic leukemia: a Children's Oncology Group study. Blood 2012;119(15):3512-22.
74. Lu N, Wang YH, Arima K, Hanabuchi S, Liu YJ. TSLP and IL-7 use two different mechanisms to regulate human CD4+ T cell homeostasis. J Exp Med 2009;206(10):2111-9.
75. Scheeren FA, van Lent AU, Nagasawa M, Weijer K, Spits H, Legrand N, et al. Thymic stromal lymphopoietin induces early human B-cell proliferation and differentiation. Eur J Immunol 2010;40(4):955-65.
76. Shochat C, Tal N, Bandapalli OR, Palmi C, Ganmore I, te Kronnie G, et al. Gain-of-function mutations in interleukin-7 receptor-alpha (IL7R) in childhood acute lymphoblastic leukemias. J Exp Med 2011;208(5):901-8.
77. Ritz O, Guiter C, Castellano F, Dorsch K, Melzner J, Jais JP, et al. Recurrent mutations of the STAT6 DNA binding domain in primary mediastinal B-cell lymphoma. Blood 2009;114(6):1236-42.
78. Koskela HL, Eldfors S, Ellonen P, van Adrichem AJ, Kuusanmaki H, Andersson EI, et al. Somatic STAT3 mutations in large granular lymphocytic leukemia. N Engl J Med 2012;366(20):1905-13.

79. Den Boer ML, van Slegtenhorst M, De Menezes RX, Cheok MH, Buijs-Gladdines JG, Peters ST, et al. A subtype of childhood acute lymphoblastic leukaemia with poor treatment outcome: a genome-wide classification study. Lancet Oncol 2009;10(2):125-34.
80. Maude SL, Tasian SK, Vincent T, Hall JW, Sheen C, Roberts KG, et al. Targeting JAK1/2 and mTOR in murine xenograft models of Ph-like acute lymphoblastic leukemia. Blood 2012;120(17):3510-8.
81. van der Veer A, Waanders E, Pieters R, Willemse ME, Van Reijmersdal SV, Russell LJ, et al. Independent prognostic value of BCR-ABL1-like signature and IKZF1 deletion, but not high CRLF2 expression, in children with B-cell precursor ALL. Blood 2013;122(15):2622-9.
82. te Kronnie G, Silvestri D, Vendramini E, Fazio G, Locatelli F, Conter V, et al. Philadelphia-Like Signature In Childhood Acute Lymphoblastic Leukemia: The AIEOP Experience. Blood 2013;122(21).
83. Roberts KG, Li Y, Payne-Turner D, Harvey RC, Yang YL, Pei D, et al. Targetable kinase-activating lesions in Ph-like acute lymphoblastic leukemia. N Engl J Med 2014;371(11):1005-15.
84. Roberts KG, Pei D, Campana D, Payne-Turner D, Li Y, Cheng C, et al. Outcomes of children with BCR-ABL1-like acute lymphoblastic leukemia treated with risk-directed therapy based on the levels of minimal residual disease. J Clin Oncol 2014;32(27):3012-20.
85. Roberts KG, Morin RD, Zhang J, Hirst M, Zhao Y, Su X, et al. Genetic alterations activating kinase and cytokine receptor signaling in high-risk acute lymphoblastic leukemia. Cancer Cell 2012;22(2):153-66.
86. Weston BW, Hayden MA, Roberts KG, Bowyer S, Hsu J, Fedoriw G, et al. Tyrosine kinase inhibitor therapy induces remission in a patient with refractory EBF1-PDGFRB-positive acute lymphoblastic leukemia. J Clin Oncol 2013;31(25):e413-6.
87. Sherman SL, Allen EG, Bean LH, Freeman SB. Epidemiology of Down syndrome. Mental retardation and developmental disabilities research reviews 2007;13(3):221-7.
88. Hasle H. Pattern of malignant disorders in individuals with Down's syndrome. Lancet Oncol 2001;2(7):429-36.
89. Izraeli S, Rainis L, Hertzberg L, Smooha G, Birger Y. Trisomy of chromosome 21 in leukemogenesis. Blood cells, molecules & diseases 2007;39(2):156-9.

90. Taub JW. Relationship of chromosome 21 and acute leukemia in children with Down syndrome. Journal of pediatric hematology/oncology 2001;23(3):175-8.
91. Day SM, Strauss DJ, Shavelle RM, Reynolds RJ. Mortality and causes of death in persons with Down syndrome in California. Developmental medicine and child neurology 2005;47(3):171-6.
92. Hill DA, Gridley G, Cnattingius S, Mellemkjaer L, Linet M, Adami HO, et al. Mortality and cancer incidence among individuals with Down syndrome. Archives of internal medicine 2003;163(6):705-11.
93. Sussan TE, Yang A, Li F, Ostrowski MC, Reeves RH. Trisomy represses Apc(Min)-mediated tumours in mouse models of Down's syndrome. Nature 2008;451(7174):73-5.
94. Hertzberg L, Vendramini E, Ganmore I, Cazzaniga G, Schmitz M, Chalker J, et al. Down syndrome acute lymphoblastic leukemia, a highly heterogeneous disease in which aberrant expression of CRLF2 is associated with mutated JAK2: a report from the International BFM Study Group. Blood 2010;115(5):1006-17.
95. Forestier E, Izraeli S, Beverloo B, Haas O, Pession A, Michalova K, et al. Cytogenetic features of acute lymphoblastic and myeloid leukemias in pediatric patients with Down syndrome: an iBFM-SG study. Blood 2008;111(3):1575-83.
96. Kearney L, Gonzalez De Castro D, Yeung J, Procter J, Horsley SW, Eguchi-Ishimae M, et al. Specific JAK2 mutation (JAK2R683) and multiple gene deletions in Down syndrome acute lymphoblastic leukemia. Blood 2009;113(3):646-8.
97. Pardanani A, Gotlib JR, Jamieson C, Cortes JE, Talpaz M, Stone RM, et al. Safety and efficacy of TG101348, a selective JAK2 inhibitor, in myelofibrosis. J Clin Oncol 2011;29(7):789-96.
98. Santos FP, Kantarjian HM, Jain N, Manshouri T, Thomas DA, Garcia-Manero G, et al. Phase 2 study of CEP-701, an orally available JAK2 inhibitor, in patients with primary or post-polycythemia vera/essential thrombocythemia myelofibrosis. Blood 2010;115(6):1131-6.
99. Verstovsek S, Kantarjian H, Mesa RA, Pardanani AD, Cortes-Franco J, Thomas DA, et al. Safety and efficacy of INCB018424, a JAK1 and JAK2 inhibitor, in myelofibrosis. N Engl J Med 2010;363(12):1117-27.

100. Tefferi A. Challenges facing JAK inhibitor therapy for myeloproliferative neoplasms. N Engl J Med 2012;366(9):844-6.
101. Verstovsek S. Janus-activated kinase 2 inhibitors: a new era of targeted therapies providing significant clinical benefit for Philadelphia chromosome-negative myeloproliferative neoplasms. J Clin Oncol 2011;29(7):781-3.
102. Verstovsek S, Mesa RA, Gotlib J, Levy RS, Gupta V, DiPersio JF, et al. A double-blind, placebo-controlled trial of ruxolitinib for myelofibrosis. N Engl J Med 2012;366(9):799-807.
103. Harrison C, Kiladjian JJ, Al-Ali HK, Gisslinger H, Waltzman R, Stalbovskaya V, et al. JAK inhibition with ruxolitinib versus best available therapy for myelofibrosis. N Engl J Med 2012;366(9):787-98.
104. Maude SL, Dolai S, Delgado-Martin C, Vincent T, Robbins A, Selvanathan A, et al. Efficacy of JAK/STAT pathway inhibition in murine xenograft models of early T-cell precursor (ETP) acute lymphoblastic leukemia. Blood 2015;125(11):1759-67.
105. Springuel L, Hornakova T, Losdyck E, Lambert F, Leroy E, Constantinescu SN, et al. Cooperating JAK1 and JAK3 mutants increase resistance to JAK inhibitors. Blood 2014;124(26):3924-31.
106. Lu M, Wang J, Li Y, Berenzon D, Wang X, Mascarenhas J, et al. Treatment with the Bcl-xL inhibitor ABT-737 in combination with interferon alpha specifically targets JAK2V617F-positive polycythemia vera hematopoietic progenitor cells. Blood 2010;116(20):4284-7.
107. Nelson EA, Walker SR, Weisberg E, Bar-Natan M, Barrett R, Gashin LB, et al. The STAT5 inhibitor pimozide decreases survival of chronic myelogenous leukemia cells resistant to kinase inhibitors. Blood 2011;117(12):3421-9.
108. Marubayashi S, Koppikar P, Taldone T, Abdel-Wahab O, West N, Bhagwat N, et al. HSP90 is a therapeutic target in JAK2-dependent myeloproliferative neoplasms in mice and humans. J Clin Invest 2010;120(10):3578-93.
109. Rambaldi A, Dellacasa CM, Finazzi G, Carobbio A, Ferrari ML, Guglielmelli P, et al. A pilot study of the Histone-Deacetylase inhibitor Givinostat in patients with JAK2V617F positive chronic myeloproliferative neoplasms. Br J Haematol 2010;150(4):446-55.
110. Weigert O, Lane AA, Bird L, Kopp N, Chapuy B, van Bodegom D, et al. Genetic resistance to JAK2 enzymatic inhibitors is overcome by HSP90 inhibition. J Exp Med 2012;209(2):259-73.

111. Narlikar GJ, Fan HY, Kingston RE. Cooperation between complexes that regulate chromatin structure and transcription. Cell 2002;108(4):475-87.
112. Johnstone RW. Histone-deacetylase inhibitors: novel drugs for the treatment of cancer. Nature reviews Drug discovery 2002;1(4):287-99.
113. Kelly WK, O'Connor OA, Krug LM, Chiao JH, Heaney M, Curley T, et al. Phase I study of an oral histone deacetylase inhibitor, suberoylanilide hydroxamic acid, in patients with advanced cancer. J Clin Oncol 2005;23(17):3923-31.
114. Butler LM, Zhou X, Xu WS, Scher HI, Rifkind RA, Marks PA, et al. The histone deacetylase inhibitor SAHA arrests cancer cell growth, up-regulates thioredoxin-binding protein-2, and down-regulates thioredoxin. Proc Natl Acad Sci U S A 2002;99(18):11700-5.
115. Della Ragione F, Criniti V, Della Pietra V, Borriello A, Oliva A, Indaco S, et al. Genes modulated by histone acetylation as new effectors of butyrate activity. FEBS letters 2001;499(3):199-204.
116. Van Lint C, Emiliani S, Verdin E. The expression of a small fraction of cellular genes is changed in response to histone hyperacetylation. Gene expression 1996;5(4-5):245-53.
117. Suzuki H, Gabrielson E, Chen W, Anbazhagan R, van Engeland M, Weijenberg MP, et al. A genomic screen for genes upregulated by demethylation and histone deacetylase inhibition in human colorectal cancer. Nat Genet 2002;31(2):141-9.
118. Leoni F, Zaliani A, Bertolini G, Porro G, Pagani P, Pozzi P, et al. The antitumor histone deacetylase inhibitor suberoylanilide hydroxamic acid exhibits antiinflammatory properties via suppression of cytokines. Proc Natl Acad Sci U S A 2002;99(5):2995-3000.
119. Skov S, Rieneck K, Bovin LF, Skak K, Tomra S, Michelsen BK, et al. Histone deacetylase inhibitors: a new class of immunosuppressors targeting a novel signal pathway essential for CD154 expression. Blood 2003;101(4):1430-8.
120. Mishra N, Reilly CM, Brown DR, Ruiz P, Gilkeson GS. Histone deacetylase inhibitors modulate renal disease in the MRL-lpr/lpr mouse. J Clin Invest 2003;111(4):539-52.
121. Reddy P, Maeda Y, Hotary K, Liu C, Reznikov LL, Dinarello CA, et al. Histone deacetylase inhibitor suberoylanilide hydroxamic acid reduces acute graft-versus-host disease and preserves graft-versus-leukemia effect. Proc Natl Acad Sci U S A 2004;101(11):3921-6.

122. Reilly CM, Mishra N, Miller JM, Joshi D, Ruiz P, Richon VM, et al. Modulation of renal disease in MRL/lpr mice by suberoylanilide hydroxamic acid. J Immunol 2004;173(6):4171-8.
123. Leng C, Gries M, Ziegler J, Lokshin A, Mascagni P, Lentzsch S, et al. Reduction of graft-versus-host disease by histone deacetylase inhibitor suberonylanilide hydroxamic acid is associated with modulation of inflammatory cytokine milieu and involves inhibition of STAT1. Exp Hematol 2006;34(6):776-87.
124. Glauben R, Batra A, Stroh T, Erben U, Fedke I, Lehr HA, et al. Histone deacetylases: novel targets for prevention of colitis-associated cancer in mice. Gut 2008;57(5):613-22.
125. Mishra N, Brown DR, Olorenshaw IM, Kammer GM. Trichostatin A reverses skewed expression of CD154, interleukin-10, and interferon-gamma gene and protein expression in lupus T cells. Proc Natl Acad Sci U S A 2001;98(5):2628-33.
126. Dinarello CA, Donath MY, Mandrup-Poulsen T. Role of IL-1beta in type 2 diabetes. Current opinion in endocrinology, diabetes, and obesity 2010;17(4):314-21.
127. Vojinovic J, Damjanov N, D'Urzo C, Furlan A, Susic G, Pasic S, et al. Safety and efficacy of an oral histone deacetylase inhibitor in systemic-onset juvenile idiopathic arthritis. Arthritis and rheumatism 2011;63(5):1452-8.
128. Leoni F, Fossati G, Lewis EC, Lee JK, Porro G, Pagani P, et al. The histone deacetylase inhibitor ITF2357 reduces production of pro-inflammatory cytokines in vitro and systemic inflammation in vivo. Molecular medicine 2005;11(1-12):1-15.
129. Reddy P, Sun Y, Toubai T, Duran-Struuck R, Clouthier SG, Weisiger E, et al. Histone deacetylase inhibition modulates indoleamine 2,3-dioxygenase-dependent DC functions and regulates experimental graft-versus-host disease in mice. J Clin Invest 2008;118(7):2562-73.
130. Matalon S, Rasmussen TA, Dinarello CA. Histone deacetylase inhibitors for purging HIV-1 from the latent reservoir. Molecular medicine 2011;17(5-6):466-72.
131. Joosten LA, Leoni F, Meghji S, Mascagni P. Inhibition of HDAC activity by ITF2357 ameliorates joint inflammation and prevents cartilage and bone destruction in experimental arthritis. Molecular medicine 2011;17(5-6):391-6.
132. Golay J, Cuppini L, Leoni F, Mico C, Barbui V, Domenghini M, et al. The histone deacetylase inhibitor ITF2357 has anti-leukemic activity in vitro and in vivo and inhibits IL-6 and

VEGF production by stromal cells. Leukemia 2007;21(9):1892-900.
133. Lust JA, Lacy MQ, Zeldenrust SR, Dispenzieri A, Gertz MA, Witzig TE, et al. Induction of a chronic disease state in patients with smoldering or indolent multiple myeloma by targeting interleukin 1{beta}-induced interleukin 6 production and the myeloma proliferative component. Mayo Clinic proceedings 2009;84(2):114-22.
134. Rambaldi A, Torcia M, Bettoni S, Vannier E, Barbui T, Shaw AR, et al. Modulation of cell proliferation and cytokine production in acute myeloblastic leukemia by interleukin-1 receptor antagonist and lack of its expression by leukemic cells. Blood 1991;78(12):3248-53.
135. Lust JA, Donovan KA. The role of interleukin-1 beta in the pathogenesis of multiple myeloma. Hematology/oncology clinics of North America 1999;13(6):1117-25.
136. Todoerti K, Barbui V, Pedrini O, Lionetti M, Fossati G, Mascagni P, et al. Pleiotropic anti-myeloma activity of ITF2357: inhibition of interleukin-6 receptor signaling and repression of miR-19a and miR-19b. Haematologica 2010;95(2):260-9.
137. Galli M, Salmoiraghi S, Golay J, Gozzini A, Crippa C, Pescosta N, et al. A phase II multiple dose clinical trial of histone deacetylase inhibitor ITF2357 in patients with relapsed or progressive multiple myeloma. Annals of hematology 2010;89(2):185-90.
138. Finazzi G, Vannucchi AM, Martinelli V, Ruggeri M, Nobile F, Specchia G, et al. A phase II study of Givinostat in combination with hydroxycarbamide in patients with polycythaemia vera unresponsive to hydroxycarbamide monotherapy. Br J Haematol 2013;161(5):688-94.
139. Guerini V, Barbui V, Spinelli O, Salvi A, Dellacasa C, Carobbio A, et al. The histone deacetylase inhibitor ITF2357 selectively targets cells bearing mutated JAK2(V617F). Leukemia 2008;22(4):740-7.
140. Amaru Calzada A, Todoerti K, Donadoni L, Pellicioli A, Tuana G, Gatta R, et al. The HDAC inhibitor Givinostat modulates the hematopoietic transcription factors NFE2 and C-MYB in JAK2(V617F) myeloproliferative neoplasm cells. Exp Hematol 2012;40(8):634-45 e10.
141. Bastian L, Hof J, Pfau M, Fichtner I, Eckert C, Henze G, et al. Synergistic activity of bortezomib and HDACi in preclinical models of B-cell precursor acute lymphoblastic leukemia via

modulation of p53, PI3K/AKT, and NF-kappaB. Clin Cancer Res 2013;19(6):1445-57.
142. Williams RT, den Besten W, Sherr CJ. Cytokine-dependent imatinib resistance in mouse BCR-ABL+, Arf-null lymphoblastic leukemia. Genes Dev 2007;21(18):2283-7.
143. Krivtsov AV, Twomey D, Feng Z, Stubbs MC, Wang Y, Faber J, et al. Transformation from committed progenitor to leukaemia stem cell initiated by MLL-AF9. Nature 2006;442(7104):818-22.
144. Somervaille TC, Cleary ML. Identification and characterization of leukemia stem cells in murine MLL-AF9 acute myeloid leukemia. Cancer Cell 2006;10(4):257-68.
145. Huntly BJ, Gilliland DG. Blasts from the past: new lessons in stem cell biology from chronic myelogenous leukemia. Cancer Cell 2004;6(3):199-201.
146. Neering SJ, Bushnell T, Sozer S, Ashton J, Rossi RM, Wang PY, et al. Leukemia stem cells in a genetically defined murine model of blast-crisis CML. Blood 2007;110(7):2578-85.
147. Hudson WA, Li Q, Le C, Kersey JH. Xenotransplantation of human lymphoid malignancies is optimized in mice with multiple immunologic defects. Leukemia 1998;12(12):2029-33.
148. Ito M, Hiramatsu H, Kobayashi K, Suzue K, Kawahata M, Hioki K, et al. NOD/SCID/gamma(c)(null) mouse: an excellent recipient mouse model for engraftment of human cells. Blood 2002;100(9):3175-82.
149. Ishikawa F, Yasukawa M, Lyons B, Yoshida S, Miyamoto T, Yoshimoto G, et al. Development of functional human blood and immune systems in NOD/SCID/IL2 receptor {gamma} chain(null) mice. Blood 2005;106(5):1565-73.
150. Cox CV, Martin HM, Kearns PR, Virgo P, Evely RS, Blair A. Characterization of a progenitor cell population in childhood T-cell acute lymphoblastic leukemia. Blood 2007;109(2):674-82.
151. Liem NL, Papa RA, Milross CG, Schmid MA, Tajbakhsh M, Choi S, et al. Characterization of childhood acute lymphoblastic leukemia xenograft models for the preclinical evaluation of new therapies. Blood 2004;103(10):3905-14.

Scope of the thesis

Novel genomic abnormalities of *CRLF2* gene leading to its overexpression have been recently reported in about 10% of pediatric BCP-ALL patients without known chromosomal aberrations and in 60% of ALL patients with Down syndrome (DS). CRLF2 associates with IL7Ra to form the heterodimeric receptor for TSLP, whose binding results in downstream activation of JAK2/STAT5 pathway. *CRLF2* overexpression leads to the deregulation of this pathway and is a poor prognostic marker identifying a subset of BCP-ALL patients that could benefit from alternative therapy targeting the *CRLF2*-related pathway.

Interestingly, in T-ALL, another subtype of ALL which accounts for about 15% of pediatric cases, alterations of CRLF2 have not been reported yet, while recently mutations in its partner *IL7Ra* have been identified in about 10% of cases. This observation makes it relevant to investigate if CRLF2 could also be affected in T-ALL. Indeed, this subtype of patients have a general worse outcome compared with BCP-ALL ones and therefore would benefit of the identification of new prognostic markers for a better therapeutic stratification.

In this work, we focused on refining the characterization, dissecting the biology and pointing out the clinical relevance of B and T ALL with *CRLF2* rearrangements, focusing on therapeutic interventions for this particularly poor prognosis subgroup of patients.

Specifically, three major lines of research have been investigated in this PhD thesis:

1. Fine tuning of surface CRLF2 expression and its associated signaling profile in childhood BCP-ALL (Chapter 1)

In this chapter we focused on refining the identification of patients with CRLF2 alterations. We aimed to demonstrate that screening of CRLF2 expression on surface of BCP-ALL patients can be successfully performed by standardized flow cytometry (FCM) protocols, allowing to identify also patients with weak or partial CRLF2 surface expression. We will also investigate whether FCM data are concordant with *CRLF2* transcript level performed by RQ-PCR.

2. Role of the hystone deacetylase inhibitor Givinostat (ITF2357) in treatment of *CRLF2* rearranged BCP-ALL (Chapter 2)

In this chapter we aim to investigate the efficacy of Givinostat, an hystone deacetylase inhibitor, in *in vitro* and *in vivo* models of *CRLF2* rearranged BCP-ALL, alone or in combination with chemotherapeutic agents currently in use for induction-remission therapy. Results from this study will provide the basis for the introduction of Givinostat in the current protocols, allowing combined therapies in patients, reducing doses and relative-associated toxicity thus maintaining therapeutic efficacy. This would provide particular benefits for that patients

which particularly suffers of chemotherapy-related toxicity (i.e. DS-ALL)

3. *CRLF2* Over-expression is a Poor Prognostic Marker in Children With High Risk T-ALL (Chapter 3)

In the last part of our work, we will investigate the incidence and prognostic impact of *CRLF2* overexpression in T-ALL. The results of this study could permit the identification of a subset of T-ALL patients that could benefit from alternative therapy.

Chapter 2

Haematologica. 2015 Jun; 100(6): e229–e232.

Fine Tuning of Surface CRLF2 Expression and Its Associated Signaling Profile in Childhood B Cell Precursor Acute Lymphoblastic Leukemia

Cristina Bugarin[1], Jolanda Sarno[1], Chiara Palmi[1], **Angela Maria Savino[1]**, Geertruy te Kronnie[2], Michael Dworzak[3], Angela Shumich[3], Barbara Buldini[2], Oscar Maglia[1], Simona Sala[1], Ilaria Bronzini[2], Jean-Pierre Bourquin[4], Ester Mejstrikova[5], Ondrej Hrusak[5], Drorit Luria[6], Giuseppe Basso[2], Shai Izraeli[6], Andrea Biondi[1,7], Giovanni Cazzaniga[1] and Giuseppe Gaipa[1]. On behalf of the I-BFM study group

1. Pediatric Clinic, University of Milano Bicocca, M. Tettamanti Research Center, Monza, Italy
2. Lab. Hemato-Oncology, University of Padua, Padua, Italy

3. Children's Cancer Research Institute and St. Anna Children's Hospital, Dept. of Pediatrics, medical University of Vienna, Vienna, Austria.
4. University of Zurich, CH-8006 Zurich, Switzerland
5. Childhood Leukaemia Investigation Prague, Department of Paediatric Haematology and Oncology, Charles University Prague, 2nd Medical School, Czech Republic
6. Pediatric Hematology Oncology, Schneider Children's Medical Center of Israel, Israel
7. Dept. Department of Pediatrics, Hospital San Gerardo/Fondazione MBBM

CORRESPONDING AUTHOR

Andrea Biondi,

Clinica Pediatrica, Università di Milano-Bicocca, Ospedale San Gerardo, via Pergolesi 33, 20900 Monza (MB), Italy.

E-mail: abiondi.unimib@gmail.com

Tel: +39 (0)39 2333661; Fax: +39 (0)39 2332167.

ACKNOWLEDGEMENTS

This work was supported by Fondazione Tettamanti, Fondazione Benedetta è la Vita ONLUS, Comitato M.L. Verga, Fondazione Città della Speranza and Grant Ric. Corrente OBG 2006/02/R/001822, Associazione Italiana per la Ricerca sul Cancro (AIRC; to ABi and FL), Fondazione Cariplo (ABi), Ministero dell'Istruzione, Università e Ricerca (MIUR; ABi). We also thank the AIEOP centers for their support. We would like to

thank Dr. Chiara Buracchi for her technical support in preparing the manuscript.

Genomic rearrangements of the cytokine receptor-like factor 2 (CRLF2*)* gene (1, 2), which is part of the thymic stromal lymphopoietin receptor (TSLPR), result in overexpression of CRLF2 itself leading to JAK2-mediated activation of STAT5, which regulates cell proliferation, survival, and apoptosis (3,4,11-13). In this regard, childhood B-cell precursor acute lymphoblastic leukemias (BCP-ALLs), bearing a rearranged CRLF2, display a high rate of relapse (5-10). Furthermore, *CRLF2* genomic rearrangements are strictly associated with its surface overexpression, rendering this marker suitable for detection by flow cytometry (FCM) (14).

To determine CRLF2 expression in childhood BCP-ALLs, we first assessed TSLPR surface expression. For this purpose, we carried out, at diagnosis, standard multiparametric FCM (Dworzak *et al.*, manuscript in preparation) on 421 consecutive diagnostic bone marrow (BM) samples from BCP-ALL children (256 males and 165 females), enrolled in six centers of the AIEOP-BFM-ALL-2009 trial between December 2010 and June 2013. Our gating strategy used to measure TSLPR surface expression (Supplemental Figure 1) allowed us to distinguish three blast subpopulations according to the intensity of TSLPR staining: the first one was defined as negative (i.e. positivity <10%), the second one was moderately positive (i.e. positivity ≥ 10% to <50%), and the third one was strongly positive (i.e.

positivity ≥ 50%). We found 383 (91.2%) negative samples, 8 (1.9%) moderately positive, and 29 (6.9%) strongly positive.

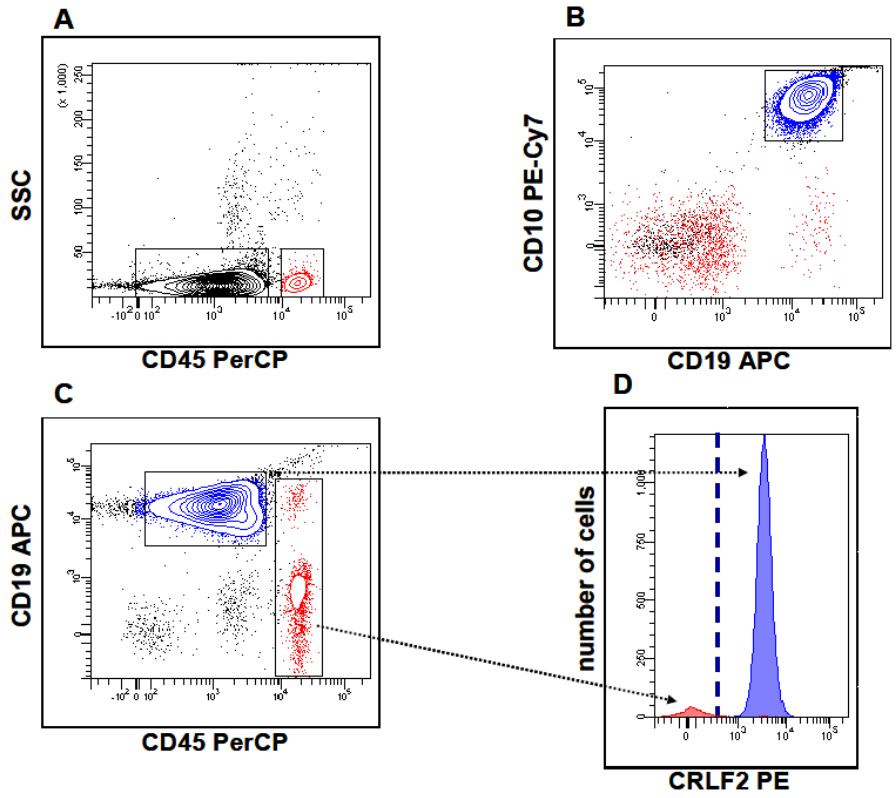

Supplemental Figure 1. Gating strategy employed to measure TSLPR surface expression in blast cells. Immature cells (black) were distinguished from mature lymphocytes (red) in SCC/CD45 dual dot plot (panel A). Within immature cells leukemic blasts (blue) are distinguished by CD19+/CD10+/CD45 intermediate immunophenotype (panel B). Based on CD19/CD45 expression (panel C), TSLPR expression is assessed as % of positive cells by setting the histogram marker exactly at the right end of mature lymphocytes peak (panel D). In all samples prevalence of mature lymphocytes was always ≥ 1.5%. Staining to measure TSLPR surface expression was performed using the combination: CRLF2PE/CD45PerCP/CD19APC/CD10PE-cy7/CD7ECD.

Inter-center distribution of patient's subgroups is shown in Table 1.

Table 1: TSLPR reactivity in BCP-ALL blasts at diagnosis analyzed in six different centers.

TSLPR profile	Centers #						Overall
	1 n=86	2 n=28	3 n=128	4 n=79	5 n=54	6 n=46	n=421
Negative	79 (91.8%)	25 (89.3%)	115 (89.9%)	76 (96.2%)	48 (88.8%)	41(89.1%)	384 (91.2%)
Moderately positive	1 (1.2%)	1 (3.6%)	4 (3.1%)	0 (0.0%)	1 (1.9%)	1 (2.2%)	8 (1.9%)
Strongly Positive	6 (7.0%)	2 (7.1%)	9 (7.0%)	3 (3.8%)	5 (9.3%)	4 (8.7%)	29 (6.9%)

Centers:

1) M. Tettamanti Research Center, Monza, Italy.
2) Lab. Hemato-Oncology, Padua, Italy.
3) Children's Cancer Research Institute and St. Anna Children's Hospital, Vienna, Austria.
4) University of Zurich, Zurich, Switzerland.
5) Pediatric Hematology Oncology, Schneider Children's Medical Center of Israel, Israel.
6) Childhood Leukaemia Investigation Prague, Department of Paediatric Haematology and Oncology, Czech Republic.

Representative examples are reported in Figure 1 panels A, B, and C.

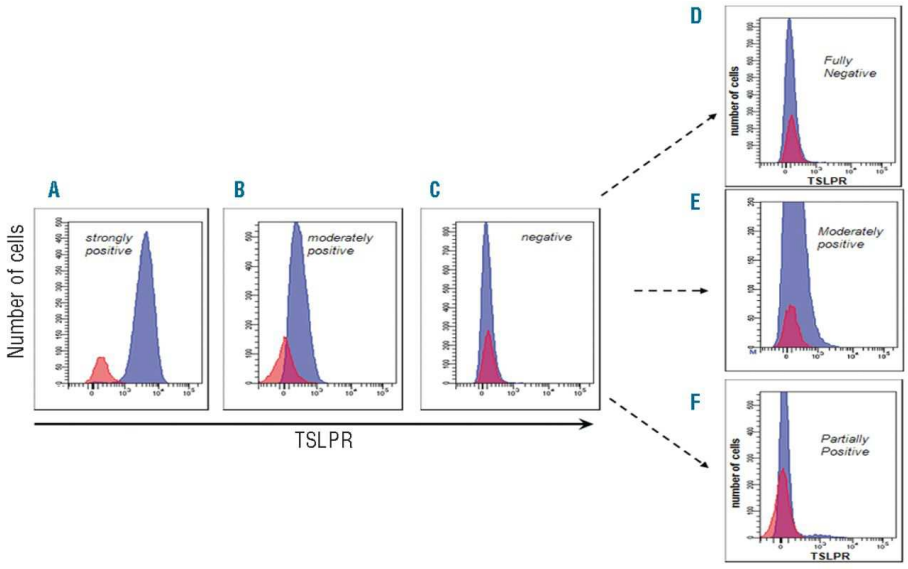

Figure 1. Different patterns of TSLPR expression in representative BCP-ALL cases: Strongly positive (positivity ≥50%, panel A), moderately positive (positivity ≥10% - <50%, panel B), and negative (positivity <10%, panel C). Fine tuning of TSLPR negative cases revealed three possible patterns of TSLPR positivity below the threshold of 10%: TSLPR fully negative (Panel D); moderately positive (Panel E); and partially positive (Panel F). The blue histograms represent the blast cells, the red ones represent the normal residual lymphocytes. Mean fluorescence intensity (MFI) of lymphocytes *vs* blasts were measured in each representative case: Panel A: 174.0 *vs* 3.899; Panel B: 149.0 *vs* 333; Panel C and panel D (same representative patient): 93.0 *vs* 97.0; Panel E: 88.0 *vs* 175.0; Panel F: 48.0 *vs* 1001.0

We then studied the immunophenotypic profile of TSLPR among the 86 patients enrolled in Center 1 during initial screening. Fine tuning of fluorescence distribution of 79/86 patients that had been previously found negative for TSLPR (i.e. positivity <10%, Table 1) allowed us to further distinguish three different expression patterns: 1) TSLPR-stained blasts

overlapping with control fluorescence (n 72, mean positivity 0.52% ± 0.52%, range 0.0% – 2.2%); 2) a second population of TSLPR-stained blasts clearly shifted to the right (n 5, mean % positivity 2.72% ± 0.16%, range 2.5% – 2.9%), which was identical to the TSLPR moderate pattern we observed previously in the diagnostic screening apart from TSLPR positivity being less than 10%; 3) a third pattern showing two clearly distinct blast populations: a larger one, TSLPR fully negative, and a smaller one positive, shifted to the right (n 2, positivity was 1% and 3.5%, respectively). Hereinafter, we will refer to these three patterns as fully negative, moderately positive (<10%), and partially positive, respectively. Representative examples are shown in Figure 1 panels D, E and F. Interestingly, one TSLPR moderately positive (<10%), and two TSLPR partially positive patients (UPNs 016, 013, and 039, respectively) showed low levels of *P2RY8-CRLF2* expression (F.C. < 0.50), suggesting the presence of a minor CRLF2 sub clone (Supplemental Table 2).

Supplemental Table 2: Phenotypic, molecular, and signaling features in 101 patients according to surface TSLPR expression.

UPN	TSLPR pattern	TSLPR surface expression (%)*	CRLF2 RQ-PCR overexpression**	CRLF2 rearrangement	CRLF2 mutation	JAK2 mutation	IL7Rα mutation	pSTAT5 response	pS6 response	p4EBP1 response	pAKT response
034	Strongly positive	99.9	Yes (132.9)	P2RY8-CRLF2	wt	neg	wt	83.6%	33.3%	36.2%	23.2%
059		99.9	Yes (108.8)	P2RY8-CRLF2	wt°	neg	wt	67.8%	68,8%	14,7%	18,7%
099		99.1	Yes (127.2)	P2RY8-CRLF2	wt	neg	wt	47.1%	34,4%	5,5%	0,0%
096		98.7	Yes (1032.7)	IGH@CRLF2	wt	R683G	wt	37.0%	41,6%	3,9%	40,4%
090		95.7	Yes (44.0)	P2RY8-CRLF2	wt	neg	wt	70.4%	n.t.	n.t.	n.t.
091		96.0	Yes (300.0)	P2RY8-CRLF2	wt	neg	wt	61.8%	n.t.	n.t.	n.t.
031		96.3	Yes (102.8)	P2RY8-CRLF2	wt	neg	S185C, T244I	66.0%	79,3%	3,5%	44,3%
032		95.2	Yes (397.6)	P2RY8-CRLF2	wt	L681-I682 insEA	wt#	67.3%	28,6%	3,4%	0,0%
097		95.1	Yes (102.2)	P2RY8-CRLF2	wt	neg	wt	49.6%	19,4%	-4,2%	0,0%
062		85.0	Yes (22.1)	wt	wt	neg	wt#	66.5%	9,7%	5,4%	0,0%
095		81.8	Yes (201.3)	P2RY8-CRLF2	wt	neg	wt	63.7%	9,4%	11.9%	3,8%
087		78.2	Yes (30.0)	P2RY8-CRLF2	wt	neg	wt	48.7%	n.t.	n.t.	n.t.
030		71.2	Yes (207.9)	wt	wt	neg	wt	n.t.	n.t.	n.t.	n.t.
013	Partially positive	3.5	No (2.49)	P2RY8-CRLF2 low§	wt	neg	wt	n.t.	n.t.	n.t.	n.t.
039		1.0	No (3.3)	P2RY8-CRLF2 low§	wt	neg	wt	n.t.	n.t.	n.t.	n.t.
073	Moderately positive (≥ 10%)	11.3	Yes (27.7)	wt (IGH@CRLF2 n.t.)	wt	neg	wt#	n.a.	n.a.	n.a.	n.a.
047	Moderately positive (<10%)	2.9	No (6.2)	wt	wt	neg	wt#	34.3%	25.4%	0.4%	1.9%
016		2.8	No (1.4)	P2RY8-CRLF2 low§	wt	neg	wt#	25.5%	1.0%	n.t.	n.t.
078		2.8	No (4.1)	wt	wt	neg	wt	16.0%	3.5%	10.7%	0.5%
067		2.6	No (12.0)	wt	wt	neg	wt#	19.0%	6.1%	1.7%	0.4%
037		2.5	No (2.4)	wt	wt	neg	wt#	17.0%	0.5%	0.0%	0.0%
004	Fully negative	2.2	No (1.8)	wt	wt	neg	wt	3.5%	0.0%	n.t.	n.t.
072		2.2	No (4.0)	wt	wt	neg	wt	1.2%	1.5%	0.3%	-0.5%
035		1.6	No (2.0)	wt	wt°	neg	wt	n.t.	n.t.	n.t.	n.t.
008		1.6	No (3.5)	wt	wt	neg	wt	n.t.	n.t.	n.t.	n.t.
028		1.5	No (2.3)	wt	wt	neg	wt#	n.t.	n.t.	n.t.	n.t.
055		1.5	No (0.6)	wt	wt°	neg	wt	0.7%	1.0%	n.t.	n.t.
049		1.5	No (9.3)	wt	wt	neg	wt	n.t.	n.t.	n.t.	n.t.
080		1.5	No (0.4)	wt	wt	neg	wt#	n.t.	n.t.	n.t.	n.t.
069		1.4	No (1.2)	wt	n.t.	n.t.	n.t.	n.t.	n.t.	n.t.	n.t.
094		1.2	No (4.0)	wt	wt	neg	wt	1.5%	-4.7%	0.2%	0.0%
061		1.1	No (0.1)	wt	wt	neg	wt#	0.4%	1.8%	3.5%	0.0%
079		1.0	No (0.7)	wt	wt	neg	wt	n.t.	n.t.	n.t.	n.t.
045		0.9	No (1.2)	wt	wt°	neg	wt#	3.0%	0.6%	n.t.	n.t.
086		0.9	No (0.1)	wt	wt	neg	wt#	n.t.	n.t.	n.t.	n.t.

Supplemental Table 2 (Continued)

082	Fully negative	0.9	No (3.6)	wt	n.t.	n.t.	n.t.	n.t.	n.t.	n.t.	n.t.
071		0.8	No (6.1)	wt	wt	neg	wt	n.t.	n.t.	n.t.	n.t.
052		0.8	No (0.7)	wt	wt	neg	wt	n.t.	n.t.	n.t.	n.t.
041		0.7	No (2.6)	P2RY8-CRLF2 low§	wt	neg	wt	n.t.	n.t.	n.t.	n.t.
036		0.7	No (0.3)	wt	wt	neg	wt	n.t.	n.t.	n.t.	n.t.
048		0.7	No (18.8)	wt	wt	neg	wt	n.t.	n.t.	n.t.	n.t.
019		0.6	No (4.1)	wt	wt	neg	wt#	n.t.	n.t.	n.t.	n.t.
101		0.6	No (0.2)	wt	wt	neg	wt#	0.2%	-5.9%	0.5%	-1.0%
066		0.6	No (3.2)	wt	wt	neg	wt	11.0%	0.1%	-7.9%	0.0%
046		0.6	No (2.3)	P2RY8-CRLF2 low§	wt	neg	wt	4.0%	n.t.	n.t.	n.t.
042		0.6	No (0.3)	wt	wt	neg	wt#	0.3%	0.0%	n.t.	n.t.
077		0.6	No (5.1)	wt	wt	neg	wt	n.t.	n.t.	n.t.	n.t.
002		0.6	No (0.5)	wt	wt	neg	wt	n.t.	n.t.	n.t.	n.t.
010		0.6	No (0.9)	wt	wt	neg	wt	n.t.	n.t.	n.t.	n.t.
001		0.5	No (0.2)	wt	wt	neg	wt	n.t.	n.t.	n.t.	n.t.
076		0.5	No (3.7)	wt	wt	neg	wt#	n.t.	n.t.	n.t.	n.t.
060		0.5	No (0.2)	wt	wt	neg	wt	0.2%	-5.1%	0.8%	0.0%
081		0.5	No (0.2)	wt	wt	neg	wt#	0.4%	2.5%	1.9%	0.0%
098		0.5	No (1.1)	wt	wt	neg	wt#	0.6%	0.0%	-4.7%	0.0%
038		0.5	No (0.6)	wt	wt	neg	wt	4.7%	0.7%	0.0%	0.0%
050		0.5	No (0.0)	wt	wt	neg	wt#	n.t.	n.t.	n.t.	n.t.
025		0.5	No (0.7)	wt	wt	neg	wt	n.t.	n.t.	n.t.	n.t.
100		0.4	No (0.1)	wt	wt°	neg	wt#	2.5%	0.0%	-0.9%	-2.8%
068		0.4	No (2.6)	wt	wt°	neg	wt#	n.t.	n.t.	n.t.	n.t.
093		0.4	No (5.4)	wt	wt	n.a.	wt	0.8%	-13.1%	2.3%	0.0%
092		0.4	No (5.9)	wt	wt	neg	wt#	3.3%	4.4%	-5.9%	0.0%
088		0.4	No (0.5)	wt	wt	n.a.	wt	6.1%	-5.0%	0.0%	0.0%
051		0.4	No (0.0)	wt	wt°	neg	wt	n.t.	n.t.	n.t.	n.t.
089		0.3	No (3.3)	wt	wt	neg	wt	1.0%	n.t.	n.t.	n.t.
075		0.3	No (2.1)	wt	wt	neg	wt	n.t.	n.t.	n.t.	n.t.
070		0.3	No (1.6)	wt	wt	neg	wt#	n.t.	n.t.	n.t.	n.t.
063		0.3	No (0.0)	wt	wt	neg	wt#	n.t.	n.t.	n.t.	n.t.
058		0.3	No (0.9)	wt	wt	neg	wt	n.t.	n.t.	n.t.	n.t.
018		0.3	No (0.2)	wt	wt	neg	wt#	n.t.	n.t.	n.t.	n.t.
003		0.3	No (0.1)	wt	wt°	neg	wt	n.t.	n.t.	n.t.	n.t.
023		0.2	No (2.8)	wt	wt	neg	wt	9.1%	0.9%	0.0%	0.0%
022		0.2	No (1.2)	wt	wt°	neg	wt#	10.8%	0.0%	0.0%	0.0%
084		0.2	Yes (33.2)	wt	wt	neg	wt	1.4%	0.0%	n.t.	n.t.
026		0.2	No (0.1)	wt	wt	neg	wt#	n.t.	n.t.	n.t.	n.t.
065		0.2	No (4.1)	wt	wt°	neg	wt	n.t.	n.t.	n.t.	n.t.
064		0.2	No (0.2)	wt	wt	neg	wt#	n.t.	n.t.	n.t.	n.t.
005		0.2	No (6.5)	wt	wt	neg	wt#	n.t.	n.t.	n.t.	n.t.

Supplemental Table 2 (Continued)

054	Fully negative	0.2	No (0.7)	wt	wt	neg	wt	n.t.	n.t.	n.t.	n.t.
040		0.2	No (0.1)	wt	wt	neg	wt[#]	n.t.	n.t.	n.t.	n.t.
033		0.2	No (0.2)	wt	wt	neg	wt[#]	n.t.	n.t.	n.t.	n.t.
085		0.1	No (0.1)	wt	wt	neg	wt	3.4%	0.7%	0.6%	n.t.
044		0.1	No (0.5)	wt	wt	neg	wt[#]	0.9%	0.2%	n.t.	n.t.
083		0.1	No (0.1)	wt	wt	neg	wt	n.t.	n.t.	n.t.	n.t.
074		0.1	No (0.4)	wt	wt	neg	wt	n.t.	n.t.	n.t.	n.t.
057		0.1	No (0.1)	wt	wt	neg	wt	n.t.	n.t.	n.t.	n.t.
056		0.1	No (0.1)	wt	wt[*]	neg	wt	n.t.	n.t.	n.t.	n.t.
053		0.1	No (0.0)	wt	wt	neg	wt[#]	n.t.	n.t.	n.t.	n.t.
043		0.1	No (0.2)	wt	wt	neg	wt[#]	n.t.	n.t.	n.t.	n.t.
029		0.1	No (0.1)	wt	wt	neg	wt	n.t.	n.t.	n.t.	n.t.
027		0.1	No (0.7)	wt	wt	neg	wt	n.t.	n.t.	n.t.	n.t.
021		0.1	No (0.1)	wt	wt[*]	neg	wt	n.t.	n.t.	n.t.	n.t.
020		0.1	No (1.5)	wt	wt[*]	neg	wt[#]	n.t.	n.t.	n.t.	n.t.
011		0.1	No (0.8)	wt	n.t.	n.t.	n.t.	n.t.	n.t.	n.t.	n.t.
024		0.1	No (0.5)	wt	n.t.	n.t.	n.t.	n.t.	n.t.	n.t.	n.t.
017		0.1	No (0.3)	wt	wt	neg	wt	n.t.	n.t.	n.t.	n.t.
014		0.1	No (0.3)	wt	wt[*]	neg	wt[#]	n.t.	n.t.	n.t.	n.t.
009		0.1	No (15.4)	wt	wt	neg	wt[#]	n.t.	n.t.	n.t.	n.t.
007		0.1	No (0.0)	wt	wt[*]	neg	wt	n.t.	n.t.	n.t.	n.t.
015		0.0	No (1.7)	wt	wt[*]	neg	wt	n.t.	n.t.	n.t.	n.t.
012		0.0	No (0.2)	wt	wt	neg	wt	n.t.	n.t.	n.t.	n.t.
006		0.0	No (0.2)	wt	wt	neg	wt[#]	n.t.	n.t.	n.t.	n.t.

n.t.= not tested; wt = wild type; n.a. = not available
* patients are listed by descendent order of values
** CRLF2 was considered over expressed in patients with levels of gene expression 20 times higher than the median of the considered cohort as described in Palmi *et al* (see ref.9)].
[§] P2RY8-CRLF2 Fold Change < 0.50
[#]These patients showed a T244I polymorphism
[*]These patients showed a V244M polymorphism
note: Among patients tested for p-STAT5, UPNs from 1 to 86 are patients from the prospective series of 421, UPNs from 87 to 101 are patients selected retrospectively from the cell bank

Next, CRLF2 transcripts levels, *CRLF2* aberrations (*P2RY8-CRLF2*, *IGH@-CRLF2*, *CRLF2* F232C), and *JAK2* and *IL7R* mutations were analyzed in 86 of our BCP-ALL samples collected in Center 1 as described previously (9). We detected CRLF2 overexpression in 9.3% of BCP-ALL patients. Seventy nine of these patients (91.8%) were negative for surface TSLPR expression as assessed by both FCM (<10%) and RQ-PCR (<20 FC), while only seven (8.1%) were concordantly positive. Intriguingly, one patient (UPN 084) showed overexpression of CRLF2, whereas TSLPR expression levels were undetectable (FC 33.2). However, this patient did not display *P2RY8-CRLF2* gene fusion. Two of the 7 patients with CRLF2 overexpression (UPN 30 and UPN 62), as assessed by both techniques, were negative for *P2RY8-CRLF2* fusion and *IGH@-CRLF2* translocation. Conversely, 5 non-overexpressed cases showed barely detectable levels of *P2RY8-CRLF2* gene fusion. Thus,

while our results seem to indicate a lack of correlation between genomic rearrangement and CRLF2 overexpression, as assessed by PCR, they clearly show that CRLF2-overexpressing BCP-ALLs are characterized by a strong positivity for TSLPR when analyzed by FCM.

To determine a functional read out CRLF2 genomic rearrangements, MUTZ5 cells (*IGH@-CRLF2*; *JAK2* R683G), MHH-CALL4 cells (*IGH@-CRLF2*; *JAK2* I682F), or primary thawed cells were subject to phospho flow cytometric assay (see supplemental materials). Likewise, a total of 41 cryopreserved BCP-ALL samples obtained according to their availability in cell banks – 28 were obtained from the consecutive series of Center 1 (total of 86) and 15 from a local cell bank – and viability after thawing (cut off ≥80%) were subject to phospho flow assay. Twenty-four BCP-ALL samples were TSLPR fully negative, 5 moderately positive (all of them <10%), and 12 strongly positive.

Next, we sought to determine basal and TSLP-induced pSTAT5 expression in CD45 intermediate/ CD10+/ CD7- blasts. The mean level of basal pSTAT5 detected in the three subgroups fully negative, moderately positive, and strongly positive for TSLPR was 0.71% ± 1.03% (range 0.0% – 4.0%), 2.64% ± 3.64% (range 0.2% – 9.0%), and 11.30% ± 18.31% (range 0.0% – 65.6%). Statistical differences were calculated by one-way ANOVA analysis of variance (p=0.0200). As expected, we observed much higher phosphorylation of STAT5 in the TSLPR strongly positive samples than the fully negative ones, with a

mean of pSTAT5+ cells of 60.79% ± 12.79% (range 37.0% – 83.6%) and 2.95% ± 3.26% (range 0.2 %– 11.0%), respectively ($p<0.001$ by Bonferroni's test) (Figure 2, Panel A). Furthermore, CRLF2-rearranged MUTZ5 and MHH-CALL4 cells showed aberrant TSLP-induced pSTAT5 compared with CRLF2 wild-type REH cells (data not shown). Interestingly, the group of 5 patients that were TSLPR moderately positive (<10%) showed enhanced pSTAT5 response with a mean of 22.36% ± 7.63% (range 16.0%- 34.3%), significantly higher than TSLPR fully negative patients (Figure 2, panel A, $p< 0.001$ by Bonferroni's test).

We also studied TSLP-induced signaling through the PI3K/AKT/mTOR pathway (S6, 4EBP1 and AKT) in 36 out of 41 BCP-ALL patients [9 TSLPR strongly positive, 5 moderately positive (i.e. <10%), and 22 fully negative]. TSLP stimulation led to a significant increase in phosphorylation levels of S6, 4EBP1, and AKT in TSLPR strongly positive samples as compared to both the fully negative and moderately positive cases (one-way ANOVA $p<0.0001$, $p= 0.0119$, and $p= 0.0065$, respectively), in good agreement with Tasian *et al* (14). Differences between groups are detailed in Figure 2, panels, B, C and D. Contrary to what reported by Tasian *et al*, in our samples, we observed no significant difference in basal phosphorylation of S6, 4EBP1, and AKT-S473 that could be ascribed to differences in TSLPR expression levels.

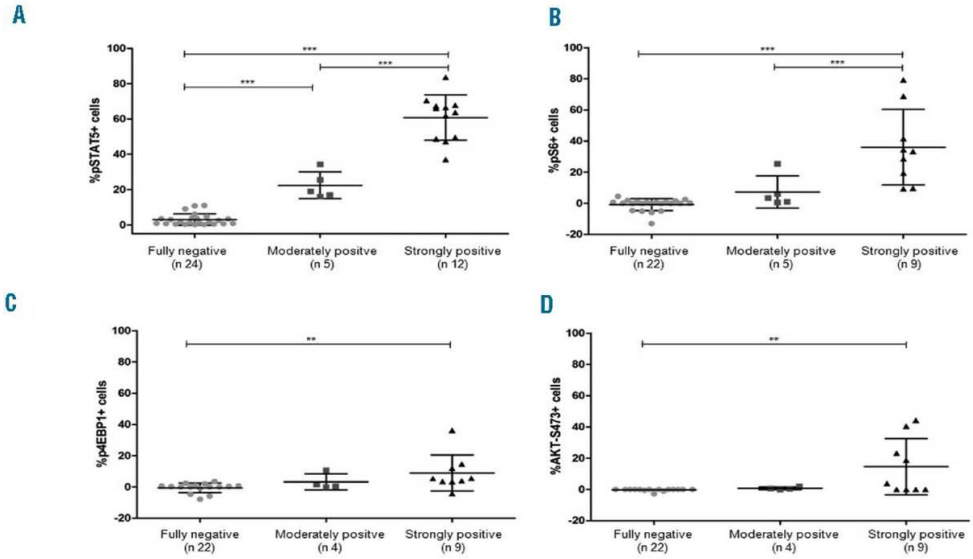

Figure 2. TSLP-induced phosphoprotein responses in BCP-ALL patients according to TSLPR expression (fully negative, moderately positive, or strongly positive). Distribution of positive cells is represented as whiskers plot of 5th and 95th percentile with means and Standard Deviations. Statistical significance among groups was determined by one-way ANOVA analysis of variance followed by post hoc Bonferroni's multiple comparison test (*p < 0.05, **p < 0.01, ***p < 0.001). Panel A shows pSTAT5 response (n 41) ; panels B, C, and D show TSLP-induced pS6, p4EBP1 and pAKT expression (n 36, 35, and 35 respectively). All groups were compared, but only those with statistical significance are indicated by stars and horizontal bars. Data were normalized to the basal phosphorylation level of each phosphoprotein.

Strikingly, neither TLSPR fully negative nor TSLPR moderately positive cases showed mutations in *JAK2*, *CRLF2*, or *IL7RA*. However, the observation of enhanced level of basal pSTAT5 in TSLPR moderately positive as compared to the fully negative patients may indicate the presence of a CRLF2 rearranged sub clone below the level of detection in this latter subgroup of

patients. In favor of this hypothesis, TSLPR strongly positive patients displayed an heterogeneous mutational profile: 10/12 carried *P2RY8-CRLF2* rearrangement - one of these also carrying a mutation in JAK insertion L681-I682 insEA and another one carrying the IL7RA mutation S185C; 1/12 displayed *IGH@-CRLF2* translocation and *JAK2* point mutation R683G; 1/12 was wild type also for *P2RY8-CRLF2* and *IGH@-CRLF2* rearrangements. SNP at codon 244 (rs151218732) of *CRLF2* as well as SNP at codon 244 (rs6897932) of *IL7RA* were randomly distributed independent of TSLPR overexpression. A summary of phenotypic, molecular and signaling features of the analyzed patients is described in Supplemental Table 2.

To the best of our knowledge, this is the first report showing BCP-ALL patients moderately positive for TSLPR characterized by aberrant pSTAT5 and pS6 expression. We are currently investigating whether this signature refers to the presence of minor clones or is due to additional mechanisms driving aberrant JAK/STAT and PI3K/mTOR signal transduction.

In this regard, Tasian *et al* has pointed to a potential diagnostic value of TSLP-mediated phosphosignaling in patients moderately positive for TSLPR staining (i.e. TSLPR-dim) as it would be a *bona fide* functional read out of the CRLF2 status. However, they did not provide any evidence of TSLPR-dim patients. In our study, we demonstrate the existence of CRLF2 moderately positive patients characterized by an activated phosphosignaling cascade. Thus, it is possible that Tasian *et al*

failed to identify TSLPR moderately positive patients because TSLPR expression was assessed after fixation and permeabilization, a procedure that is known to mask the presence of several surface antigens.

In summary, screening of TSLPR expression in BCP-ALL patients can be successfully achieved using standardized FCM protocols. FCM and PCR are highly concordant in detecting both CRLF2 overexpressed and non-overexpressed patients. However, patients characterized by a moderately or partially positive TSLPR expression associated with aberrant pSTAT5 and pS6 expression could only be detected by FCM analysis. Thus, our findings might prove useful in refining future diagnostic screening of ALL patients and help develop novel CRLF2 inhibitor-based therapies. In this regard, it is important to point out that approximately 50% of ALL patients with a Ph-like gene expression profile, which is associated with a poor outcome, have *CRLF2* rearrangements (15).

References

1. Mullighan CG, Collins-Underwood JR, Phillips LA, et al. Rearrangement of CRLF2 in B-progenitor- and Down syndrome-associated acute lymphoblastic leukemia. Nat Genet. 2009 Nov;41(11):1243-1246.
2. Russell LJ, Capasso M, Vater I, et al. Deregulated expression of cytokine receptor gene, CRLF2, is involved in lymphoid transformation in B-cell precursor acute lymphoblastic leukemia. Blood. 2009 Sep 24;114(13):2688-2698.
3. Harvey RC, Mullighan CG, Chen IM, et al. Rearrangement of CRLF2 is associated with mutation of JAK kinases, alteration of

IKZF1, Hispanic/Latino ethnicity, and a poor outcome in pediatric B-progenitor acute lymphoblastic leukemia. Blood. 2010 Jul 1;115(26):5312-5321.
4. Roll JD, Reuther GW. CRLF2 and JAK2 in B-progenitor acute lymphoblastic leukemia: a novel association in oncogenesis. Cancer Res. 2010 Oct 1;70(19):7347-7352.
5. Attarbaschi A, Morak M, Cario G, et al. Treatment outcome of CRLF2-rearranged childhood acute lymphoblastic leukaemia: a comparative analysis of the AIEOP-BFM and UK NCRI-CCLG study groups. Br J Haematol. 2012 Sep;158(6):772-777.
6. Cario G, Zimmermann M, Romey R, et al. Presence of the P2RY8-CRLF2 rearrangement is associated with a poor prognosis in non-high-risk precursor B-cell acute lymphoblastic leukemia in children treated according to the ALL-BFM 2000 protocol. Blood. 2010 Jul 1;115(26):5393-5397.
7. Chen IM, Harvey RC, Mullighan CG, et al. Outcome modeling with CRLF2, IKZF1, JAK, and minimal residual disease in pediatric acute lymphoblastic leukemia: a Children's Oncology Group study. Blood. 2012 Apr 12;119(15):3512-3522.
8. Ensor HM, Schwab C, Russell LJ, et al. Demographic, clinical, and outcome features of children with acute lymphoblastic leukemia and CRLF2 deregulation: results from the MRC ALL97 clinical trial. Blood. 2011 Feb 17;117(7):2129-2136.
9. Palmi C, Vendramini E, Silvestri D, et al. Poor prognosis for P2RY8-CRLF2 fusion but not for CRLF2 over-expression in children with intermediate risk B-cell precursor acute lymphoblastic leukemia. Leukemia. 2012 Oct;26(10):2245-2253.
10. van der Veer A, Waanders E, Pieters R, et al. Independent prognostic value of BCR-ABL1-like signature and IKZF1 deletion, but not high CRLF2 expression, in children with B-cell precursor ALL. Blood. 2013 Oct 10;122(15):2622-2629.
11. Isaksen DE, Baumann H, Trobridge PA, Farr AG, Levin SD, Ziegler SF. Requirement for stat5 in thymic stromal lymphopoietin-mediated signal transduction. J Immunol. 1999 Dec 1;163(11):5971-5977.
12. Levin SD, Koelling RM, Friend SL, et al. Thymic stromal lymphopoietin: a cytokine that promotes the development of IgM+ B cells in vitro and signals via a novel mechanism. J Immunol. 1999 Jan 15;162(2):677-683.
13. Rochman Y, Kashyap M, Robinson GW, et al. Thymic stromal lymphopoietin-mediated STAT5 phosphorylation via kinases JAK1 and JAK2 reveals a key difference from IL-7-induced signaling. Proc Natl Acad Sci U S A. 2010 Nov 9;107(45):19455-19460.

14. Tasian SK, Doral MY, Borowitz MJ, et al. Aberrant STAT5 and PI3K/mTOR pathway signaling occurs in human CRLF2-rearranged B-precursor acute lymphoblastic leukemia. Blood. 2012 Jul 26;120(4):833-842.
15. Roberts KG, Morin RD, Zhang J, et al. Genetic alterations activating kinase and cytokine receptor signaling in high-risk acute lymphoblastic leukemia. Cancer Cell. 2012 Aug 14;22(2):153-166.

Supplemental methods

Phospho flow cytometry

MUTZ5 cells harboring IGH@-CRLF2 translocation and JAK2 R683G mutation, MHHCALL4 displaying IGH@-CRLF2 translocation and JAK2 I682F mutation, or primary thawed cells were subject to phospho flow cytometric assay. For this purpose, cells were starved in X-vivo medium and rested at 37°C for 16 hours or 1 hour. Then, cells were stimulated with rh-TSLP (10 ng/mL) for 30 minutes at 37°C to allow signal transduction, and treated according to an established internal protocol. Starved cells were fixed with paraformaldehyde (1.5%) and permeabilized with 90% ice-cold methanol and then incubated with anti-phospho-protein-directed MoAbs (or isotype matched IgG) and surface antigen-directed MoAbs. Characteristics of MoAbs and staining combinations are described in Supplemental Table 1.

Supplemental Table 1: Characteristics of selected antibodies and staining combinations for TSLPR immunophenotypic screening and phosphoflow cytometry assay.

Selected Antibodies					
Reactivity	Clone	Fluorochrome	Source	Ig class	Use
TSLPR	1D3	PE	Biolegend	mouse IgG2aλ	10µl/1x10^{5}cells
TSLPR	1B4	PE	Biolegend	Mouse IgG1K	10µl/1x10^{5}cells
CD19	SJ25C1	APC	BD	mouse IgG1 k	3µl/1x10^{5}cells
CD10	HI10a	PE	Biolegend	mouse IgG1 k	2µl/1x10^{5}cells
CD10	HI10a	PE-CY7	BD	mouse IgG1 k	2µl/1x10^{5}cells
CD45	2D1	PerCP	BD	mouse IgG1 k	2µl/1x10^{5}cells
CD7	8H8	ECD	Beckman Coulter	mouse IgG2a	1µl/1x10^{5}cells
IgG1 k Isotype control	MOPC-21	Alexa Fluor 488	BD	mouse IgG1 k	10µl/1x10^{5}cells
IgG1 k Isotype control	MOPC-21	Alexa Fluor 647	BD	mouse IgG1 k	10µl/1x10^{5}cells
p-Stat5 (Y694)	47	Alexa Fluor 488	BD	mouse IgG1	10µl/1x10^{5}cells
p-S6 (pS235/pS236)	N7-548	Alexa Fluor 647	BD	mouse IgG1 k	10µl/1x10^{5}cells
IgG Isotype control	236B4	Alexa Fluor 488	Cell Signaling	rabbit IgG	2µl/1x10^{5}cells
IgG Isotype control	DA1E	Alexa Fluor 647	Cell Signaling	rabbit IgG	2µl/1x10^{5}cells
p-4E-BP1 (Thr37/46)	236B4	Alexa Fluor 488	Cell Signaling	rabbit IgG	2µl/1x10^{5}cells
anti p-AKT (S473)	D9E	Alexa Fluor 647	Cell Signaling	rabbit IgG	8µl/1x10^{5}cells

Staining panel for Immunophenotyping					
Tube 1	TSLPR PE	CD45 PerCP	CD10 PE-CY7	CD19 APC	CD7 ECD

Staining panel for Phosphoflow					
Tube 1	IgG1 k Isotype control Alexa 488	IgG1 k Isotype control Alexa 647	CD10 PE	CD45 PerCP	CD7
Tube 2	p-Stat5 Alexa 488	p-S6 Alexa 647	CD10 PE	CD45 PerCP	CD7

Cells were acquired on a FACSaria™ flow cytometer (BD) equipped with 488-nm, 633-nm and 405-nm lasers. Data were collected (at least 100000 events per tube) and analyzed using DIVA™ software (BD). Positivity threshold for phosphoprotein expression was established by the use of isotype IgG-negative control (Supplemental Figure 2 panel A). Basal levels of each

phosphoprotein were then calculated as percentage (%) of phosphoprotein positive (p-positive) cells in unstimulated conditions (Supplemental Figure 2 panel B). Response to each cytokine (rhTSLP) was calculated by subtracting the % of p-positive cells in the basal state from that obtained upon exposure to cytokine (Supplemental Figure 2 panel C).

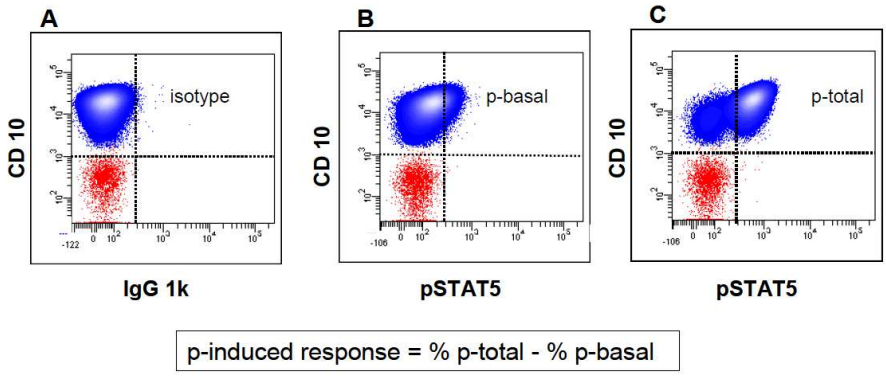

Supplemental Figure 2. Representative phosphoflow analysis in leukemic blast population (blue) gated on CD45-intermediate/SSC-low/CD10+ cells to measure signaling response after cytokine stimulation. Positivity threshold was established by an isotype IgG phospho-specific antibody (panel A). Basal and total levels of p-proteins were calculated as % of positive cells in unstimulated (panel B) and stimulated (panel C) conditions, respectively. p-induced response was then calculated by the indicated formula.

Quantitative expression of CRLF2

CRLF2 transcript levels on diagnostic samples were analyzed using TaqMan Gene Expression Assay Hs00913509_s1 (Applied Biosystems, Foster City,CA,USA) following the manufacturer's instructions. The presence and level of the fusion transcript P2RY8-CRLF2 was analyzed by Universal Probe Library System (UPL) (Roche Diagnostic, Basel,

Switzerland) as well as the housekeeping GUS gene transcript, tested as internal control. Optimal primers and probe for P2RY8-CRLF2 and GUS amplification were selected using the Roche ProbeFinder software (https://www.roche-appliedscience.com/sis/rtpcr/upl). In particular, for P2RY8-CRLF2 amplification we used primers designed in the first exon of P2RY8 (5'-gctacttctgccgctgctt-3') and in the first exon of CRLF2 (5'-gcagaaagacggcagctc-3') with the UPL probe n. 28 (Roche UPL cat. n. 04687604001). Each cDNA sample (20 ng RNA equivalent) was tested in duplicate (Ct range between replicates <1.5). The amplification reaction was performed on the 7900HT FAST Real Time PCR System instrument (Applied Biosystems) for CRLF2 expression and on the Light Cycler 480 (Roche) for P2RY8-CRLF2 with the following protocol: initial step at 95°C for 10 min, then 50 cycles at 95°C for 15s and at 60°C for 1 min. Relative gene expression (indicated as fold change) was quantified by the 2-DDCt method (22). The DDCts for CRLF2 expression were calculated by subtracting the median of the DCt of a published cohort of 464 BCPALL patients enrolled in Italy in the AIEOP-BFM ALL2000 study from February 2003 to July 2005 (22) to the DCt of each sample. The DDCts for P2RY8-CRLF2 expression were calculated by subtracting the DCt of a selected positive patient external to this cohort to the DCt of each sample.

Mutational screening of JAK2, CRLF2 and IL7Rα

Mutational screening of JAK2, CRLF2 and IL7Rα was performed in 82/86 consecutive patients and in 15/15 patients (13/15 for JAK2) selected retrospectively from Monza's cell bank for phospho flow analysis. High Resolution Melting (HRM) analysis was applied to identify JAK2 mutations in exon 16 using HRM Master (Roche Diagnostics) as previously described (21). Sequencing of CRLF2 exon 6 and IL7R exons 5 and 6 was performed by Sanger sequencing of PCR products from patients DNA after whole genome amplification using GenomePhi V2 DNA Amplification Kit (GE Healthcare Life Science); we designed the following primers for CRLF2-F (5'-AGGGAGACTGGTTAGGGATGA-3'), CRLF2-R (5'-TGGGCATTGTATGGAAACTG -3') and for IL7R exon 5 IL7R-F (5'-GCAACACCTCTTTTCCATC-3') and IL7R-R (5'-GGGAACAAAAACTCTACCACCA-3') and exon 6 IL7R-F(5'-TGCATGGCTACTGAATGCTC-3') and IL7R-R (5'-CCCACACAATCACCCTCTTT- 3').

Statistical analysis

Statistical significance of phosphoprotein levels among groups of patients with different TSLPR pattern (strongly positive, moderately positive, and fully negative) was determined by one-way ANOVA analysis of variance followed by post hoc Bonferroni's multiple comparison test. P values less than 0.05 were considered statistically significant. All data were presented as mean ± standard deviation (SD). GraphPad PrismV5.0

(GraphPadSoftware, San Diego, CA, USA) was used for statistical analysis.* $p < 0.05$, ** $p < 0.01$, ***$p < 0.001$.

Chapter 3

Role of the hystone deacetylase inhibitor Givinostat (ITF2357) in treatment of CRLF2 rearranged acute lymphoblastic leukemia

A.M. Savino [1], J.Sarno [1], L.Trentin [2], M. Vieri [1], G. Fazio [1], M. Bardini [1], C. Bugarin [1], G. Fossati [3], K. Davis [4], G. Gaipa [1], L.H. Meyer [5], G. Te Kronnie [2], A. Biondi [1], C. Palmi [1]* and G. Cazzaniga [1]*.

*These authors contributed equally to this work

1. Centro Ricerca M. Tettamanti, Clinica Pediatrica, Università di Milano Bicocca, Fondazione MBBM/Ospedale San Gerardo, Monza, Italy.
2. Laboratory of Onco-Hematology, Department of Pediatrics, Università di Padova, Italy.

3. Preclinical R&D Department, Italfarmaco S.p.A., Cinisello Balsamo, Milan, Italy.
4. Baxter Laboratory in Stem Cell Biology, Department of Microbiology and Immunology, Stanford University, Stanford, CA 94305, USA; Hematology and Oncology, Department of Pediatrics, Stanford University, Stanford, CA 94305, USA.
5. Department of Pediatrics and Adolescent Medicine, Ulm University Medical Center, Ulm, Germany.

CORRESPONDING AUTHORS

Giovanni Cazzaniga,
Centro Ricerca M. Tettamanti, Università di Milano-Bicocca, Ospedale San Gerardo, via Pergolesi, 33, 20900 Monza (MB), Italy.
E-mail: gianni.cazzaniga@hsgerardo.org
Tel: +39 (0)39 2333661 ; Fax: +39 (0)39 2332167

and

Andrea Biondi,
Clinica Pediatrica, Università di Milano-Bicocca, Ospedale San Gerardo, via Pergolesi 33, 20900 Monza (MB), Italy.
E-mail: abiondi.unimib@gmail.com
Tel: +39 (0)39 2333661; Fax: +39 (0)39 2332167.

ABSTRACT

Recently, in a subset of poor prognosis childhood ALL patients, genomic alterations of *CRLF2* and *JAK2* genes leading to the deregulation of JAK/STAT pathway have been reported. Inhibition of CRLF2/JAK2 signaling has the potential to become a therapeutic intervention for this subgroup of patients. In addition to the use of JAK2 inhibitors, numerous reports indicated that a broader antitumor activity is necessary to effectively treat tumor cells with aberrant *CRLF2* related signaling. Previous studies have shown that the HDAC inhibitor Givinostat/ITF2357 has potent anti-tumor activity against hematological malignancies, including myeloproliferative neoplasms (MPN) carrying the JAK2V617F mutation and consequent deregulation of JAK/STAT pathway. Here we demonstrated that Givinostat, at low concentrations, inhibited proliferation and induced apoptosis of BCP-ALL *CRLF2*-rearranged MHH-CALL4 and MUTZ 5 cell lines positive for exon 16 *JAK2* mutations and of blasts from patients carrying *CRLF2* rearrangments. At low doses (0.2 µM), Givinostat downregulated genes belonging to JAK/STAT pathway and inhibited the basal and TSLP- induced signaling reducing the phoshporylation of STAT5. *In vivo*, Givinostat was able to significantly reduce engraftment of human blasts in xenograft models of CRLF2 positive BCP-ALL. Furthermore, Givinostat increased the effect of current chemotherapy in *in vitro* and *ex vivo* models. In conclusion, this drug may represent a novel and

effective tool, in combination with current chemotherapy, to treat this difficult and bad prognosis subset of ALL.

INTRODUCTION

B Cell Precursor Acute Lymphoblastic Leukemia (BCP-ALL) is one of the most common pathologies in pediatric age and represents 35% of all tumors. The cure rate for this disease approaches 90% with current treatment regimen (1), however the probability of survival of patients who relapse is only 30%. Therefore there is an urgent need to focus on particular subgroups of patients with hallmarks of bad prognosis that could benefit of novel therapeutic approaches. Recently, alterations of *CRLF2* (*Cytokine Receptor-like Factor 2*), a new negative prognostic factor in pediatric BCP-ALL (2), have been identified in up to 7% of patients (3-5). In particular, these patients represent half of Ph-like ALLs (6) and of Down Syndrome-associated BCP-ALL (3,7). Rearrangements in *CRLF2* cause the overexpression of this component of the heterodimeric cytokine receptor for thymic stromal lymphpoietin (TSLP) and lead to deregulation of JAK/STAT and PI3K/mTOR pathways causing hyperactive signaling (4,8,9). Moreover, *CRLF2* overexpression is highly associated with point mutations in JAK family members (4,6,10,11) and experimental data showed that the introduction of *CRLF2* rearrangements and *JAK2* mutations together induced transformation of the murine BCP cell line BaF3 (7). These observations emphasize the role

of JAK/STAT pathway in *CRLF2* rearranged subset of BCP-ALL and lead to hypothesize that inhibition of this hyperactive signaling network could have a therapeutic relevance. Several reports described the employment of JAK inhibitors to target JAK/STAT pathway. Maude et al. (12) showed the efficacy of a JAK1/2 inhibitor, in *in vivo* xenograft models of Ph-like BCP-ALL and in a subset of T-ALL, ETP-ALL, in which the hyperactivation of JAK/STAT pathway is a common feature (13). However, the development of new resistance mechanisms to JAK inhibitors is growing (14) impairing their efficacy, thus emphasizing the need for innovative therapeutic strategies. In this issue we propose a novel epigenetic approach using an already known class I/II HDAC inhibitor (HDACi), Givinostat/ITF2357, as therapeutic tool to treat *CRLF2* rearranged patient with deregulation of JAK/STAT pathway. This drug is already in clinic for myeloproliferative neoplasms (MPNs) such as polycythemia vera and has an already established safety profile with controlled side effects (15). This study establishes the *in vitro* and *in vivo* efficacy of Givinostat in cases with *CRLF2* rearrangements, alone or in combination with conventional chemotherapy. We show that Givinostat causes transcriptional modulation of genes involved in JAK/STAT pathway leading to the inactivation of this signaling network. Overall, this drug may represent a novel and effective tool to treat this difficult and bad prognosis subset of ALL.

MATERIALS AND METHODS

Cell culture

For this study, we used human BCP-ALL cell lines MHH-CALL4 and MUTZ5, human essential thrombocythemia SET2 and human chronic myeloid leukemia K562. MHH-CALL4 and MUTZ5 overexpressed *CRLF2* via *IGH@-CRLF2* translocation and harbored *JAK2* mutations (*JAK2* I682F and R683G, respectively). SET2 cell line bearing V617F mutation of *JAK2* was chosen as positive control for sensitivity to Givinostat and the *BCR/ABL*- positive K562 cell line was included as negative one (16). Cells were kept in RPMI medium supplemented with 10-20% fetal bovine serum, 1% L-glutammine and 1% penicillin/streptomycin at 37°C in humidified air with 5% CO_2.

Patient samples

Five patients were selected for this study on the basis of their positivity for *CRLF2* alterations and availability of biological material. The analyzed patients were diagnosed and treated according to AIEOP-BFM ALL 2000 and 2009 protocols (NCT00613457 and NCT01117441) from 2005 to 2012. BCP-ALL diagnosis was made according to standard cytomorphology, cytochemistry and immunophenotypic criteria. Immunophenotyping was carried out using APC conjugated anti-human CD10, FITC-conjugated anti-human CD19 (EBioscience, San Diego, California, USA) and PE-conjugated human CRLF2 (Biolegend, London,UK). Cells were collected on

a FACSCanto II™ flow cytometer (BD, Becton Dickinson Biosciences, San Jose, California, USA) and analyses were performed with DIVA™ software. *CRLF2* overexpression and *P2RY8-CRLF2* fusion were analyzed as previously described (17). Briefly, relative gene expression (indicated as fold change) was quantified by the 2-DDCt method. For *CRLF2* expression, the DDCts were calculated by subtracting the median of the DCt of a published cohort of 464 BCP-ALL patients enrolled in Italy in the AIEOP-BFM ALL2000 study from February 2003 to July 2005 (18) to the DCt of each sample. Patients were considered *CRLF2* overexpressed when relative gene expression was 20 fold-above the median. The DDCts for *P2RY8-CRLF2* expression were calculated by subtracting the DCt of a selected positive patient external to this cohort to the DCt of each sample (19). Patients were further characterized for JAK2 alterations by HRM technique (17) and for other BCP-ALL associated aberrations by Multiplex Ligation-dependent Probe Amplification (MLPA; SALSA MLPA P335-A3 ALL-IKZF1 probemix, MRC-Holland, Amsterdam, The Netherlands) according to the manufacturer's instruction (20,21). Informed consent to participate in the study was obtained for all patients by parents or legal guardians. Investigation has been conducted in accordance with the ethical standards, with the Declaration of Helsinki and with the national and international guidelines and has been approved by the authors' institutional review board.

Establishment of xenograft model

Primary leukemia cells from bone marrow of the above mentioned patients were injected into sublethal irradiated (250 rad) non-obese diabetic/severe combined immunodeficient (NOD. Cg-*Prkdc*^{scid} also termed NOD/SCID, Charles River Laboratories, Wilmington, MA, USA) mice. Samples were injected at a dose of 7-10 x10^6 cell per mouse. Cells from bone marrow of successfully engrafted mice (more than 80% of human blasts in bone marrow) were re-injected (10^6 cells/mouse) to create secondary or tertiary xenografts for treatment studies. Engraftment was determined by flow cytometric analysis of samples collected by bone marrow aspiration using antibodies against human CD10, CD19 and CRLF2 and, to exclude false positivity, mouse CD45.1 (Percp-Cy5.5-conjugated, EBioscience). For *ex vivo* studies, blasts were isolated from infiltrated bone marrow or spleens of primary and secondary mice (more than 80% BCP-ALL blasts). Blasts were cultured on a confluent layer of OP9 stroma and kept in alpha-MEM medium supplemented with 20% fetal bovine serum, 1% Glutamax (GIBCO® Life Technologies, Carlsbad, California, USA) and 1% penicillin/streptomycin at 37°C in humidified air with 5% CO_2 (22). Human recombinant TSLP (Immunotools, Friesoythe¸Germany) was added in the medium at a concentration of 10 ng/ml.

In vitro and *ex vivo* analysis of leukemia cells

Cells lines and xenograft leukemia blasts were incubated with Givinostat (ITF2357,Italfarmaco, Cinisello Balsamo, Italy) dissolved in DMSO, or only DMSO as vehicle, in 24-well plates for 72h (blasts were cultured on OP9 stroma). Citotoxicity assays were performed with Annexin V-FITC Apoptosis Detection Kit Plus (BioVision, San Francisco, California, USA) following the manufacturer instructions. Live cells (negative for both Annexin V and Sytox staining) were assessed by cytofluorymetric technique. Proliferation assays were performed only for cell lines by counting live cells by FACS. Experiments were performed in triplicate. STAT5 phosphorylation was measured by phosphoflow as previously described (23). Cells were assessed for viability >75% by Trypan blu exclusion. Cell lines and xenograft blasts were incubated for 24h with Givinostat at 0.2 µM or DMSO at 37°C. After treatment, cells were stimulated with rh-TSLP (0.1-10 ng/mL) for 30 minutes at 37°C to allow signal transduction. After stimulation, cells were immediately fixed with paraformaldehyde (1.5%) and permeabilized with 90% ice-cold methanol (24). Samples were than stained with Alexa-Fluor 488-conjugated anti-phospho-STAT5 Tyr 694 (BD Bioscience Franklin Lakes, NJ, USA) or isotype matched IgG and surface antigen-directed MoAbs (anti human CD10 and anti mouse CD45.1).Cells were acquired on FACSCantoII™ flow cytometer. Data were collected and analyzed using DIVA™ software and Cytobank. Positivity threshold for phosphoprotein expression was

established using isotype IgG-negative control. For Givinostat and vehicle treated samples, the levels of STAT5 phosphoprotein in response to rh-TSLP stimulus were normalized to the basal STAT5 phosphorylation levels for each cell line and patient for data display.

Microarray analysis and qRT-PCR assay

Gene expression analysis was carried out on *ex-vivo* treated xenograft leukemia cells from primary or secondary transplantation (N=5) after 6h of incubation with Givinostat or vehicle in alpha-MEM without stroma. RNA was extracted using TRIZOL reagent (Invitrogen, Life Technologies, Carlsbad, California, USA). RNA quality was assessed on an Agilent 2100 Bioanalyzer (Agilent Technologies, Waldbronn, Germany). Gene expression analysis was performed using the Affymetrix GeneChip Human Genome U133 Plus 2.0 array and the Affymetrix GeneChip 3' IVT PLUS reagent kit. From each sample 100 ng of RNA were converted in double-stranded cDNA and then labeled cRNA was generated by in vitro transcription. For the fragmentation 15 µg of purified cRNA were used. Hybridization, washing, staining and scanning protocols were performed following manufacturer's instructions. All data analysis was performed in R (http://www.R-project.org/ version 3.0.2) using Bioconductor and R packages. Probe level signals were converted to expression values using the robust multi-array averaging (RMA) algorithm (25). Differentially

expressed genes were identified using Significance Analysis of Microarray algorithm coded in the samr R package (26). In SAM, we estimate the number of false positive predictions (i.e., False Discovery Rate, FDR) with 1000 permutations. To identify genes up- and down-regulated by Givinostat, we selected those probe sets with FDR<0.05. Gene Ontology (GO) analysis was performed using DAVID version 6.7 (http://david.abcc.ncifcrf.gov/). Pathway analysis was carried out using Graphite (http://graphiteweb.bio.unipd.it/) that combines topological and multivariate pathway analysis with an efficient system of network visualizations (27). Gene set enrichment analysis (GSEA) was done comparing the expression profiles of treated versus control samples using the C2KEGG and C2cgp gene sets within the molecular signatures databases (MSigDB) collection (28). The signal to noise metric and the gene_set permutation were used to identify statistical enrichment of the selected gene sets in Givinostat treated versus DMSO treated cells.

Validation of differentially expressed genes was performed by qRT-PCR using TaqMan Gene Expression Assays and the Universal Probe Library System (UPL) (Roche Diagnostic, Basel, Switzerland). Optimal primers and probes were selected using the Roche ProbeFinder software (https://www.roche-appliedscience.com/sis/rtpcr/upl). Genes analyzed included: *STAT5A*, *JAK2*, *IL7Rα*, *cMYC*, *BCL2L1*, *PTPN1* and the housekeeping *GUS* gene, tested as internal control. Each cDNA sample was tested in triplicate (Ct range between

replicates <1.0). Differences in gene expression before and after treatment were statistically evaluated using the student t-test. Differences were considered statistically significant at p values <0.05, indicated in experiments with asterisks: * $p<0.05$; ** $p<0.01$; *** $p<0.001$.

CyTOF analysis

CyTOF analysis was performed used diagnostic samples for patient 1,2,3,5 and xenograft-derived blasts for patient 4, according to the availability of the cells. One million single cells per sample have been treated with Givinostat (0.2 μM) for 24 hours and then analyzed via CyTOF using previously described approach (29). The expression of 25 phenotypic proteins were contemporary measured at single cell level. Cells were gated to exclude cPARP positive, myeloid, T-cells and red blood cells and then clusterized for 16 parameters typical of B-cell signature. Supplementary Table 1 summarize the panel of metal-conjugated antibodies used for the analysis. Checkmarks indicate the markers used for the analysis by viSNE clustering software (30). The plots are colored for different protein expression's and colorimetric depiction for each plot indicates the different level of expression of the considered marker in the cell population analyzed. Blue dots represents blasts negative for that antigen while positivity is indicated by a colorimetric range that goes from yellow to red. SPADE software was used to further represent data. Cells were clusterized according to

their positivity for surface or intracellular markers and clusters were represented by spheres. The size of the spheres was depicted according to the number of events in each cluster. Bigger spheres represents clusters with more cells positive or negative for the selected marker. The colorimetric range from negativity to positivity for that marker reflected the one used by viSNE. The spheres have been further grouped in bubbles (black circles) according to the expression of CRLF2, CD10 and CD45.

In vivo treatment

All *in vivo* experiments were conducted on protocols approved by Ministero della Salute (64/2014 PR) For efficacy studies, mice were randomized to treatment or vehicle (3-5 mice per arm) once xenografts had engrafted (0,1-1% human blasts in the bone marrow). Givinostat or vehicle (1% DMSO+PEG-H2O 1:1) was administered for 7 weeks (5 days/week) by intraperitoneal injection at a dose of 30 mg/kg. At the end of treatment, mice were sacrificed and spleens and bone marrows were harvested. Disease burden was assessed at this end point, by measuring absolute number of splenic and bone marrow blasts (total splenic or bone marrow count x %human CD10+/CD19+/CRLF2+ cells).

Combination assays

To mimick the effect of remission/induction chemotherapy, Methyl-prednisolone (Sanofi, Italy) or a mix of Asparaginase (EUSA Pharma, UK), Vincristine (Pfizer, Italy) and Dexamethasone (Farmaceutici CABER, Italy) were used for combination assays. The doses employed for the combination were chosen under the IC50 value for each agent, calculated with Compusyn software (Compusyn; Biosoft, Cambridge, UK), performing single dose/effect curves (data not shown) for each cell line or xenograft blasts. Cells were incubated with vehicle, drugs alone or in combination for 72 hours and then inhibition of proliferation or cytotoxic effect was tested as previously described.

Drug additivity or synergy was determined by using the criteria described by Greco et al. (31). Briefly, the effect of each drug was expressed as the ratio of drug treated sample/vehicle. For each point, synergy or additivity was calculated using the Bliss independence model defined by the equation: $E_{xy}=E_x+E_y-(E_xxE_y)$, where (E_{xy}) is the additive effect of drugs x and y as predicted by their observed individual effects (E_x and E_y). Therefore E_{xy} represents the Expected value (EV) in case of additivity of the compounds, while the Actual value (AV) indicated the real observed effect of the combination. Since in this issue the effect was evaluated as the reduction of proliferating cells/live cells, we considered both drugs additive when AV=EV, synergic: AV>EV and antagonists when AV<EV.

RESULTS

Givinostat inhibits growth, induces apoptosis and blocks STAT5 phosphorylation in *CRLF2* rearranged cell lines

We measured the effect of Givinostat on inhibition of proliferation and induction of apoptosis in long term culture of BCP-ALL cell lines MHH-CALL4 and MUTZ5, both harboring *IGH@-CRLF2* rearrangement and *JAK2* mutation. SET2 essential thrombocytemia cell line, bearing V617F mutation of JAK2, was chosen as positive control and K562 chronic myelogenous leukemia cell line, (*BCR/ABL* positive), was included as negative one (16). As shown in figure 1, treatment with Givinostat reduced the proliferation of MHH-CALL4 and MUTZ5 cells within 72 hours with IC50 values of 0.08±0.05uM and 0.17±0.07uM, respectively. Moreover, Givinostat induced a decrease in viable cells with IC50 of 0.17±0.03uM for MHH-CALL4 and 0.25±0.03 uM for MUTZ5 cell line. Of note, the observed IC50 values for MHH-CALL4 were lower than those for SET2 positive control both for proliferation (IC50: 0.08±0.05uM vs. 0.14±0.03uM) and apoptosis (IC50: 0.17±0.03 vs. 0.22±0.04uM) (Figure 1, panel A-B). In order to investigate if Givinostat could have an effect on modulating CRLF2-mediated JAK/STAT pathway, we examined the phosphorylation status of STAT5 after treatment with the drug, in basal state or after TSLP stimulation. As expected, due to JAK2 point mutation, high basal level of pSTAT5 was observed in MHH-CALL4 e

MUTZ5. Low concentration of TSLP (1 ng/ml) robustly increased pSTAT5 (1.5 to 2.2 fold increase for MHH-CALL4 and MUTZ5, respectively). Givinostat (0.2uM) inhibited pSTAT5 in both cell lines in basal conditions (we detected 3.9 and 4.5 fold decreases of median values of pSTAT5 for MUTZ5 and MHH-CALL4, respectively) and reduced phosphorylation below basal levels after cytokine stimulation (2.8 and 2.1 fold decreases under basal levels for MUTZ5 and MHH-CALL4, respectively) (Figure 1, panel C).

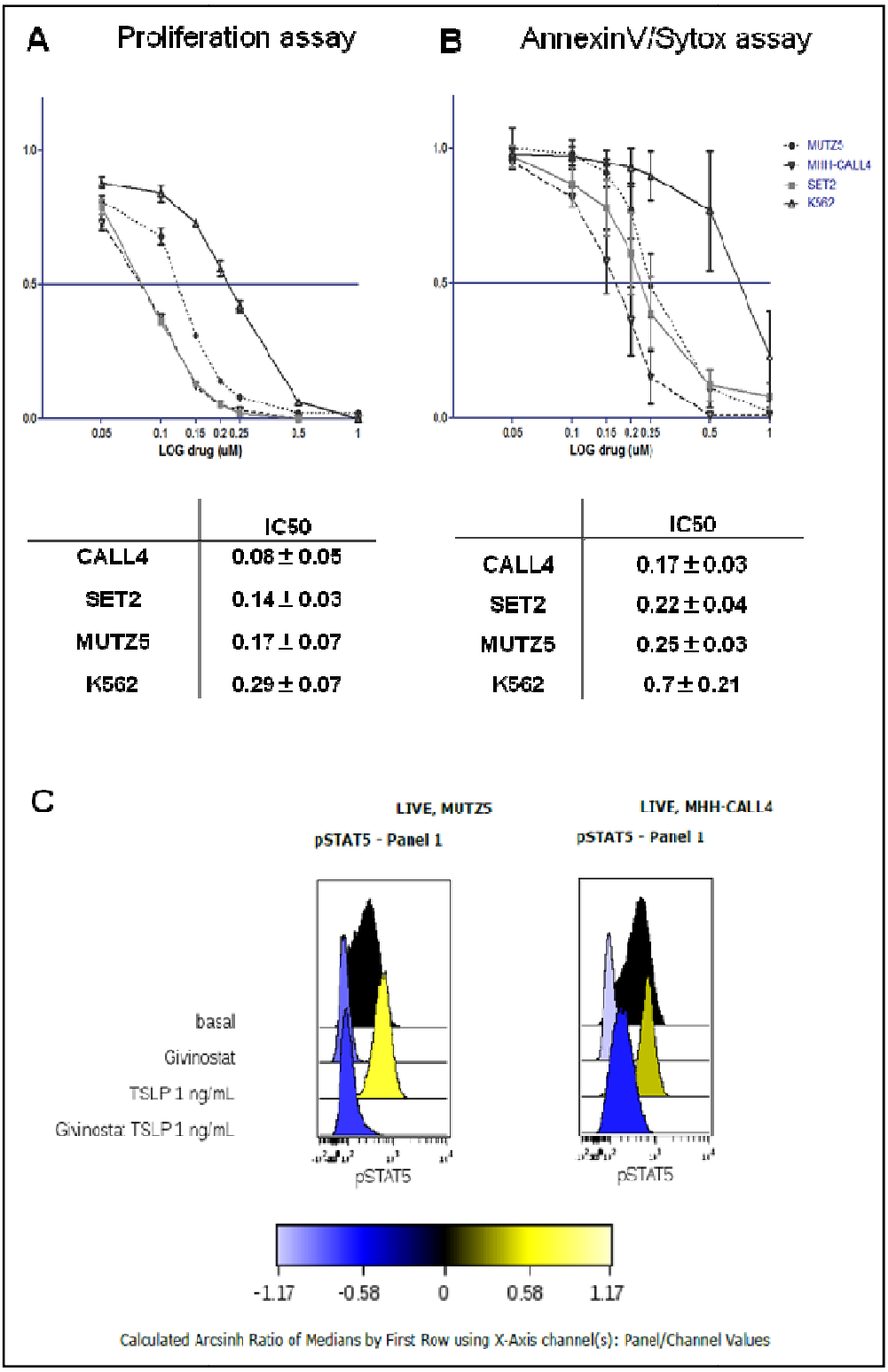

	IC50
CALL4	0.08 ± 0.05
SET2	0.14 ⊥ 0.03
MUTZ5	0.17 ⊥ 0.07
K562	0.29 ± 0.07

	IC50
CALL4	0.17 ± 0.03
SET2	0.22 ± 0.04
MUTZ5	0.25 ± 0.03
K562	0.7 ± 0.21

Figure 1. Anti-proliferative and pro-apoptotic effect of Givinostat on cell lines (A) *Analysis of proliferation performed by flow cytometric count of live cells (Annex V/Sytox double negative) measured in a defined time interval (30').* ***(B)*** *Analysis of apoptosis by Annexin V/Sytox assay on MHH-CALL4, MUTZ5, SET2 and K562 cell lines. Y axis: percentage of Givinostat treated live cells (Annexin V/Sytox double negative) normalized on percentage of vehicle treated cells. X axis: logaritmic increasing doses of Givinostat. The IC50 of individual samples are shown in reported tables both for proliferation and apoptosis. (**C**) Inhibition of basal and TSLP-induced STAT5 phosphorylation after treatment with Givinostat in CRLF2 rearranged cell lines. MHH-CALL4 and MUTZ5 were plated at 0.1x10^6 cells/well in 24 wells for 24 hours in presence of 0.2uM Givinostat or vehicle. Data were normalized to the basal pSTAT5 phosphorylation level for colorimetric depiction of signaling changes. Blue indicates inhibition and yellow is stimulation.*

Patient-derived ALL-xenograft samples

To confirm the data obtained with cell lines, we decided to further investigate the effect of Givinostat on blasts from *CRLF2* rearranged BCP-ALL patients. To this purpose we developed xenograft models of human *CRLF2* rearranged ALL to expand cells from patients and to recapitulate human leukemia in recipient mice. Diagnostic specimens from 5 patients were intravenously injected into immunodeficient mice and engraftment was determined measuring the percentage of human CD10+/CD19+/CRLF2+ blasts in the bone marrow by flow cytometry. These 5 samples were all *CRLF2* rearranged (*CRLF2r*) with *P2RY8-CRLF2* fusion and 1 out of 5 harbored *JAK2* mutation (*JAKm*) as listed in Table 1. The mutation consist of a not yet described insertion (L681-I682 insEA) in exon 16.

Table 1

Clinical Characteristics and genetic lesions of BCP-ALL samples

Sample no.	protocol	age at diagnosis (years)	sex	WBC x10^3/ul	Down Syndrome	Immunophenotype	Prednisone response	MRD risk	Final risk	CRLF2r	JAK2	Other genetic lesions
Pt # 1	ALL2000	5	F	16600	no	CALL	PGR	SR	SR	*P2RY8-CRLF2*	wt	del *CDKN2A/2B* ; del *BTG1*
Pt # 2	ALL2009	3	F	87210	no	B-II	PGR	SR	B-SR	*P2RY8-CRLF2*	wt	del *CDKN2A/2B* ; del *PAX5*
Pt # 3	ALL2009	2	M	23940	yes	B-II	PGR	SR	B-SR	*P2RY8-CRLF2*	wt	del *CDKN2A/2B*
Pt # 4	ALL2009	15	M	1870	yes	B-II	PGR	MR-SER	HR	*P2RY8-CRLF2*	L681-I682 insEA	del *IKZF* ; del omo *CDKN2A/2B* ; del *PAX5*
Pt # 5	ALL2009	4	F		yes	B-III	PGR	MR	HR	*P2RY8-CRLF2*	wt	del *PAX5* ; del *BTG1*

PGR = prednisone good responder; SR= standard risk; MR=medium risk; HR=high risk; SER= slow responder.

All 5 samples successfully engrafted in NOD/SCID mice. The animals were sacrificed when they reached 80% of human blasts in bone marrow and spleen, and the recovered cells were used for *ex-vivo* analyses and for further serial transplantations to perform preclinical *in vivo* studies.

Givinostat induces apoptosis of *CRLF2* rearranged xenograft blasts

ALL blasts isolated from xenografted mice were co-cultured on OP9 stroma to perform *ex vivo* assays. In contrast with cell lines, blasts are not able to expand and proliferate when cultured *ex vivo* (32), for this reason in this system we only evaluated induction of apoptosis. Consistent with our findings in cell lines, Givinostat (0.2uM) reduced the percentage of live cells (Annexin V/Sytox negative) in all xenograft blasts treated with the drug up to one week of observation (Figure 2A). In particular, Givinostat, after 72 hours, was able to kill about 100% of blasts of all tested patients. The induction of cell death in Givinostat treated samples was confirmed using CyTOF technology. In Figure 2B, we showed the modification of the expression of 4 surface markers after treatment with the drug for a representative sample (patient 2). The analysis and the data representation was performed by viSNE software. The complete panel of analysis with the remaining 8 out of 12 markers is shown in supplementary figure 1. CRLF2, CD10,and the most proliferative Ki67 positive blasts notably diminished after 24 hours of treatment with Givinostat, while CD45 high,

IgMi, IgMs positive cells, representative of the normal hematopoietic counterpart, remained unchanged. Moreover, the analysis performed with another software named SPADE showed that, in this patient, the total number of recorded events was lower in Givinostat treated sample (25% of reduction) and most of the missing cells after treatment were CD10 positive and specifically CRLF2 high. Indeed, the bubble indicating CD10+ cells changed from 70% of total events to 44% after treatment and CRLF2+ cells decreased from 42% to 18.4%. On the contrary, normal CD45 high cells were 8.9% of total events before and after treatment (supplementary figure 2). The results were confirmed in 3 other patients (data not shown)

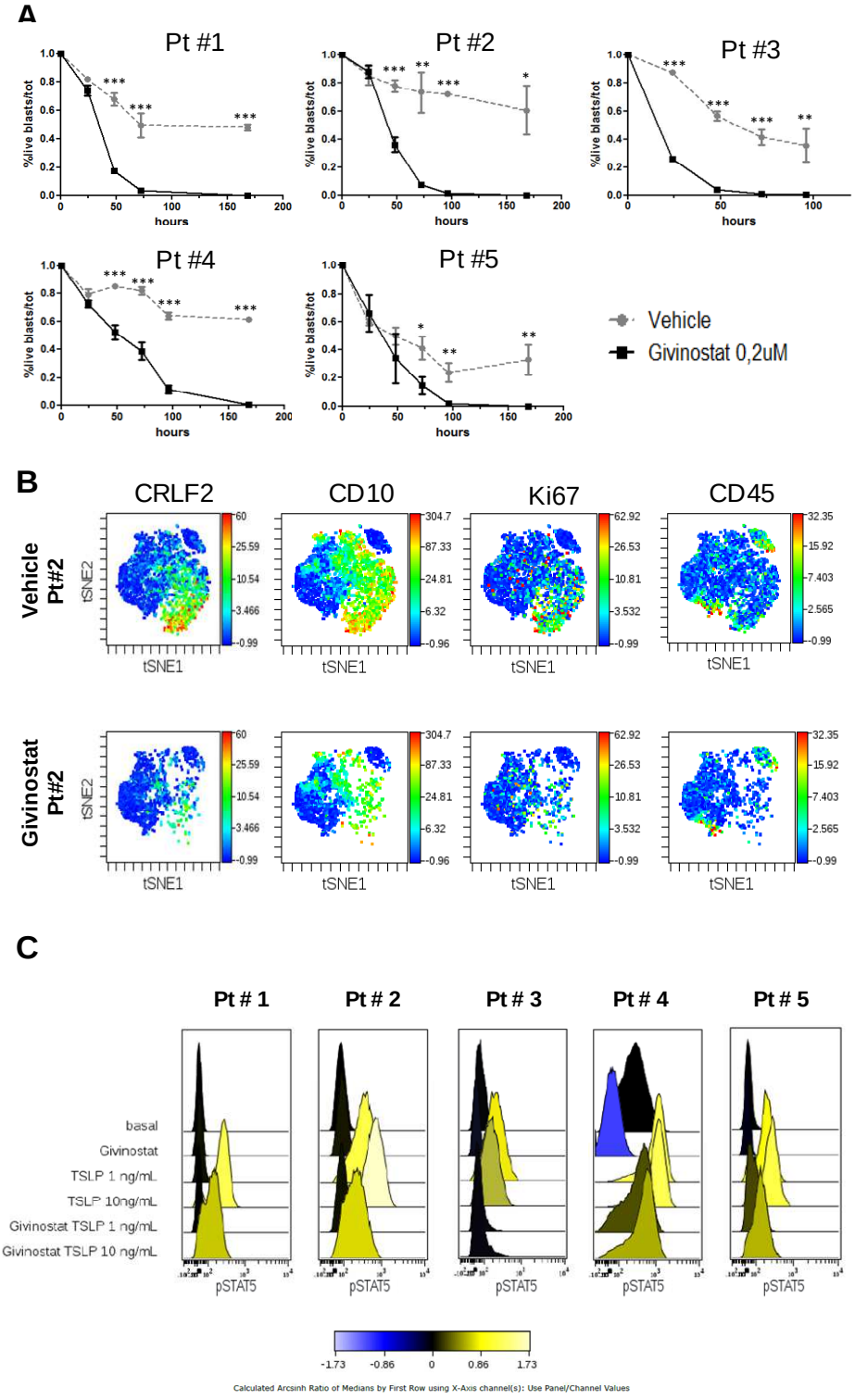
A
Pt #1
Pt #2
Pt #3
Pt #4
Pt #5
%live blasts/tot
hours
Vehicle
Givinostat 0,2uM
B
CRLF2
CD10
Ki67
CD45
Vehicle Pt#2
Givinostat Pt#2
tSNE1
tSNE2
C
Pt # 1
Pt # 2
Pt # 3
Pt # 4
Pt # 5
basal
Givinostat
TSLP 1 ng/mL
TSLP 10ng/mL
Givinostat TSLP 1 ng/mL
Givinostat TSLP 10 ng/mL
pSTAT5
Calculated Arcsinh Ratio of Medians by First Row using X-Axis channel(s): Use Panel/Channel Values

Figure 2. Induction of cell death on xenograft blasts by Givinostat *(A) Analysis of apoptosis of CRLF2 rearranged xenograft blasts after exposure to Givinostat ex-vivo. Freshly isolated blasts from xenograft models listed in Table 1 were plated in medium on a layer of confluent OP9 stroma in presence of Givinostat (0.2μM) or vehicle. After 24h up to one week (168h), non-adherent cells were collected and cellular viability analyzed on the FACS by Annexin V/Sytox staining. The percentage of live (Annexin V/Sytox double negative) human CD10+/mouse CD45.1 negative cells, normalized on their T0, was shown in each panel. (B) Application of viSNE to leukemic bone marrow sample from patient 2 before and after treatment with Givinostat (0.2μM for 24 hours). Each point in the viSNE map represents an individual cell and is colored according on the intensity of selected marker. Here we show only 4 selected markers from the original panel (CRLF2, CD10, Ki67, CD45). After treatment with Givinostat the number of dots belonging to high expressing CRLF2, CD10 and Ki67 group was drastically diminished whereas the high CD45 residue remains unaffected. (C) Inhibition of STAT5 phosphorylation after treatment with Givinostat in xenograft blasts. Xenograft blasts were plated on OP9 stroma and exposed to 0.2uM Givinostat or vehicle for 24 hours. Stimulation with 1-10 ng/ml TSLP-induced phosphorylation of STAT5 in vehicle treated blasts and Givinostat was able to inhibit this effect. Xeno 4 had an increased level of pSTAT5 probably due to Jak2 mutation. Data were normalized to the basal phosphorylation level of STAT5 protein for colorimetric depiction of signaling changes. Blue indicates inhibition and yellow is stimulation.*

Givinostat inhibits signal transduction in *CRLF2* rearranged xenograft blasts

We examined the effect of Givinostat on STAT5 phosphorylation in *CRLF2* rearranged xenograft blasts. Basal pSTAT5 level was lower in blasts than in cell lines, except for patient 4 who presented an insertion in *JAK2* gene sequence, probably hyperactivating. This patient showed a value of pSTAT5 5.7 fold higher than the mean of basal pSTAT5 of the other four patients. Low concentration of TSLP (1ng/ml)

induced STAT5 activation in all xenograft blasts except for patient 1. Therefore, we tested a higher dose of the cytokine (10ng/ml) too. Givinostat (0.2uM) inhibited pSTAT5 after cytokine stimulation in all tested xenograft blasts (mean fold decrease of pSTAT5: 2.4±0.6) (Figure 2C). For patient 4, the inhibition was markedly observed also in basal conditions (pSTAT5 fold decrease: 6.6).

Givinostat modulates the JAK/STAT pathway in *CRLF2* rearranged leukemia cells

To gain insights into molecular processes modulated by Givinostat in leukemia cells harboring the CRLF2 rearrangement, we analyzed the gene expression profiles of primary leukemia cells (N=5) isolated from ALL bearing recipients incubated ex vivo with 0.2 µM Givinostat or DMSO (vehicle) for 6 hours. Givinostat is an epigenetic drug and acts as an HDACi; as expected, it induced a drastic modification at the transcriptome level resulting in almost a distinct clustering between treated and untreated samples already by unsupervised analysis (Figure 3A). Furthermore, gene set enrichment analysis (GSEA) identified a positive enrichment in Givinostat treated specimens for epigenetically silenced cancer genes up-regulated also upon treatment with 5-aza-2'-deoxycytidine (Aza-dC) and/or trichostatin A (TSA), which supports the action of the compound as an epigenetic modifier (Supplementary Figure 3A). According to SAM (Significance

Analysis of Microarrays) analysis, we identified 1228 unique genes (2068 probe sets) differentially expressed between control and treated samples with a FDR<0.05. In particular, 493 and 735 genes resulted up- and down-regulated in Givinostat treated samples, respectively as shown in the supervised analysis (Supplementary Figure 3B). According to Gene Ontology (GO) analysis, the 1228 genes were grouped into 6 main functional categories: phosphorilation, alternative splicing, SH2 domain (i.e. the protein phospho-tyrosine binding domain), actin-binding, Kinase and cytoplasm (p-value<0.05 and FDR<0.05). To reveal relevant biological processes affected by Givinostat we performed a pathway analysis interrogating the KEGG database. Apoptosis, cell cycle, B cell receptor signaling, insulin signaling, p53 signaling and, even more intriguingly, JAK/STAT signaling resulted within the top 20 ranked pathways modulated by the treatment (Supplementary Table 2 and Supplementary Figure 3C). In particular, the transcriptional modification induced by Givinostat in genes related to the JAK/STAT signaling pathway was also confirmed by the negative enrichment of the JAK/STAT gene signature according to GSEA in the treated samples, Figure 3B. Different regulation of Genes included in the JAK/STAT signaling pathway: *STAT5A*, *JAK2*, *IL7Rα*, *CRLF2* was validated also by quantitative RT-PCR (Figure 3C). In addition, STAT5 target genes with oncogenic function, *BCL2L1* and *cMYC* were downregulated by the treatment. On the contrary, *PTPN1* gene,

coding for a tyrosine phosphatase able to dephosphorylate JAK2 was upregulated in 3 out of 4 tested patients.

Moreover, the down regulation of *CRLF2* gene was also confirmed at a protein level upon Givinostat administration by flow cytometry. Blasts were gated for human CD10 expression and MFI values of CRLF2 positive population were evaluated. Downmodulation of CRLF2 protein on cell surface was measured in all tested xenograft blasts after treatment with Givinostat at 0,2uM for 24 hours. One representative experiment performed on patient 3 was showed in figure 3D. For this patient, the median of CRLF2 peak of Givinostat treated sample was 2.4 fold lower than vehicle.

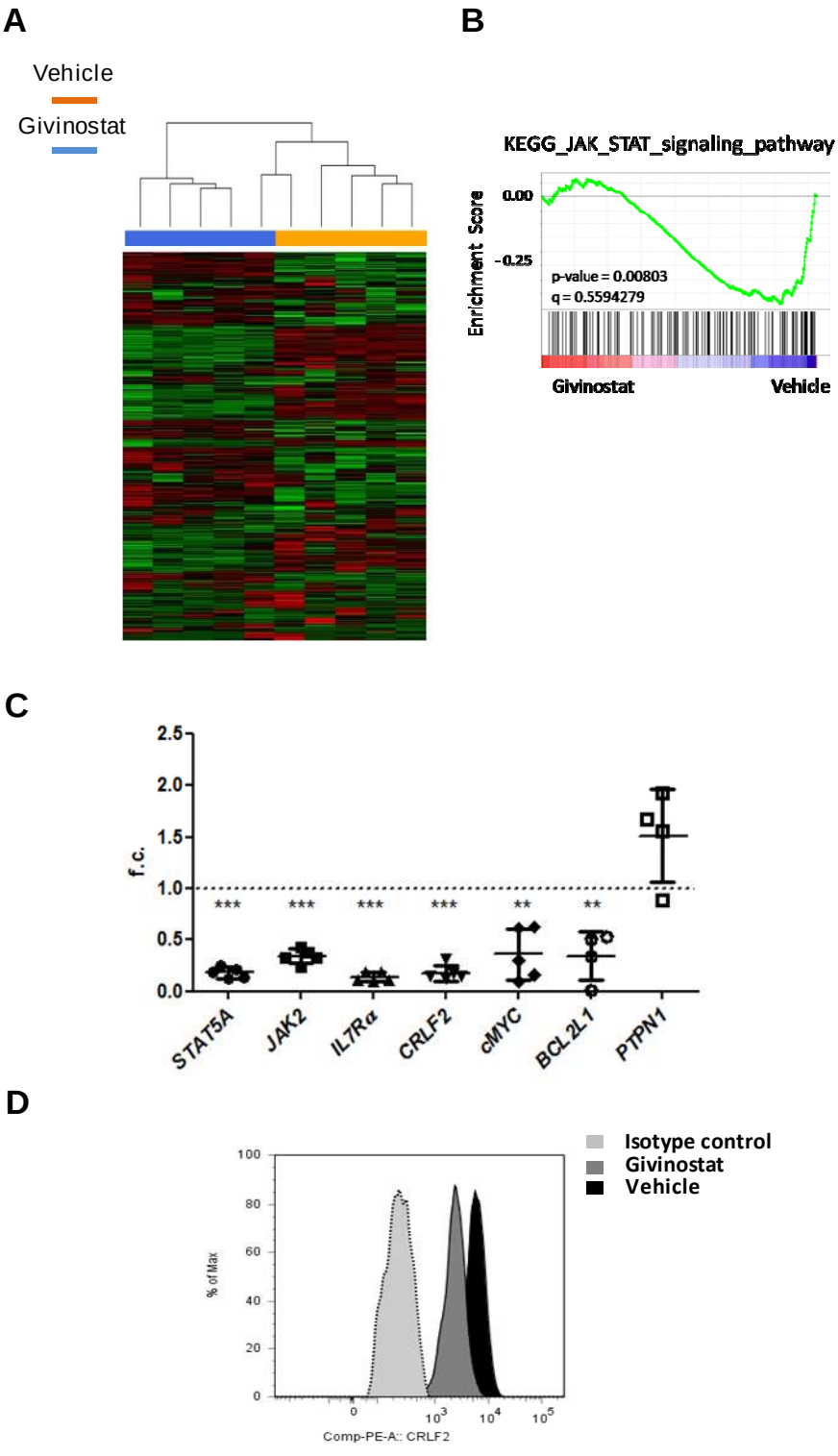
A
Vehicle
Givinostat
B
KEGG_JAK_STAT_signaling_pathway
Enrichment Score
0.00
-0.25
p-value = 0.00803
q = 0.5594279
Givinostat
Vehicle
C
f.c.
2.5
2.0
1.5
1.0
0.5
0.0
***
***
***
***
**
**
STAT5A
JAK2
IL7Rα
CRLF2
cMYC
BCL2L1
PTPN1
D
Isotype control
Givinostat
Vehicle
% of Max
100
80
60
40
20
0
0
10^3
10^4
10^5
Comp-PE-A:: CRLF2

Figure 3. Effect of Givinostat on genes involved in JAK/STAT pathway. *(A) Unsupervised hierarchical clustering analysis using probe sets values normalized with RMA and filtered by variance >90% between treated (in blue) and control samples (orange) to highlight associations between clusters of samples and clusters of genes. (C) GSEA analysis plot showing the negative enrichment of the "KEGG_JAK_STAT_signaling_pathway" gene set in Givinostat treated samples (negative Normalized Enrichment Score, NES= -1.4461855) and the corresponding positive enrichment in Vehicle treated samples. The green curve reflects the enrichment score of the genes included in the considered gene set and the ranked differentially regulated genes between the two considered phenotypes (i.e. Givinostat versus Vehicle). (C) Genes involved in JAK/STAT pathway were measured by RQ-PCR. The graphs report the relative gene expression of the indicated genes in drug-treated cells versus untreated cells whose gene expression was conventionally set at value 1. (D) Surface expression of CRLF2 after treatment with Givinostat. MFI are plotted for a representative patient (pt 2).*

Givinostat inhibits engraftment of blasts in xenograft models of *CRLF2* rearranged BCP-ALL

To determine the efficacy and the therapeutic activity of Givinostat, *in vivo* models of CRLF2+ BCP-ALL was set up by injecting intravenously blasts from patients 1, 2 and 3 listed in Table 1, as previously described. Seven days after transplantation, mice were randomized and received Givinostat at 30 mg/kg or vehicle via i.p (5 days/week). Disease burden was assessed after 7 weeks of treatment when mice were sacrificed and bone marrow and spleen were collected for analysis. All three *CRLF2* rearranged xenograft models exhibited decreased leukemia burden with Givinostat treatment compared to vehicle, evidenced by a decreased of total blast

count in the bone marrow of treated mice (ranging from 1.9 to 34 fold decrease). Moreover, in patient 1 derived xenograft, was observed also a decrease of disease burden in the spleen (128 fold decrease). Unfortunately, the effect of Givinostat in the spleen was not evaluable for the other patient derived xenografts, since in these mice very low level of blast engraftment was observed even in absence of the drug (figure 4).

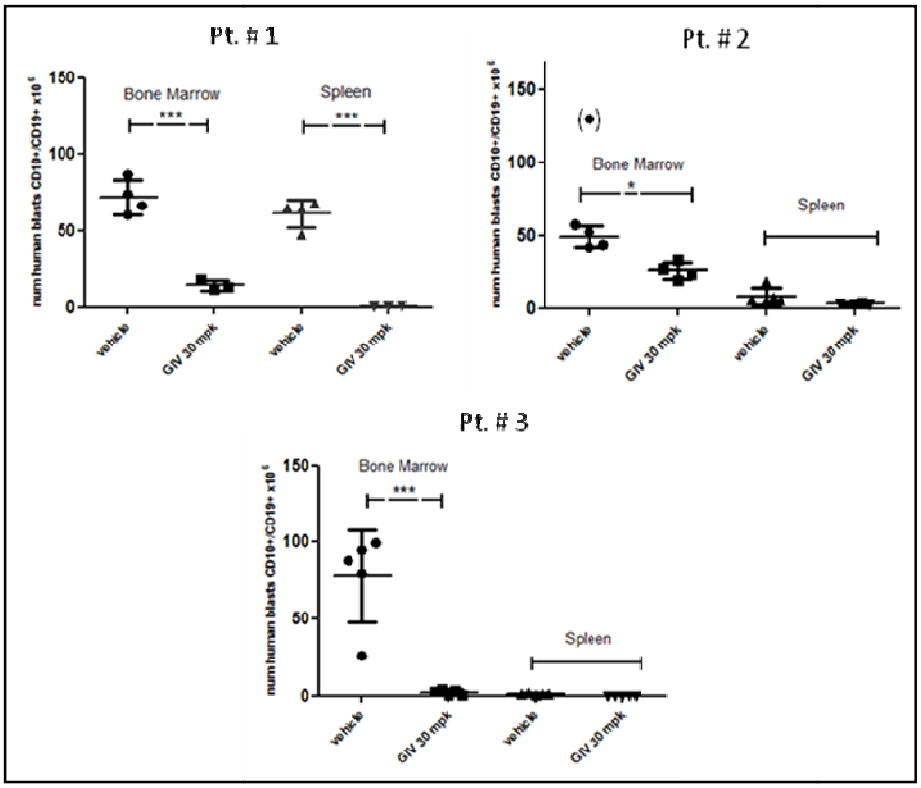

Figure 4. Efficacy of Givinostat in xenograft model of CRLF2 rearranged BCP-ALL. *Bone marrow and spleen blast counts at sacrifice in patient 1, 2, 3 xenograft models (3-5 mice per arm). Distribution of absolute blast count identified as human CD10/CD19 double positive cells with means and standard deviation are graphed. One outlier in vehicle treated group (xenograft of patient 2) is plotted in brackets, it has been analyzed but excluded from the statistics.*

Givinostat increases the effect of chemotherapy in CRLF2 rearranged cell lines and in xenograft blasts

Having established the single-agent efficacy of Givinostat, we next evaluated the effect of the drug in combination with remission induction chemotherapeutics used in pediatric protocols. First of all, we tested the combination of Givinostat with Methyl-prednisolone, the first drug administered to patients in induction regimen and a strong predictor of clinical outcome. Initially, we measured the *in vitro* sensitivity of MHH-CALL4 and MUTZ5 cell lines to Methyl-prednisolone as monotherapy and we found that, while MUTZ5 cells were sensitive (33) to Methyl-prednisolone (IC50 for cytotoxicity: 0,007ug/ml), MHH-CALL4 (IC50 for cytotoxicity: 4,5ug/ml) were never completely killed by the chemotherapeutic, even at high doses of the drug (about 30% of resistant cells). As result of these observations, we decided to test the anti-proliferative and cytotoxic effect of the combination of Givinostat with Methyl-prednisolone in MHH-CALL4 cell line. We demonstrated that Givinostat was able to sensitize these cells to Methyl prednisolone and a synergic effect of the drugs was measured using the Bliss formula (Figure 5A and 5B).

Moreover, we demonstrated that Givinostat was also able to synergize with a mix of chemiotherapeutics currently used in remission induction therapy: Vincristine, Dexamethasone and Asparaginase (VDA). Monotherapy efficacy studies were performed for each drug (data not shown) and values under IC50 were chosen for the combination setting. The doses used

to create the mix of the three drugs were different for MHH-CALL4 and MUTZ5 according to the diverse IC50 values calculated for the single agents. We showed that a low dose of Givinostat (0,1uM) increased the ability of VDA to induce inhibition of proliferation and cell death in MHH-CALL4 cell line *in vitro*. The observed effect on proliferation and apoptosis was significantly higher than the effect reached with single agents and of that expected by the combination (calculated with Bliss formula), indicating synergism of the drugs. One representative experiment out of three was shown in figure 5, panel C-D. Combination assays performed on MUTZ5 are shown in supplementary figure 4.

We then confirmed the data on xenograft blasts co-cultured *ex-vivo* on OP9 stroma. Xenograft blasts showed a substantial decrease of vitality after 72 hours of culture even in the absence of drugs but, as shown in figure 5 panel E, we found a significative strong cytotoxic activity of Givinostat in combination with both Methyl-prednisolone and VDA. In particular, the effect of combination, evaluated with Bliss formula, showed an additive effect for patients 1, 2, 3 and a synergic effect for patient 4 both of Methyl-prednisolone and of VDA with Givinostat.

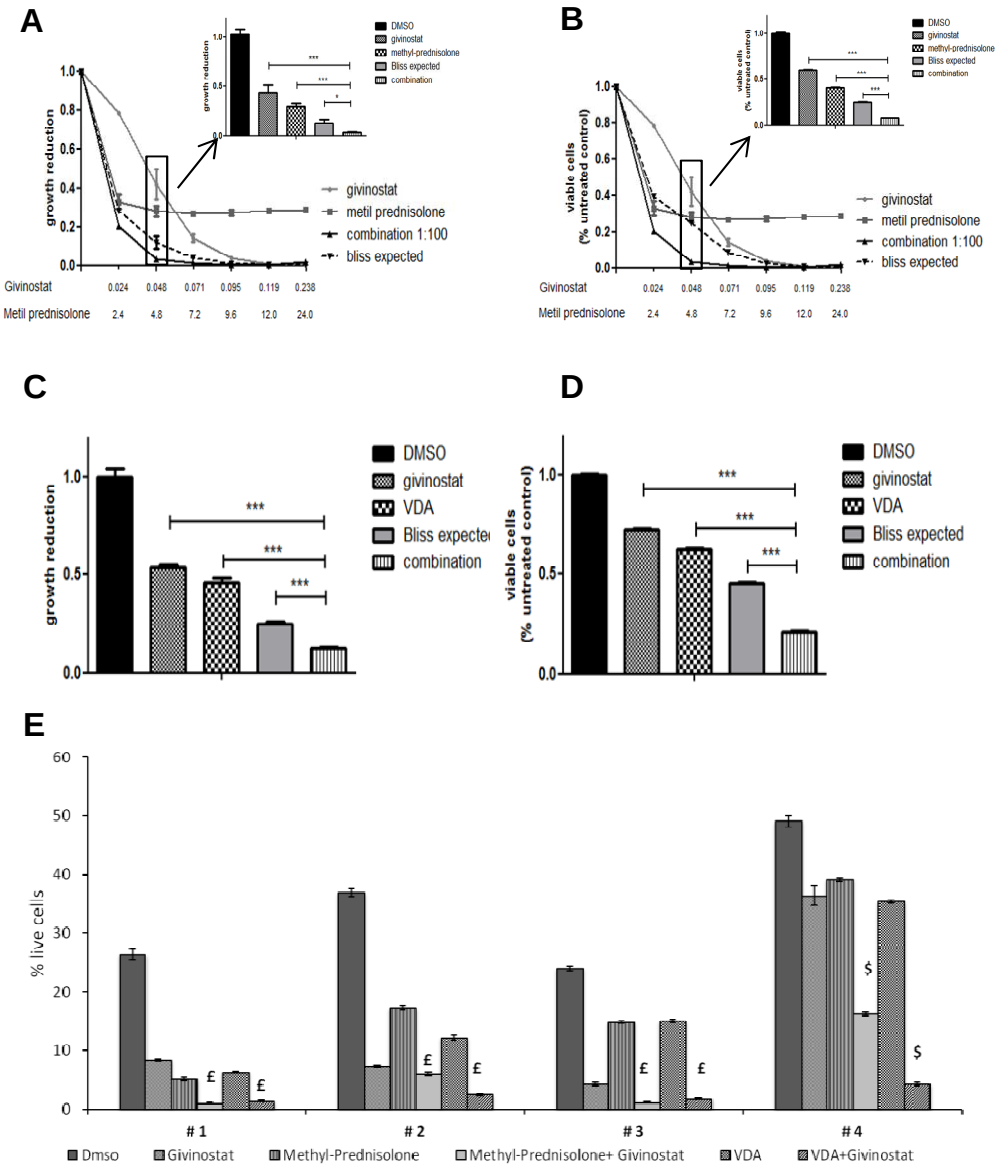

p value	# 1	# 2	# 3	# 4
VDA+GIV vs VDA	<0,001	<0,001	<0,001	<0,001
VDA+GIV vs GIV	<0,001	<0,001	<0,001	<0,001
PREDN+GIV vs PREDN	<0,001	0,0014	<0,001	<0,001
PREDN+GIV vs GIV	<0,001	ns	<0,001	<0,001

***Figure 5. Effect of combination of Givinostat with conventional chemotherapy**. In vitro response of MHH-CALL4 at Methyl-prednisolone and Givinostat alone or in combination determined by proliferation assay (A) and Annexin/Sytox assay (B) in a dose escalation expressed in µg/ml after 72 hours of treatment. Dotted lines indicate the expected effect of the combination calculated with Bliss formula. The significance for the lowest dose of both drugs with the highest effect were shown in the black box in detail. Proliferation (C) and Annexin/Sytox assay (D) performed on MHH-CALL4 with Givinostat (0.1 µM) and VDA (Asparaginase 0,23 ug/ml; Desametasone 0,01 ug/ml; Vincristine 0,001 ug/ml). The expected effect is represented by grey column. (E) Effect of combination on xenograft blasts from patient 1 to 4 after 72 hours of treatment. Givinostat (0.1 µM) was combined with VDA (Asparaginase 0,12 ug/ml; Desametasone 0,01 ug/ml; Vincristine 0,001 ug/ml) and Methyl-prednisolone (4.8 ug/ml). The percentage of viable cells are reported on Y axis. The £ represents additivity (Bliss formula: EV=AV) and the $ indicates synergy (EV<AV). The significant differences between conditions with their p-values are reported in the table.*

DISCUSSION

Rearrangements of *CRLF2*, leading to overexpression of this component of the heterodimeric cytokine receptor for TSLP, are present in up to 7% of childhood BCP-ALL overall and 60-70% of DS-ALL. This subgroup of patients is characterized by a particularly bad prognosis. Recent phosphoflow cytometry results indicate that BCP-ALL leukemic samples which arbor *CRLF2* rearrangements (with or without concomitant *JAK* mutations) have increased signaling strength trough JAK2/STAT5 or PI3K/mTOR pathway that could be potentially be targeted with JAK or PI3K inhibitors (9). The JAK/STAT pathway represent one of the main signaling cascade mediating cytokine receptor and plays a role in hematopoietic cell growth, proliferation, differentiation and survival (34). A variety of

hematologic malignancies activate JAK pathway signaling inappropriately through several mechanisms, including activating mutations, fusions and downregulation of negative regulators (35-39). Nowadays, few data exist on effective treatment strategies for *CRLF2* rearranged and *JAK* mutated ALL. Some reports demonstrated efficacy of heat shock protein 90 inhibition and minimal activity of JAK inhibitor BVB808 in *CRLF2* rearranged BCP-ALL (40). Recently, Maude et al. reported *in vivo* efficacy of JAK1/2 inhibitor Ruxolitinib on ALL xenograft with JAK activating lesions. However, in *CRLF2* overexpressed cases without JAK mutation, Ruxolitinib showed a modest effect in reducing tumor burden, indicating that a broader anti tumoral effect was requested in this cases (12). In the present work we investigated the effect of Givinostat, a pan hystone deacetylase inhibitor, on *CRLF2* rearranged cases. This drug is already in clinic for the treatment of myeloproliferative disorders. In particular, Givinostat demonstrated to be significantly active in Polycythemia Vera cases with *JAK2 V617F* mutant, an alteration which induced an hyperactivation of JAK/STAT signaling pathway.

We showed here the efficacy of Givinostat in inhibiting proliferation and inducing cell death of BCP-ALL *CRLF2* rearranged cell lines at very low doses, with an IC50 similar or lower than positive control JAK2 V617F mutated SET2 cells. The cytotoxic effect was confirmed also on primary blasts from patients harboring *CRLF2* rearrangements. Importantly, Givinostat was able to efficiently kill blast cells preserving the

normal hematopoietic counterpart. This consideration could be exerted evaluating the data coming from CyTOF analyses. CyTOF represents a new generation of single cell technology that overcomes the limitations of fluorescence-based flow cytometry (41) because stable isotopes are used as reporters instead of fluorophores. This enables a significant increase in the number of measurable parameters per cell and furthermore we can benefit of a quantitatively accurate platform with linear sensitivity across four orders of magnitude. This single cell analysis allow to understand how the single populations changes in response to the drugs and, in this case in particular, it showed that the cellular population particularly affected by Givinostat was represented by blasts with high expression of CRLF2, while the CD45+ normal hematopoietic cells remain unaffected by the treatment.

Since Givinostat is an epigenetic drug able to remodel chromatine and to affect transcription, we focused on its effect on genes involved in JAK/STAT pathway. Of particular interest was the observed downmodulation of the activator of transcription *STAT5* and of its targets *cMYC* and *BCL2L1*. These results highlight the potential for targeting 'undragable' oncogenic transcription factors with epigenetic regulators involved in chromatine remodeling, since the direct targeting of STAT proteins remain a great challenge. Interestingly, Givinostat downmodulated also *CRLF2* gene itself and consequently, the expression of the surface protein was reduced. This is particularly important in this subtype of ALL,

since the overexpression of this receptor drives proliferation and survival processes. Furthermore, Givinostat was able to impair the signaling network related to CRLF2 as it reduced the STAT5 phosphorylation level both at basal condition and after TSLP stimulation. It remains to be investigated if the effect on STAT5 phosphorylation observed was due to an impairment of signaling cascade or to a decrease of total amount of STAT5 protein. Further investigation will be necessary to elucidate this aspect but the final goal of reducing pSTAT5 was anyway achieved. Nevertheless, the effect of inhibition of the pathway was reached involving different players at different levels of regulation. *PTPN1* gene for instance, coding for a tyrosine phosphatase able to dephosphorylate and inhactivate JAK2, was upregulated by the drug.

Importantly, we have established the preclinical *in vivo* efficacy of Givinostat on xenograft models of three different *CRLF2* rearranged patients. Moreover, we demonstrated the efficacy of Givinostat in combination with other chemotherapeutics on cell lines and on blasts from *CRLF2* rearranged patients. Of note, the most responsive patient to Givinostat in combination with Methyl-prednisolone and VDA was a DS-ALL patient belonging to MRD high risk group, thus resulting refractory to the conventional therapy. Furthermore this case showed hyperactivation of JAK/STAT network due probably to a not yet described *JAK2* insertion.

The strong effect of low doses of Givinostat in combination with current chemotherapy is intriguing because it elevates the

potential of epigenetic therapies in pediatric ALLs and suggests a role for these therapies in at least some subtypes of high risk ALL like *CRLF2* rearranged BCP-ALL for which cytotoxic chemotherapy yields suboptimal cure rates. Of note, in our cohort three out of five patients were DS-ALL. In the future, it would be helpful to focus on this cathegory of patients which particularly suffer of therapy- related side effects and then that could benefit on the introduction of new therapeutic agents in their present regimen of chemotherapy in order to reduce the doses of currently used chemotherapeutics and their related toxicity and morbidity.

REFERENCES

1. Hunger SP, Lu X, Devidas M, Camitta BM, Gaynon PS, Winick NJ, et al. Improved survival for children and adolescents with acute lymphoblastic leukemia between 1990 and 2005: a report from the children's oncology group. J Clin Oncol 2012;30(14):1663-9.
2. Chen IM, Harvey RC, Mullighan CG, Gastier-Foster J, Wharton W, Kang H, et al. Outcome modeling with CRLF2, IKZF1, JAK, and minimal residual disease in pediatric acute lymphoblastic leukemia: a Children's Oncology Group study. Blood 2012;119(15):3512-22.
3. Mullighan CG, Collins-Underwood JR, Phillips LA, Loudin MG, Liu W, Zhang J, et al. Rearrangement of CRLF2 in B-progenitor- and Down syndrome-associated acute lymphoblastic leukemia. Nat Genet 2009;41(11):1243-6.
4. Russell LJ, Capasso M, Vater I, Akasaka T, Bernard OA, Calasanz MJ, et al. Deregulated expression of cytokine receptor gene, CRLF2, is involved in lymphoid transformation in B-cell precursor acute lymphoblastic leukemia. Blood 2009;114(13):2688-98.
5. Ensor HM, Schwab C, Russell LJ, Richards SM, Morrison H, Masic D, et al. Demographic, clinical and outcome features of

children with acute lymphoblastic leukemia and CRLF2 deregulation: results from the MRC ALL97 clinical trial. Blood 2011;117(7):2129-36.
6. Harvey RC, Mullighan CG, Wang X, Dobbin KK, Davidson GS, Bedrick EJ, et al. Identification of novel cluster groups in pediatric high-risk B-precursor acute lymphoblastic leukemia with gene expression profiling: correlation with genome-wide DNA copy number alterations, clinical characteristics, and outcome. Blood 2010;116(23):4874-84.
7. Hertzberg L, Vendramini E, Ganmore I, Cazzaniga G, Schmitz M, Chalker J, et al. Down syndrome acute lymphoblastic leukemia, a highly heterogeneous disease in which aberrant expression of CRLF2 is associated with mutated JAK2: a report from the International BFM Study Group. Blood 2010;115(5):1006-17.
8. Carpino N, Thierfelder WE, Chang MS, Saris C, Turner SJ, Ziegler SF, et al. Absence of an essential role for thymic stromal lymphopoietin receptor in murine B-cell development. Mol Cell Biol 2004;24(6):2584-92.
9. Tasian SK, Doral MY, Borowitz MJ, Wood BL, Chen IM, Harvey RC, et al. Aberrant STAT5 and PI3K/mTOR pathway signaling occurs in human CRLF2-rearranged B-precursor acute lymphoblastic leukemia. Blood 2012;120(4):833-42.
10. Mullighan CG, Zhang J, Harvey RC, Collins-Underwood JR, Schulman BA, Phillips LA, et al. JAK mutations in high-risk childhood acute lymphoblastic leukemia. Proc Natl Acad Sci U S A 2009;106(23):9414-8.
11. Yoda A, Yoda Y, Chiaretti S, Bar-Natan M, Mani K, Rodig SJ, et al. Functional screening identifies CRLF2 in precursor B-cell acute lymphoblastic leukemia. Proc Natl Acad Sci U S A 2010;107(1):252-7.
12. Maude SL, Tasian SK, Vincent T, Hall JW, Sheen C, Roberts KG, et al. Targeting JAK1/2 and mTOR in murine xenograft models of Ph-like acute lymphoblastic leukemia. Blood 2012;120(17):3510-8.
13. Maude SL, Dolai S, Delgado-Martin C, Vincent T, Robbins A, Selvanathan A, et al. Efficacy of JAK/STAT pathway inhibition in murine xenograft models of early T-cell precursor (ETP) acute lymphoblastic leukemia. Blood 2015;125(11):1759-67.
14. Springuel L, Hornakova T, Losdyck E, Lambert F, Leroy E, Constantinescu SN, et al. Cooperating JAK1 and JAK3 mutants increase resistance to JAK inhibitors. Blood 2014;124(26):3924-31.

15. Rambaldi A, Dellacasa CM, Finazzi G, Carobbio A, Ferrari ML, Guglielmelli P, et al. A pilot study of the Histone-Deacetylase inhibitor Givinostat in patients with JAK2V617F positive chronic myeloproliferative neoplasms. Br J Haematol 2010;150(4):446-55.
16. Amaru Calzada A, Todoerti K, Donadoni L, Pellicioli A, Tuana G, Gatta R, et al. The HDAC inhibitor Givinostat modulates the hematopoietic transcription factors NFE2 and C-MYB in JAK2(V617F) myeloproliferative neoplasm cells. Exp Hematol 2012;40(8):634-45 e10.
17. Palmi C, Vendramini E, Silvestri D, Longinotti G, Frison D, Cario G, et al. Poor prognosis for P2RY8-CRLF2 fusion but not for CRLF2 over-expression in children with intermediate risk B-cell precursor acute lymphoblastic leukemia. Leukemia 2012;26(10):2245-53.
18. Conter V, Bartram CR, Valsecchi MG, Schrauder A, Panzer-Grumayer R, Moricke A, et al. Molecular response to treatment redefines all prognostic factors in children and adolescents with B-cell precursor acute lymphoblastic leukemia: results in 3184 patients of the AIEOP-BFM ALL 2000 study. Blood 2010;115(16):3206-14.
19. Bugarin C, Sarno J, Palmi C, Savino AM, Te Kronnie G, Dworzak M, et al. Fine Tuning of Surface CRLF2 Expression and Its Associated Signaling Profile in Childhood B Cell Precursor Acute Lymphoblastic Leukemia. Haematologica 2015;100(6):e229-32.
20. Palmi C, Valsecchi MG, Longinotti G, Silvestri D, Carrino V, Conter V, et al. What is the relevance of Ikaros gene deletions as a prognostic marker in pediatric Philadelphia-negative B-cell precursor acute lymphoblastic leukemia? Haematologica 2013;98(8):1226-31.
21. Palmi C, Lana T, Silvestri D, Savino A, Kronnie GT, Conter V, et al. Impact of IKZF1 deletions on IKZF1 expression and outcome in Philadelphia chromosome negative childhood BCP-ALL. Reply to "incidence and biological significance of IKZF1/Ikaros gene deletions in pediatric Philadelphia chromosome negative and Philadelphia chromosome positive B-cell precursor acute lymphoblastic leukemia". Haematologica 2013;98(12):e164-5.
22. Cazzaniga V, Bugarin C, Bardini M, Giordan M, te Kronnie G, Basso G, et al. LCK over-expression drives STAT5 oncogenic signaling in PAX5 translocated BCP-ALL patients. Oncotarget 2015;6(3):1569-81.

23. Krutzik PO, Nolan GP. Intracellular phospho-protein staining techniques for flow cytometry: monitoring single cell signaling events. Cytometry Part A : the journal of the International Society for Analytical Cytology 2003;55(2):61-70.
24. Kotecha N, Flores NJ, Irish JM, Simonds EF, Sakai DS, Archambeault S, et al. Single-cell profiling identifies aberrant STAT5 activation in myeloid malignancies with specific clinical and biologic correlates. Cancer Cell 2008;14(4):335-43.
25. Irizarry RA, Hobbs B, Collin F, Beazer-Barclay YD, Antonellis KJ, Scherf U, et al. Exploration, normalization, and summaries of high density oligonucleotide array probe level data. Biostatistics 2003;4(2):249-64.
26. Tusher VG, Tibshirani R, Chu G. Significance analysis of microarrays applied to the ionizing radiation response. Proc Natl Acad Sci U S A 2001;98(9):5116-21.
27. Sales G, Calura E, Cavalieri D, Romualdi C. graphite - a Bioconductor package to convert pathway topology to gene network. BMC bioinformatics 2012;13:20.
28. Subramanian A, Tamayo P, Mootha VK, Mukherjee S, Ebert BL, Gillette MA, et al. Gene set enrichment analysis: a knowledge-based approach for interpreting genome-wide expression profiles. Proc Natl Acad Sci U S A 2005;102(43):15545-50.
29. Bendall SC, Simonds EF, Qiu P, Amir el AD, Krutzik PO, Finck R, et al. Single-cell mass cytometry of differential immune and drug responses across a human hematopoietic continuum. Science 2011;332(6030):687-96.
30. Amir el AD, Davis KL, Tadmor MD, Simonds EF, Levine JH, Bendall SC, et al. viSNE enables visualization of high dimensional single-cell data and reveals phenotypic heterogeneity of leukemia. Nat Biotechnol 2013;31(6):545-52.
31. Greco WR, Bravo G, Parsons JC. The search for synergy: a critical review from a response surface perspective. Pharmacological reviews 1995;47(2):331-85.
32. Manabe A, Coustan-Smith E, Behm FG, Raimondi SC, Campana D. Bone marrow-derived stromal cells prevent apoptotic cell death in B-lineage acute lymphoblastic leukemia. Blood 1992;79(9):2370-7.
33. Spijkers-Hagelstein JA, Pinhancos SS, Schneider P, Pieters R, Stam RW. Chemical genomic screening identifies LY294002 as a modulator of glucocorticoid resistance in MLL-rearranged infant ALL. Leukemia 2014;28(4):761-9.

34. Heim MH. The Jak-STAT pathway: cytokine signalling from the receptor to the nucleus. Journal of receptor and signal transduction research 1999;19(1-4):75-120.
35. Baxter EJ, Scott LM, Campbell PJ, East C, Fourouclas N, Swanton S, et al. Acquired mutation of the tyrosine kinase JAK2 in human myeloproliferative disorders. Lancet 2005;365(9464):1054-61.
36. Kralovics R, Passamonti F, Buser AS, Teo SS, Tiedt R, Passweg JR, et al. A gain-of-function mutation of JAK2 in myeloproliferative disorders. N Engl J Med 2005;352(17):1779-90.
37. Levine RL, Wadleigh M, Cools J, Ebert BL, Wernig G, Huntly BJ, et al. Activating mutation in the tyrosine kinase JAK2 in polycythemia vera, essential thrombocythemia, and myeloid metaplasia with myelofibrosis. Cancer Cell 2005;7(4):387-97.
38. Oh ST, Simonds EF, Jones C, Hale MB, Goltsev Y, Gibbs KD, Jr., et al. Novel mutations in the inhibitory adaptor protein LNK drive JAK-STAT signaling in patients with myeloproliferative neoplasms. Blood 2010;116(6):988-92.
39. Roberts KG, Morin RD, Zhang J, Hirst M, Zhao Y, Su X, et al. Genetic alterations activating kinase and cytokine receptor signaling in high-risk acute lymphoblastic leukemia. Cancer Cell 2012;22(2):153-66.
40. Weigert O, Lane AA, Bird L, Kopp N, Chapuy B, van Bodegom D, et al. Genetic resistance to JAK2 enzymatic inhibitors is overcome by HSP90 inhibition. J Exp Med 2012;209(2):259-73.
41. Bjornson ZB, Nolan GP, Fantl WJ. Single-cell mass cytometry for analysis of immune system functional states. Curr Opin Immunol 2013;25(4):484-94.

SUPPLEMENTARY FIGURES AND TABLES

Supplementary Table 1. ***Complete panel of metal-conjugated antibodies used for CyTOF analyses.***

[illegible]	[illegible]	[illegible]	[illegible]	[illegible]	[illegible]
CD235		S	In	115	Lineage
CD61		S	In	113	Lineage
CD45	✔	S	In	115	Bcell maturity
cPARP			La	139	Apoptosis
CD49	✔	S	Pr	141	Bcell maturity
CD22		S	Pr	143	Bcell maturity
CD79b	✔	S	Pr	144	Bcell maturity
CD20	✔	S	Sm	147	Bcell maturity
CD24	✔	S	Pr	148	Bcell maturity
CD179a	✔		Sm	149	Bcell maturity
H3			Sm	152	Cell No.
IgM	✔		Eu	153	Bcell maturity
kappa Lambda		S	Sm	154	Bcell maturity
CD10	✔	S	Gd	156	Bcell maturity
CD38		S	Gd	157	Bcell maturity
CD179b	✔		Gd	158	Bcell maturity
CD21	✔	S	Gd	160	Bcell maturity
TSLPR	✔	S	Dy	161	Bcell maturity
CD27	✔	S	Dy	162	Bcell maturity
CD43	✔	S	Er	167	Bcell maturity
CD5	✔	S	Er	168	Bcell maturity
CD3		S	Tm	169	Bcell maturity
CD5		S	Er	170	Lineage
CD66 CD15		S	Yb	171	Lineage
HLA-DR		S	Yb	172	Bcell maturity
IgD	✔	S	Lu	175	Bcell maturity
pCREB			Yb	176	pBCR signaling
DNA			Ir	191,193	
Cisplatin - Viability			Pt	195	

Supplementary Table 2

Serial	Pathway	Pathway Genes	Mapped Genes
1	Natural killer cell mediated cytotoxicity	137	16
2	Osteoclast differentiation	123	16
3	Apoptosis	86	15
4	B cell receptor signaling pathway	73	15
5	Vascular smooth muscle contraction	113	14
6	Cell cycle	124	13
7	Fc gamma R-mediated phagocytosis	95	13
8	Hepatitis B	136	12
9	Insulin signaling pathway	137	12
10	Leukocyte transendothelial migration	85	12
11	Oocyte meiosis	108	12
12	p53 signaling pathway	68	12
13	HIF-1 signaling pathway	109	11
14	Jak-STAT signaling pathway	99	11
15	Cholinergic synapse	95	10
16	Circadian entrainment	96	10
17	Gap junction	89	10
18	Neurotrophin signaling pathway	116	10
19	T cell receptor signaling pathway	98	10
20	Tight junction	118	10
21	Chronic myeloid leukemia	73	9
22	Fc epsilon RI signaling pathway	62	9
23	Glutamatergic synapse	92	9
24	Salivary secretion	48	9
25	VEGF signaling pathway	67	9
26	Acute myeloid leukemia	57	8
27	Alzheimer's disease	49	8
28	Amoebiasis	46	8
29	Chagas disease (American trypanosomiasis)	89	8
30	Dopaminergic synapse	124	8
31	Epstein-Barr virus infection	83	8
32	ErbB signaling pathway	88	8
33	Glioma	65	8
34	Glycerophospholipid metabolism	84	8
35	GnRH signaling pathway	85	8
36	Melanogenesis	101	8
37	NF-kappa B signaling pathway	80	8
38	Pancreatic cancer	69	8
39	Phosphatidylinositol signaling system	76	8
40	PPAR signaling pathway	64	8
41	Progesterone-mediated oocyte maturation	80	8
42	Prostate cancer	87	8
43	Renal cell carcinoma	60	8
44	Small cell lung cancer	82	8
45	Wnt signaling pathway	144	8
46	Axon guidance	118	7
47	Measles	102	7
48	Morphine addiction	55	7
49	Toll-like receptor signaling pathway	103	7
50	Adherens junction	70	6

Supplementary Figure 1

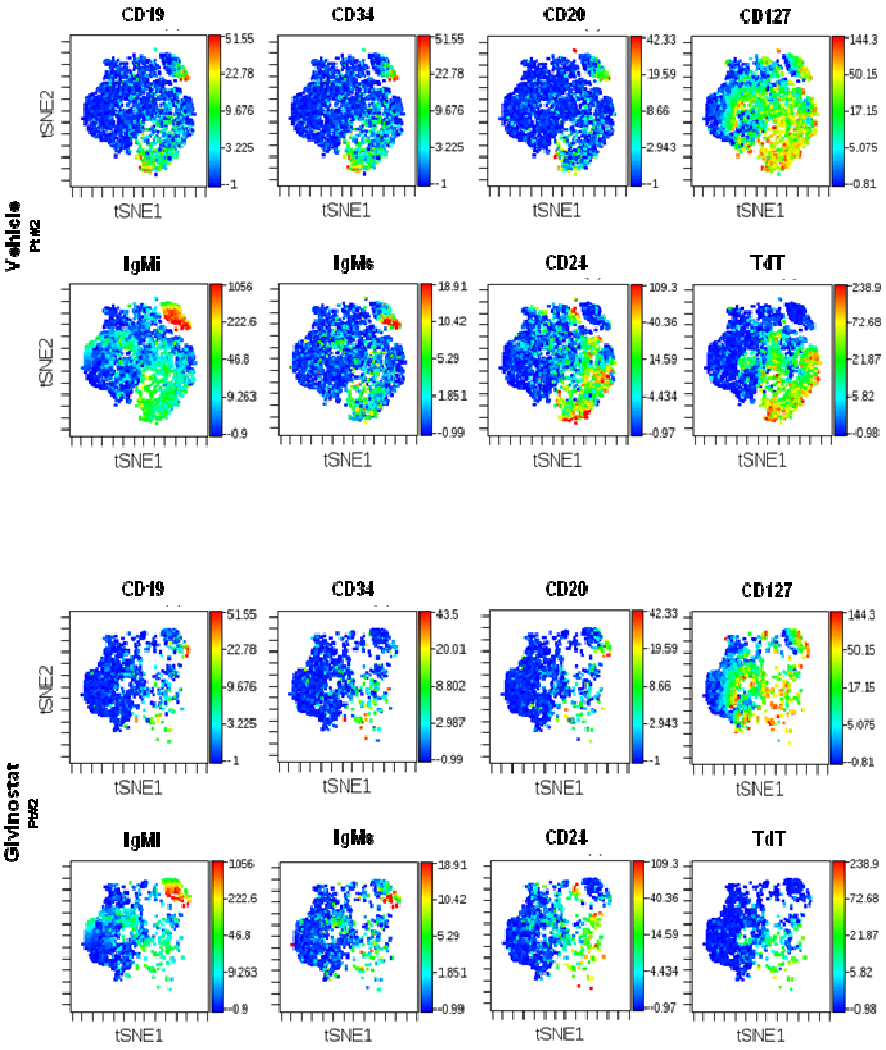

Figure S1. Complete panel of viSNE analyses with the remaining 8 out of 12 markers for patient 2.

Supplementary Figure 2

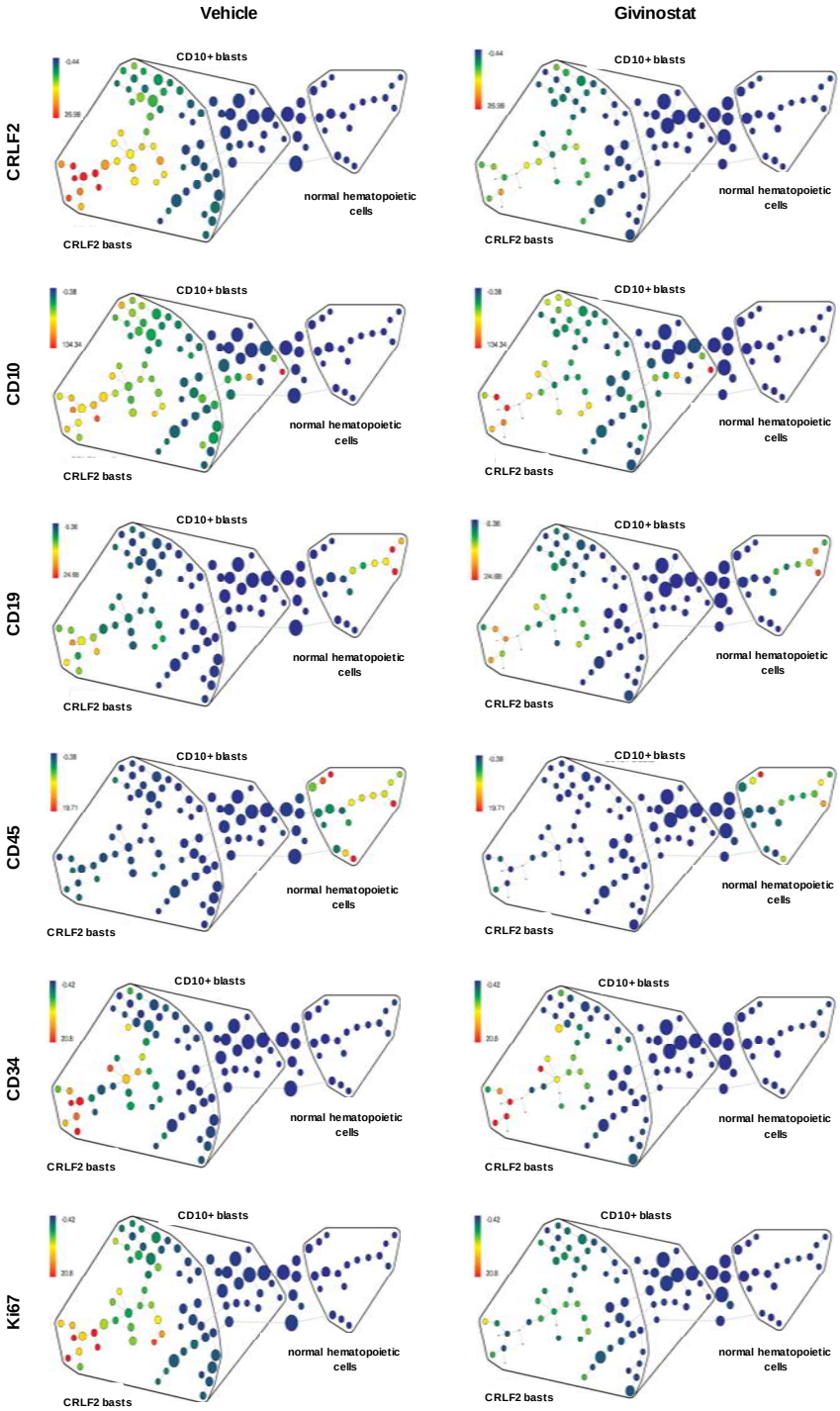

Supplementary Figure 2 (continued)

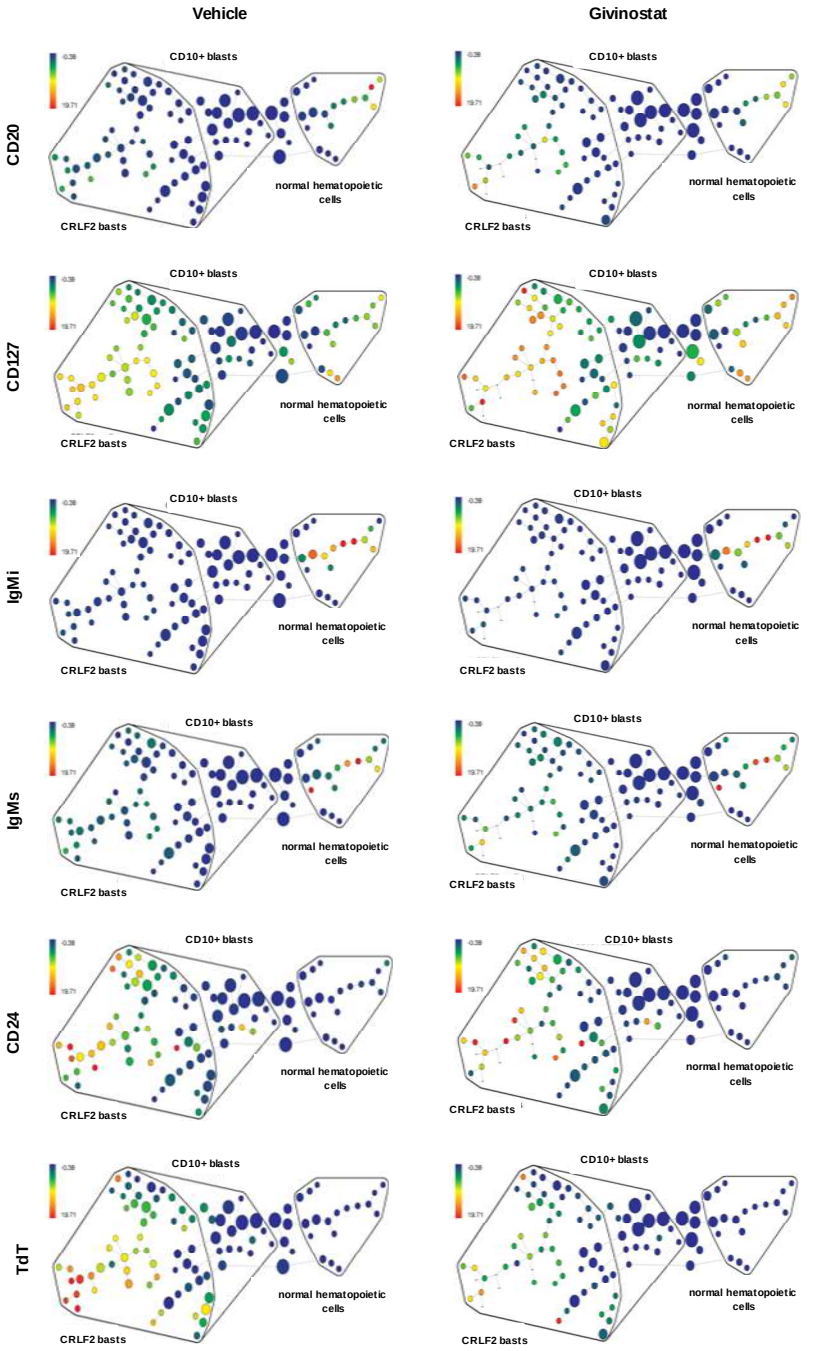

	CD10+	CRLF2+	normal	total events
vehicle	32741 (70.0%)	19821 (42.0%)	4129 (8.9%)	46565 (100%)
Givinostat	15348 (44.0%)	6413 (18.4%)	3104 (8.9%)	34843 (100%)

Figure S2. Figure Figure S2. Analyses of blasts from patient 2 with SPADE tool. *The positivity for selected markers was graphically represented by the color and was used to clusterize blasts in spheres. The size of the spheres changed accordingly to the number of blasts selected. The spheres were furthermore grouped in bubbles, according to their positivity for CD10, CRLF2 and normal cells (CD45high, intra cellular and surface IgM positive). After treatment with Givinostat not only the color but also the size of the spheres was reduced. Number and percentage of events registered for each bubble before and after treatment with Givinostat are shown.*

Supplementary Figure 3

A

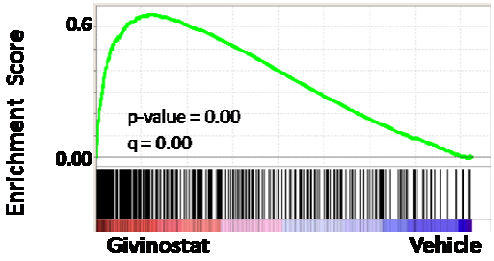

B

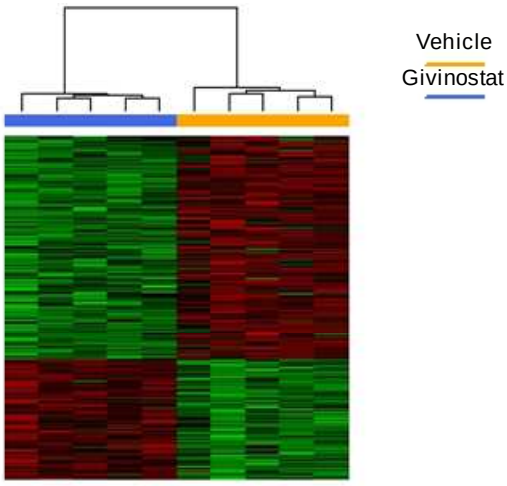

C

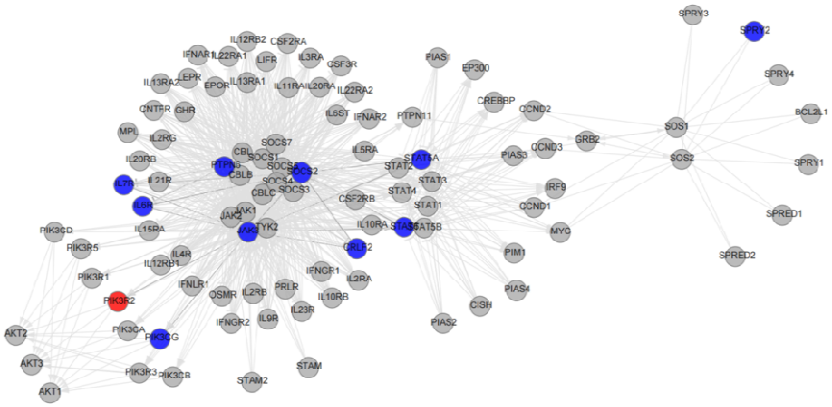

Figure S3. *(A) GSEA plot showing the positive enrichment (positive Normalized Enrichment Score, NES= 2.7727435) in the Givinostat treated samples for HDAC target genes. (B) Supervised hierarchical clustering analysis using the 2068 probe sets differentially regulated with FDR< 0.05 according to SAM between Givinostat treated (blue) versus vehicle treated (orange) samples. Down- and up-regulated genes are shown in the heat map in green and red, respectively. (C) Graphite network showing the genes enclosed in the KEGG JAK-STAT signaling pathway; genes down-regulated by Givinostat and included in the differentially regulated genes according to SAM are shown in blue. Genes up-regulated are shown in red.*

Supplementary Figure 4

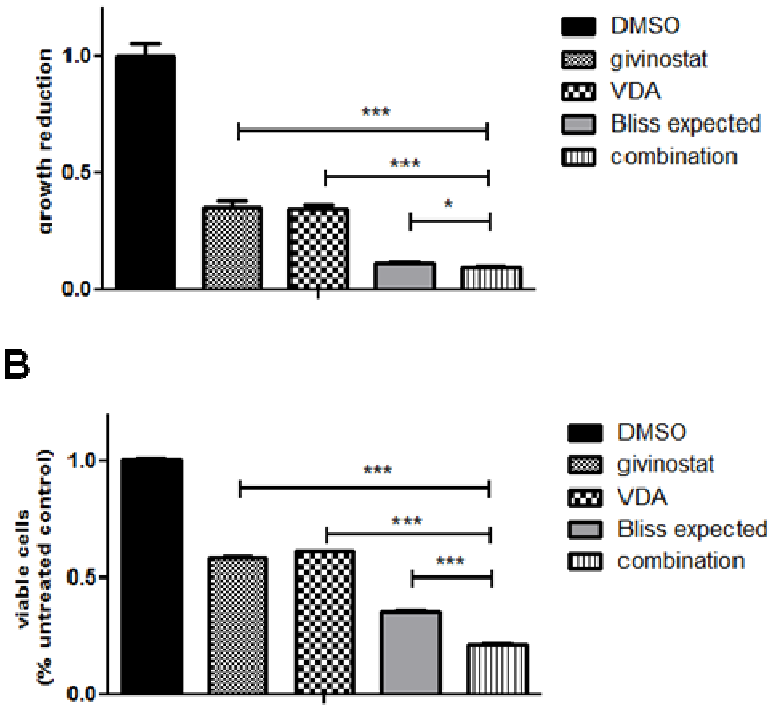

Figure S4. *Proliferation (A) and Annexin V/Sytox assay (D) performed on MUTZ5 cells in presence of Givinostat (0.1 µM) and VDA (Asparaginase 0,023 ug/ml; Desametasone 0,001 ug/ml; Vincristine 0,0001 ug/ml) alone and in combination. The expected effect, calculated by Bliss formula, is represented by grey column.*

Chapter 4

Manuscript in preparation

CRLF2 Over-expression is a Poor Prognostic Marker in Children with High Risk T-Cell Acute Lymphoblastic Leukemia.

Chiara Palmi[1], **Angela Maria Savino**[1], Daniela Silvestri[2], Ilaria Bronzini[3], Gunnar Cario[4], Maddalena Paganin[3], Barbara Buldini[3], Marta Galbiati[1], Martina U. Muckenthaler[5], Maurizio Aricò,[6] Elena Barisone,[6] Fiorina Casale,[6] Franco Locatelli,[6] Luca Lo Nigro,[6] Concetta Micalizzi,[6] Rosanna Parasole,[6] Andrea Pession,[6] Caterina Putti,[6] Nicola Santoro,[6] Anna Maria Testi,[6] Ottavio Ziino,[6] Andreas Kulozik[5], Martin Zimmermann[7], Martin Schrappe[4], Cristina Bugarin[1], Giuseppe Gaipa[1], Giuseppe Basso[3], Andrea Biondi[8], Maria Grazia Valsecchi[2], Martin Stanulla[7], Valentino

Conter[6,8], Geertruy te Kronnie[3] and Giovanni Cazzaniga[1].

8. Centro Ricerca M. Tettamanti, Clinica Pediatrica, Università di Milano Bicocca, Fondazione MBBM/Ospedale San Gerardo, Monza, Italy.
9. Centro Operativo e di Ricerca Statistica, Università di Milano Bicocca, Monza, Italy.
10. Laboratory of Onco-Hematology, Department of Pediatrics, Università di Padova, Italy.
11. Department of Pediatrics, University Hospital Schleswig-Holstein, Campus Kiel, Kiel, Germany.
12. Department of Pediatric Oncology, Hematology and Immunology, University of Heidelberg, Heidelberg, Germany.
13. ALL Working Group, Italian Association of Pediatric Hematology and Oncology (AIEOP).
14. Department of Paediatric Haematology and Oncology, Hannover Medical School, Hannover, Germany.
15. Clinica Pediatrica, Università di Milano Bicocca, Fondazione MBBM/Ospedale San Gerardo, Monza, Italy.

ACKNOWLEDGEMENTS

C. Palmi is supported by a grant from Beat Leukemia Foundation (www.beat-leukemia.org). This study was supported by grants from: Fondazione Città della Speranza (Padova), Fondazione Tettamanti (Monza), Associazione Italiana Ricerca sul Cancro (AIRC) (to GteK, GB, GiC, AB, FL and MGV),

CARIPARO project of excellence (to GteK), MIUR (to AB and GB), Fondazione Cariplo (to AB, GiC and GteK), Deutsche Krebshilfe (to GuC, MSt and MSc), Madeleine-Schickedanz-Kinderkrebsstiftung (to GuC, MSt and MSc), TRANSCAN _TRANSCALL (to MUM, AK, GC, MS, GB, AB, GiC and GteK).

We thank Dr Stefan Nagel (DSMZ - German Collection of Microorganisms and Cell Cultures GmbH) for the *CRLF2* expression screening on T-ALL cell lines; Simona Songia, Lilia Corral, Valentina Carrino, Eugenia Mella, Tiziana Villa (Monza), Elena Seganfreddo and Katia Polato (Padova) for MRD monitoring of children treated in AIEOP centers; all medical doctors of the AIEOP and BFM centers.

CORRESPONDING AUTHORS

Giovanni Cazzaniga,
Centro Ricerca M. Tettamanti, Università di Milano-Bicocca, Ospedale San Gerardo, via Pergolesi, 33, 20900 Monza (MB), Italy.
E-mail: gianni.cazzaniga@hsgerardo.org
Tel: +39 (0)39 2333661 ; Fax: +39 (0)39 2332167

and

Andrea Biondi,
Clinica Pediatrica, Università di Milano-Bicocca, Ospedale San Gerardo, via Pergolesi 33, 20900 Monza (MB), Italy.
E-mail: abiondi.unimib@gmail.com
Tel: +39 (0)39 2333661; Fax: +39 (0)39 2332167.

RUNNING HEAD

Poor outcome for *CRLF2* over-expression in childhood T-ALL.

ABSTRACT

Purpose

Although introduction of risk-adapted therapy improved their prognosis, pediatric T acute lymphoblastic leukemia (T-ALL) patients still have a worse outcome compared to patients with B Cell Precursor (BCP)-ALL and they could benefit from the identification of new prognostic markers.

Alteration of Cytokine Receptor-like Factor 2 (*CRLF2*) gene, a hallmark correlated with poor outcome in BCP-ALL, has not been reported in T-ALL. However, aberrations in IL7Rα that heterodimerizes with CRLF2 have been described. This observation prompted us to investigate if CRLF2 could also be affected in T-ALL.

Patients and Methods

We analyzed *CRLF2* expression in 212 T-ALL patients enrolled in the AIEOP-BFM ALL 2000 study in Italian (AIEOP) and German (BFM-G) centers.

Results

Seventeen AIEOP patients out of 120 (14.2%) presented *CRLF2* expression 5 times higher than the median (‘*CRLF2-high*’) with a significantly inferior 5-years EFS (41.2%±11.9 vs. 68.9%±4.6, p=0.006) and an increased CIR (52.9%±12.1 vs. 26.2%±4.3, p=0.007) compared to *CRLF2-low* patients. The prognostic value of *CRLF2* over-expression was validated in the BFM-G cohort. Cox model analysis showed that patients with

CRLF2-high expression had a 2.5-fold increased risk of relapse. Interestingly, *CRLF2* over-expression was associated with a poor prognosis in the high risk (HR) subgroup where *CRLF2-high* patients were more frequently allocated.

From a biological perspective, in *CRLF2-high* blasts we found a tendency to a stronger TSLP-induced pSTAT5 response sensitive to the JAK inhibitor Ruxolitinib. Moreover, gene set enrichment analysis showed an inverse correlation between the expression of *CRLF2* and of cell cycle regulators.

Conclusion

CRLF2 over-expression is a poor prognostic marker identifying a subset of HR T-ALL patients that could benefit from alternative therapy, potentially targeting the *CRLF2* pathway.

INTRODUCTION

Notwithstanding improved survival rates obtained with risk-adjusted therapy, 25% of T-ALL patients have little or no expectancy of cure. Indeed, this ALL subtype has a generally worse outcome compared with BCP-ALL and the prognosis after relapse remains dramatically poor.[1,2] In the AIEOP-BFM ALL 2000 study, risk group stratification for BCP and T-ALL was largely based on Minimal Residual Disease (MRD) monitoring as a measure of early response to therapy.[1,2] In BCP-ALL, chromosomal translocations have been also incorporated in the risk stratification employed for choosing treatment.[3,4] Meanwhile in T-ALL, although several genomic abnormalities have been described, only few were shown to have prognostic value, and

none has been included in treatment protocols as patient stratification criteria.[5-9] Hence, identification of prognostic factors and development of innovative therapeutic approaches for T-ALL remain a critical task for leukemia research.

Among recently reported genomic abnormalities in ALL, a subset of BCP-ALL patients has been characterized by over-expression of the Cytokine Receptor-like Factor 2 (*CRLF2*) gene, associated with either an intra-chromosomal deletion causing the *P2RY8-CRLF2* fusion or the *IGH@-CRLF2* translocation.[10,11] These two *CRLF2* rearrangements have been shown to correlate with poor outcome in BCP-ALL patients.[12-16]

CRLF2 heterodimerizes with IL-7Ra to form a receptor for thymic stromal lymphopoietin (TSLP), an epithelial cell-derived cytokine that strongly activates dendritic cells (DC) and regulates DC-mediated central tolerance, peripheral T cell homeostasis and inflammatory Th2 responses.[17] TSLP receptor has been detected on many types of immune cells, including B and T cells. Signaling from TSLP receptor activates signal transducer and activator of transcription (STAT5) by JAK1 and JAK2 phosphorylation.[18,19]

CRLF2 rearrangements are a new prognostic marker for BCP-ALL, and the inhibition of JAK/STAT5 signaling represents a potential new therapeutic approach for this subgroup of patients.

Alterations of *CRLF2* have not yet been reported in T-ALL, while recently mutations in its partner *IL7Rα* have been identified in about 10% of T-ALL patients.[20,21] This observation

prompted us to investigate if CRLF2 could also be affected in T-ALL. Here, we report on the incidence of *CRLF2* over-expression at diagnosis in 212 T-ALL patients and its prognostic impact. Patients had been consecutively enrolled in the AIEOP-BFM ALL 2000 study of the Associazione Italiana Ematologia Oncologia Pediatrica (AIEOP) and the Berlin-Frankfurt-Munster (BFM) group in Italian and in German centers.

PATIENTS AND METHODS

Patients

One hundred and twenty T-ALL patients, consecutively enrolled in the AIEOP-BFM ALL 2000 protocol in AIEOP Centers from September 2000 to July 2005, were included in the study as a test cohort.

The clinical characteristics of patients analyzed in this study compared to patients enrolled in the same protocol but not analyzed here are shown in Supplementary Table 1.

No significant differences were observed between patients included or not in this study with respect to sex, age, WBC count, immunophenotype, prednisone response, risk group stratification (Supplementary Table 1) and event-free survival (EFS) (Supplementary Figure 1A).

Supplementary Table 1. Clinical features of T-ALL patients enrolled in the Italian and German AIEOP-BFM ALL 2000 protocol, analyzed and not analyzed for *CRLF2* expression

	AIEOP					BFM-G				
Characteristics	**P-value**	**Analyzed**		**Not analyzed**		**P-value**	**Analyzed**		**Not analyzed**	
		N	**%**	**N**	**%**		**N**	**%**	**N**	**%**
All patients		120	*100.0*	131	*100.0*		92	*100.0*	289	*100.0*
Gender	0.81					0.16				
Male		94	*78.3*	101	*77.1*		93	*77.2*	91	*69.6*
Female		26	*21.7*	30	*22.9*		27	*22.8*	40	*30.4*
Age	0.08					0.51				
1-5 Yrs		43	*35.8*	37	*28.2*		31	*26.1*	33	*25.3*
6-9 Yrs		26	*21.7*	48	*36.7*		35	*29.4*	29	*22.5*
10-14 Yrs		41	*34.2*	36	*27.5*		36	*30.4*	45	*34.2*
15-17 Yrs		10	*8.3*	10	*7.6*		17	*14.1*	24	*18.0*
WBC (X1000/µl)	0.64					<0,001				
< 20		27	*22.5*	35	*26.7*		10	*8.7*	42	*31.8*
20-100		41	*34.2*	46	*35.1*		42	*34.8*	50	*38.5*
≥ 100		52	*43.3*	50	*38.2*		68	*56.5*	39	*29.7*
Immunophenotype	0.07					0.02				
Early-T		36	*30.0*	54	*41.2*		18	*15.2*	34	*26.3*
Thym		64	*53.3*	50	*38.2*		86	*71.7*	70	*53.3*
Mature T		15	*12.5*	18	*13.7*		14	*12.0*	20	*14.9*
Not specified		5	*4.2*	9	*6.9*		1	*1.1*	7	*5.5*
Prednisone Response	0.47					0.58				
Good		77	*64.2*	89	*67.9*		74	*62.0*	83	*63.3*
Poor		41	*34.2*	39	*29.8*		44	*36.9*	43	*32.9*
Unknown		2	*1.6*	3	*2.3*		1	*1.1*	5	*3.8*
MRD	0.33					0.74				
SR		16	*13.3*	11	*8.4*		14	*11.9*	17	*12.8*
MR		40	*33.3*	53	*40.5*		73	*60.9*	66	*50.2*
HR		21	*17.5*	25	*19.1*		20	*16.3*	16	*12.4*
Unknown		43	*35.8*	42	*32.0*		13	*10.9*	32	*24.6*
Final Risk	0.36					0.71				
no-HR		68	*56.7*	76	*58.0*		53	*57.6*	180	*62.3*
HR		52	*43.3*	55	*42.0*		51	*42.4*	49	*37.7*

WBC, White Blood Cell count; MRD, Minimal Residual Disease; HR, High Risk; MR, Medium Risk; SR, Standard Risk.

A

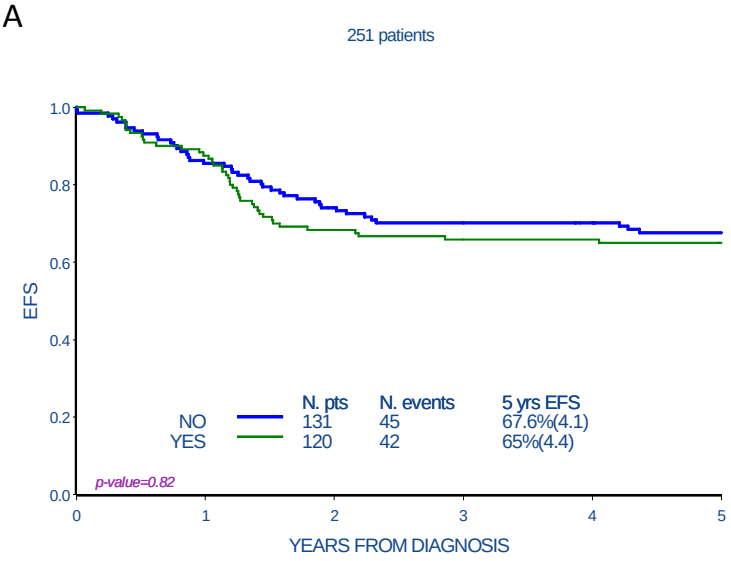

B

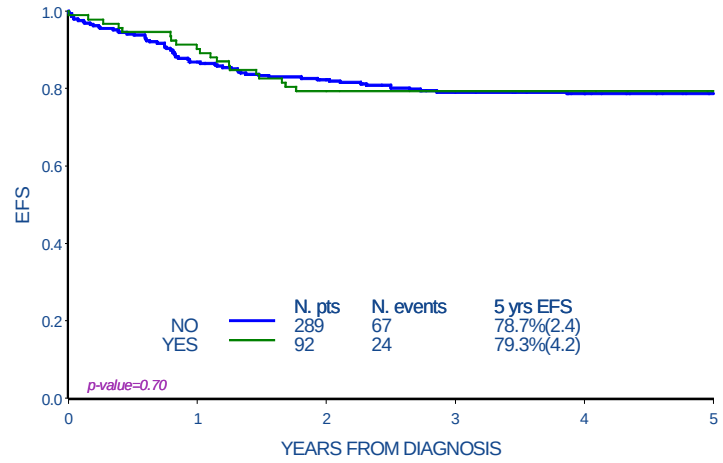

Supplementary Figure 1. Treatment outcome of study cohort.
EFS of AIEOP (A) and BFM-G (B) patients included and non-included in the study cohort.

In addition, 92 consecutive patients enrolled in the AIEOP-BFM ALL 2000 study and treated in German Centers (BFM-G) from January 2001 to December 2004 were analyzed as a validation cohort. The clinical characteristics of the German patients analyzed in this study compared to those not analyzed are shown in Supplementary Table 1: more patients with a higher white blood cell (WBC) count at diagnosis (≥ 100,000/µl: 56.5% vs. 29.7%, p=<0.001) and less with early T-ALL phenotype (15.2% vs. 26.3%, p=0.01) were included in the analysis. However, no significant differences were observed with respect to EFS (Supplementary Figure 1B). Further details are in Supplementary.

Informed consent to participate in the study was obtained for all patients from parents or legal guardians. Details on risk group definitions and final stratification, treatment outlines, were previously reported[1] and briefly summarized in Supplementary .

Quantitative expression of CRLF2

CRLF2 transcript levels on AIEOP and BFM-G samples were centrally analyzed by RQ-PCR.[15] Relative gene expression (indicated as *fold change*) was quantified by 2^{-DDCt} method.[22] The DDCt for AIEOP and BFM-G samples was referred to the median DCt of their respective cohort. Details are in Supplementary.

Statistical analysis

EFS curves were estimated according to the Kaplan-Meier method, and compared using the log-rank test. Cumulative incidence of relapse/resistance (CIR) was estimated by adjusting for competing risks of other events. The Cox regression model was applied to evaluate the prognostic value of two different genetic features on the cause-specific hazard of relapse/resistance after stratifying for risk group. Follow-up was updated in January 2014. Analyses were carried out using SAS version 9.2. The study protocol was registered at http://clinicaltrials.gov (NCT00613457 for AIEOP, NCT00430118 for BFM).

RESULTS

CRLF2 alterations and other genetic aberrations in AIEOP T-ALL patients at diagnosis

Similarly to what is seen in BCP-ALL,[12,15] a sigmoid curve was observed for the distribution of *CRLF2* expression levels in AIEOP T-ALL patients, with *CRLF2* expression at diagnosis ranging from a 0.06- to an 82- fold change with respect to the median value (Figure 1A).

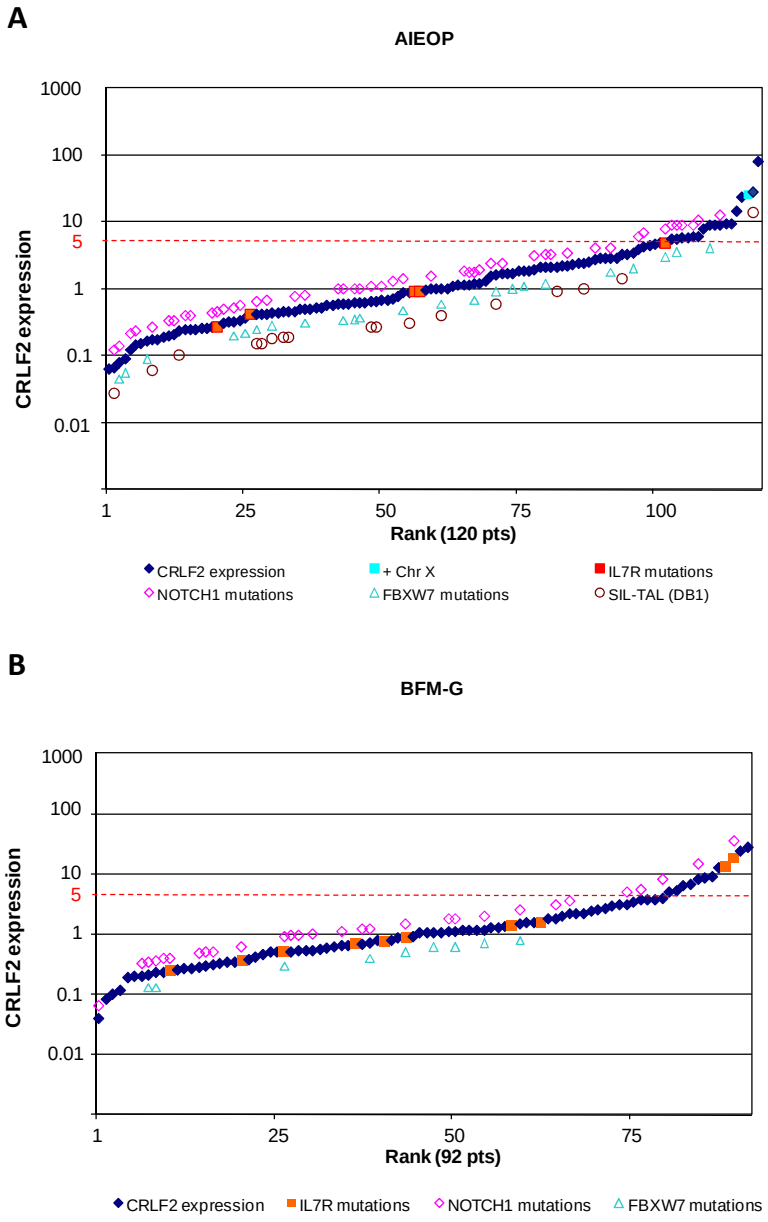

Figure 1. *CRLF2* expression and genomic alterations
CRLF2 expression in AIEOP (A) and BFM-G (B) T-ALL patients at diagnosis. For each specimen results are reported as fold changes on the median expression value of their respective cohort. Positivity for additional genomic aberrations is indicated.

As previously reported for *CRLF2* expression in BCP-ALL,[15] in order to define *CRLF2* high-expressing ("*CRLF2-high*") patients, the CIR hazard ratio was calculated for each numerical increase in the *CRLF2* expression expressed as fold change with respect to the median value. The lowest threshold for *CRLF2* expression showing a significant difference ($p \leq 0.01$) in CIR between two groups was 5 times the median, which was then adopted as cut-point. (Supplementary Figure 2).

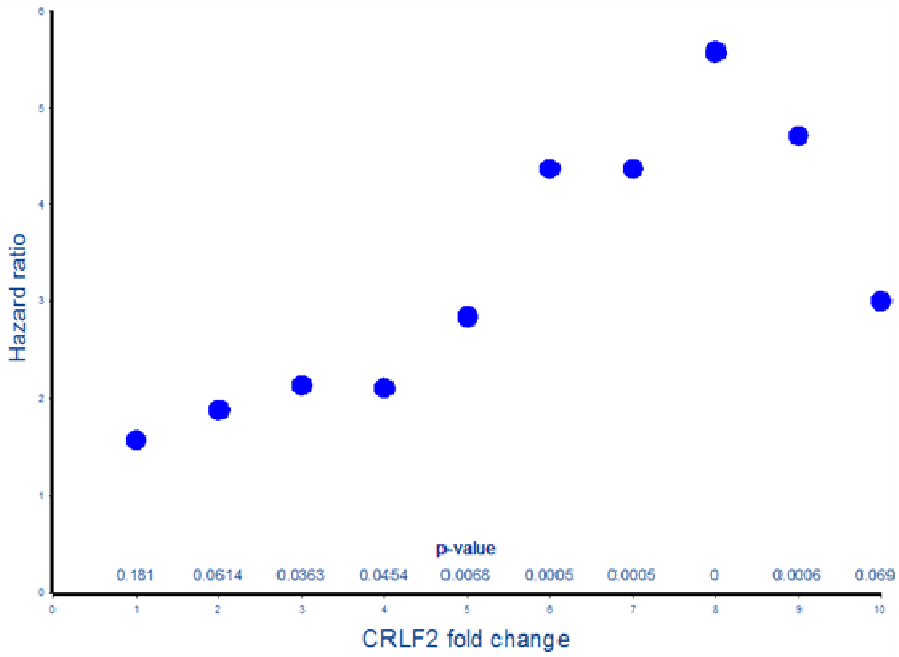

Supplementary Figure 2. CIR hazard ratio associated with different cut-points of *CRLF2* expression.
Potential cut-points of *CRLF2* expression were evaluated. The estimated hazard ratios quantified the ability to discriminate prognosis in terms of the CIR hazard at each of the cut-points. P-value for each cut-point were indicated.

Seventeen patients out of 120 (14.2%) presented *CRLF2* expression 5 times higher or equal than the median.

Clinical characteristics of *CRLF2-high* patients at diagnosis vs. *CRLF2-low* patients (*CRLF2* expression less than 5 times the median) are reported in Table 1. Unlike *CRLF2-low* patients, the majority of *CRLF2-high* patients were poor prednisone responder (PPR) (10/17 patients, 58.8%; p=0.02), while no significant differences were observed with respect to sex, age, WBC count and immunophenotype (in particular 2 *CRLF2-low* patients vs. 1 *CRLF2-high* fulfilled the immunophenotypic criteria to be classified as early T-cell precursor ALL (ETP-ALL), data not shown). While *CRLF2* over-expression did not statistically correlate with MRD classification, consistent with the more frequent incidence of PPR, *CRLF2-high* patients were frequently allocated to the HR group (Table 1).

Table 1. Clinical features of AIEOP and BFM-G study cohort patients positive or negative for *CRLF2* overexpression

	AIEOP					BFM-G				
Characteristics	**P-value**	***CRLF2-low***		***CRLF2-high***		**P-value**	***CRLF2-low***		***CRLF2-high***	
		N	**%**	**N**	**%**		**N**	**%**	**N**	**%**
All patients		103	*100.0*	17	*100.0*		80	*100.0*	12	*100.0*
Gender	0.40					0.99				
Male		82	*79.6*	12	*70.6*		62	*77.5*	9	*75.0*
Female		21	*20.4*	5	*29.4*		18	*22.5*	3	*25.0*
Age	0.48					0.15				
1-5 Yrs		38	*36.9*	5	*29.4*		23	*28.8*	1	*8.3*
6-9 Yrs		22	*21.4*	4	*23.5*		24	*30.0*	3	*25.0*
10-14 Yrs		36	*35.0*	5	*29.4*		24	*30.0*	4	*33.3*
15-17 Yrs		7	*6.8*	3	*17.6*		9	*11.3*	4	*33.3*
WBC (X1000/µl)	0.21					0.42				
< 20		26	*25.2*	1	*5.9*		6	*7.5*	2	*16.7*
20-100		34	*33.0*	7	*41.2*		27	*33.8*	5	*41.7*
≥ 100		43	*41.7*	9	*52.9*		47	*58.8*	5	*41.7*
Immunophenotype	0.93					<0,001				
Early-T		30	*29.1*	6	*35.3*		8	*10.0*	6	*50.0*
Thym		55	*53.4*	9	*52.9*		62	*77.5*	4	*33.3*
Mature T		13	*12.6*	2	*11.8*		9	*11.3*	2	*16.7*
Not specified		5	*4.9*	0	*0.0*		1	*1.3*	0	*0.0*
Prednisone Response	0.02					0.09				
Good		70	*68.0*	7	*41.2*		53	*66.3*	4	*33.3*
Poor		31	*30.1*	10	*58.8*		27	*33.8*	7	*58.3*
Unknown		2	*1.9*	0	*0.0*		0	*0.0*	1	*8.3*
MRD	0.73					0.88				
SR		15	*14.6*	1	*5.9*		10	*12.5*	1	*8.3*
MR		35	*34.0*	5	*29.4*		51	*63.8*	5	*41.7*
HR		18	*17.5*	3	*17.6*		13	*16.3*	2	*16.7*
Unknown		35	*34.0*	8	*47.1*		6	*7.5*	4	*33.3*
Final Risk	0.05					0.11				
no-HR		62	*60.2*	6	*35.3*		49	*61.3*	4	*33.3*
HR		41	*39.8*	11	*64.7*		31	*38.8*	8	*66.7*
P2RY8-CRLF2	-					-				
No		90	*87.4*	16	*94.1*		78	*97.5*	12	*100.0*
Yes		0	*0.0*	0	*0.0*		0	*0.0*	0	*0.0*
Unknown		13	*12.6*	1	*5.9*		2	*2.5*	0	*0.0*

WBC, White Blood Cell count; MRD, Minimal Residual Disease; HR, High Risk; MR, Medium Risk; SR, Standard Risk.

Interestingly, none of *CRLF2-high* patients resulted to be positive for the *P2RY8-CRLF2* fusion (16/17 tested) or the *IGH@-CRLF2* translocation (5/17 tested) and only 1/7 showed a supernumerary X chromosome (Figure 1 and Table 1).

JAK2 and *CRLF2* mutations were absent in all analyzed cases, while *IL7Rα* mutations were detected in 5/107 patients (4.7%), but they were not associated with *CRLF2* over-expression. No statistically significant difference was found in the incidence of recurrent T-ALL genetic aberrations (mutations in *NOTCH1* and *FBXW7* genes and *TAL* deletion) in *CRLF2-low vs. CRLF2-high* patients (Figure 1 and Supplementary Table 2).

Supplementary Table 2. Molecular features of AIEOP study cohort patients positive or negative for *CRLF2* overexpression

	AIEOP					BFM-G				
Characteristics	P-value	*CRLF2-low*		*CRLF2-high*		P-value	*CRLF2-low*		*CRLF2-high*	
		N	%	N	%		N	%	N	%
All patients		103	*100.0*	17	*100.0*		80	*100.0*	12	*100.0*
CRLF2 mutations	-					-				
No		71	*68.9*	13	*76.5*		-	-	-	-
Yes		0	*0.0*	0	*0.0*		-	-	-	-
Unknown		32	*31.1*	4	*23.5*		-	-	-	-
JAK2 mutations	-		*0.0*		*0.0*	-				
No		76	*73.8*	14	*82.4*		-	-	-	-
Yes		0	*0.0*	0	*0.0*		-	-	-	-
Unknown		27	*26.2*	3	*17.6*		-	-	-	-
IL7R α mutations	0.99					0.18				
No		89	*86.4*	13	*76.5*		37	*46.3*	2	*16.7*
Yes		5	*4.9*	0	*0.0*		8	*10.0*	2	*16.7*
Unknown		9	*8.7*	4	*23.5*		35	*43.8*	8	*66.7*
NOTCH1 mutations	0.75					0.99				*0.0*
No		28	*27.2*	5	*29.4*		18	*22.5*	2	*16.7*
Yes		42	*40.8*	6	*35.3*		27	*33.8*	2	*16.7*
Unknown		33	*32.0*	6	*35.3*		35	*43.8*	8	*66.7*
FBXW7 mutations	0.72					0.99				*0.0*
No		59	*57.3*	9	*52.9*		36	*45.0*	4	*33.3*
Yes		21	*20.4*	2	*11.8*		9	*11.3*	0	*0.0*
Unknown		23	*22.3*	6	*35.3*		35	*43.8*	8	*66.7*
SIL-TAL1	0.46					-				
No		82	*79.6*	16	*94.1*		-	-	-	-
Yes		16	*15.5*	1	*5.9*		-	-	-	-
Unknown		5	*4.9*	0	*0.0*		-	-	-	-

Prognostic impact of CRLF2 over-expression at diagnosis

CRLF2-high AIEOP patients had a significantly lower EFS (41.2%±11.9 vs. 68.9%±4.6, p=0.006) and an increased CIR (52.9%±12.1 vs. 26.2%±4.3, Hazard ratio=2.84, p=0.007) compared to *CRLF2-low* patients (Figure 2A and 2B).

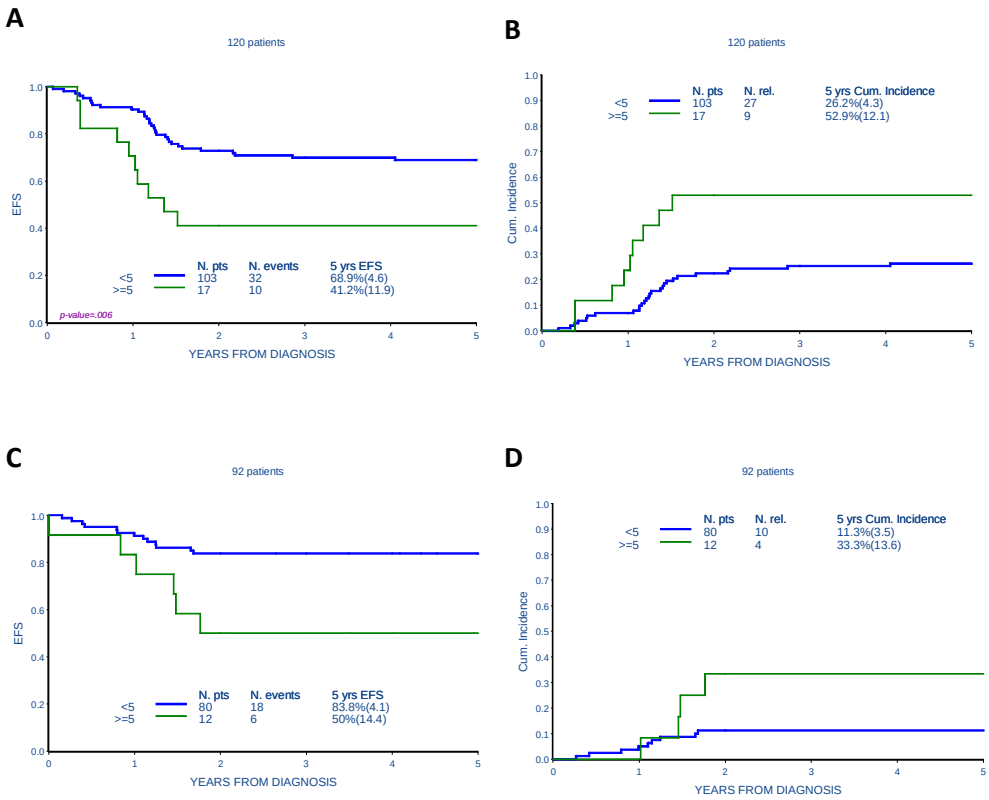

Figure 2. Association of *CRLF2* over-expression to treatment outcome

(A) EFS and (B) CIR of AIEOP study cohort patients according to *CRLF2* expression: *CRLF2-low* and *CRLF2-high*. (C) EFS and (D) CIR of BFM-G study cohort patients according to *CRLF2* expression: *CRLF2-low* and *CRLF2-high*.

In order to validate these results, we analyzed *CRLF2* over-expression in the cohort of 92 consecutive patients treated in German Centers according to the same AIEOP-BFM ALL 2000 study (BFM-G).

Twelve patients (13.0%) were *CRLF2-high* (Figure 1B). Clinical characteristics of BFM-G *CRLF2-high* patients at diagnosis vs. *CRLF2-low* patients are described in Table 1. Unlike *CRLF2-low* patients, a large proportion of *CRLF2-high* patients presented an early-T immunophenotype (6/12 patients, 50.0%; p=<0.001) and in particular 4 out of 6 early-T fulfilled the immunophenotypic criteria to be classified as ETP-ALL, while no significant differences were observed with respect of sex, age, WBC count, risk group stratification and incidence of recurrent T-ALL genetic aberrations (Table 1, Supplementary Table 2 and Figure 1B). Moreover, similar to what observed in the AIEOP cohort, none of the 92 patients resulted positive for *P2RY8-CRLF2* fusion, while IL7Ra mutations were detected in 8/45 *CRLF2-low* patients and in 2/4 *CRLF2-high* patients (Table 1, Supplementary Table 2 and Figure 1B).

We confirmed in the BFM-G cohort that *CRLF2* over-expression was associated to a significant inferior EFS (50.0%±14.4 vs. 83.8%±4.1, p-value=0.01) and a higher CIR (33.3%±13.6 vs. 11.3%±3.5, Hazard ratio=3.37, p-value= 0.04) (Figure 2C and 2D).

Cox model analysis on 212 patients included in this study (merge AIEOP/BFM-G cohort), was performed to assess the prognostic value of *CRLF2* over-expression after adjusting for

final risk stratification. *CRLF2-high* expression had a relevant prognostic impact on the risk of relapse, with a 2.5-fold increase in the risk for positive patients (Hazard ratio 2.47; 95% CI 1.30-4.70; p=0.006) (Table 2).

Table 2. Cox model on hazard of relapse in AIEOP/BFM-G patient cohort

Characteristics	P-value	Hazard ratio	95% CI
CRLF2 expression			
CRLF2-*low*		1	
CRLF2-*high*	0.006	2.47	1,30-4,70
Final Risk			
no-HR		1	
HR	0.002	2.53	1,41-4,55

Moreover, 10 out of the 34 samples of relapses that had occurred in the AIEOP cohort during the observation time of this study were evaluated for *CRLF2* expression levels. Samples at relapse showed a median value of *CRLF2* expression 3.5 times higher than the respective samples at diagnosis (4.95 vs. 1.43) (Supplementary Figure 3).

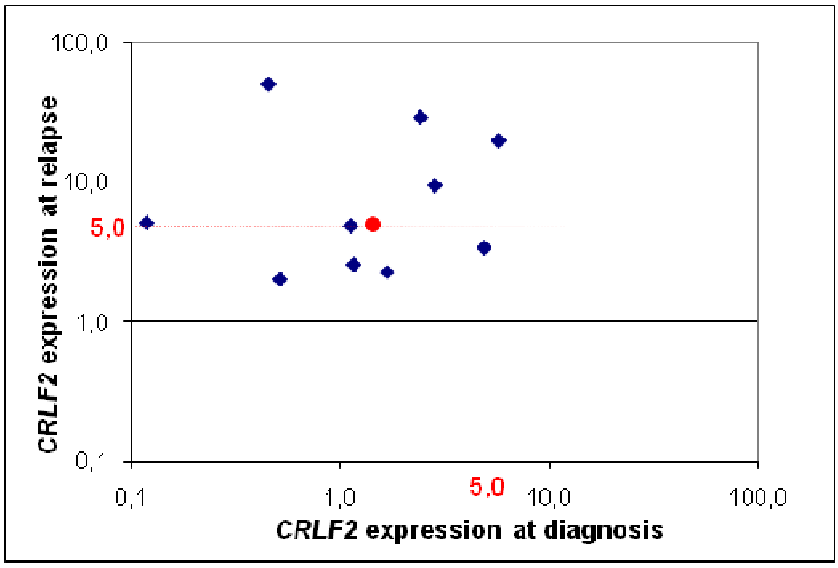

Supplementary Figure 3. *CRLF2* expression at relapse.
Log-log plot of the *CRLF2* expression value for 10 paired diagnosis and relapsed specimens. Samples at relapse showed a median value of *CRLF2* expression 3.5 times higher than the respective samples at diagnosis (4.95 vs. 1.43), as indicated with the red point.

Outcome and risk group

We further analyzed the prognostic value of *CRLF2* over-expression jointly in AIEOP and BFM-G cohorts within no-HR and HR patient subgroups respectively. Interestingly, *CRLF2-high* patients were more frequently allocated to the HR group, being found in 10 out of 121 no-HR patients (8.3%) vs. 19 out of 91 HR patients (20.9%; p=0.008). Only in the HR subgroup, *CRLF2* over-expression was significantly associated with a lower EFS (31.6%±10.7 vs 62.5%±5.7, p-value=0.01) and a higher CIR (57.9%±11.5 vs 29.2%±5.4, Hazard ratio =2.70, p-value=0.008) (Figure 3).

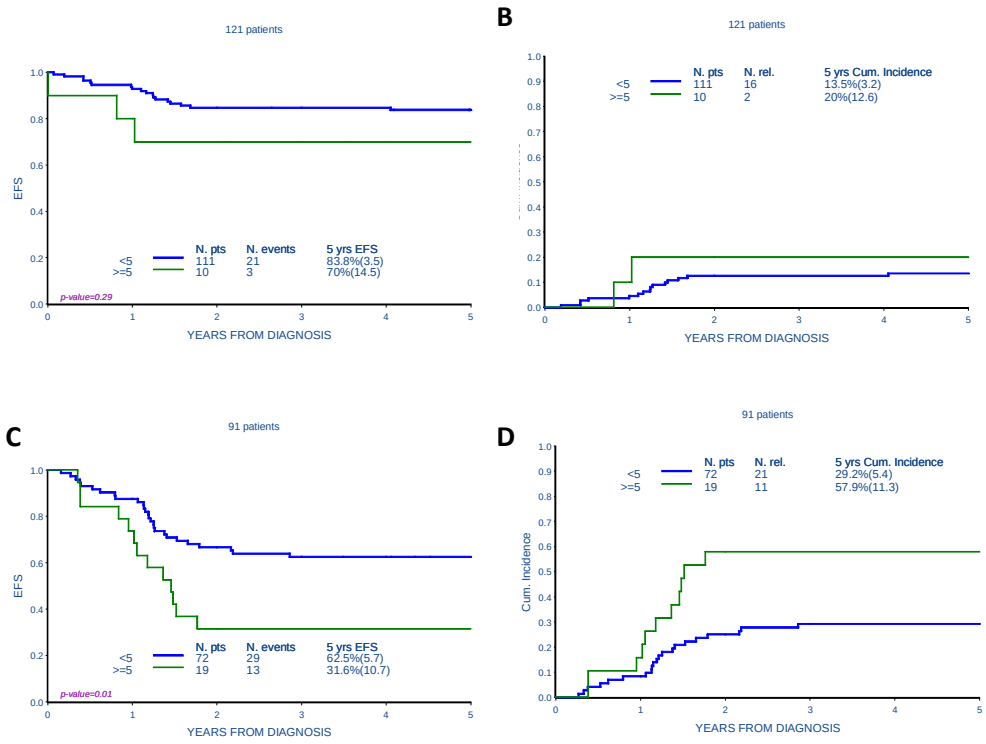

Figure 3. Association of *CRLF2* over-expression to treatment outcome in Risk subgroups
(A) EFS and (B) CIR of no-HR AIEOP/BFM-G patients according to *CRLF2* expression: *CRLF2-low* and *CRLF2-high*. (C) EFS and (D) CIR of HR AIEOP/BFM-G patients according to *CRLF2* expression: *CRLF2-low* and *CRLF2-high*.

When analyzed according to prednisone response, the majority of *CRLF2-high* patients were PPR (Table 1) and were allocated in the specific HR subgroup 'PPR-only' (no-HR by other features: they achieved a complete remission after phase IA and not present high levels of PCR-MRD at day 78). Even if the number of 'PPR-only' analyzed cases was low, in this subgroup *CRLF2-high* patients retained lower EFS (55.6%±16.6 vs

80.6%±6.6, p-value=0.24), and borderline-significant higher CIR (44.4%±16.6 vs 11.1%±5.2, Hazard ratio =4.02, p-value=0.05) (Supplementary Figure 4A and 4B).

Moreover, high levels of *CRLF2* were associated with poor outcome also when patients with ETP immunophenotype[23-26] were excluded from the analysis (EFS: 45.8%±10.2 vs 75.7%±3.2, p-value=<0.001; CIR: 45.8%±10.2 vs 19.2%±3, Hazard ratio =3.23, p-value=<0.001) (Supplementary Figure 4C and 4D).

In addition, no association between N642H mutation activating STAT5B[27] and *CRLF2* over-expression was observed (0/4 STAT5B N642H positive among *CRLF2-high* patients and 1/35 among *CRLF2-low* patients).

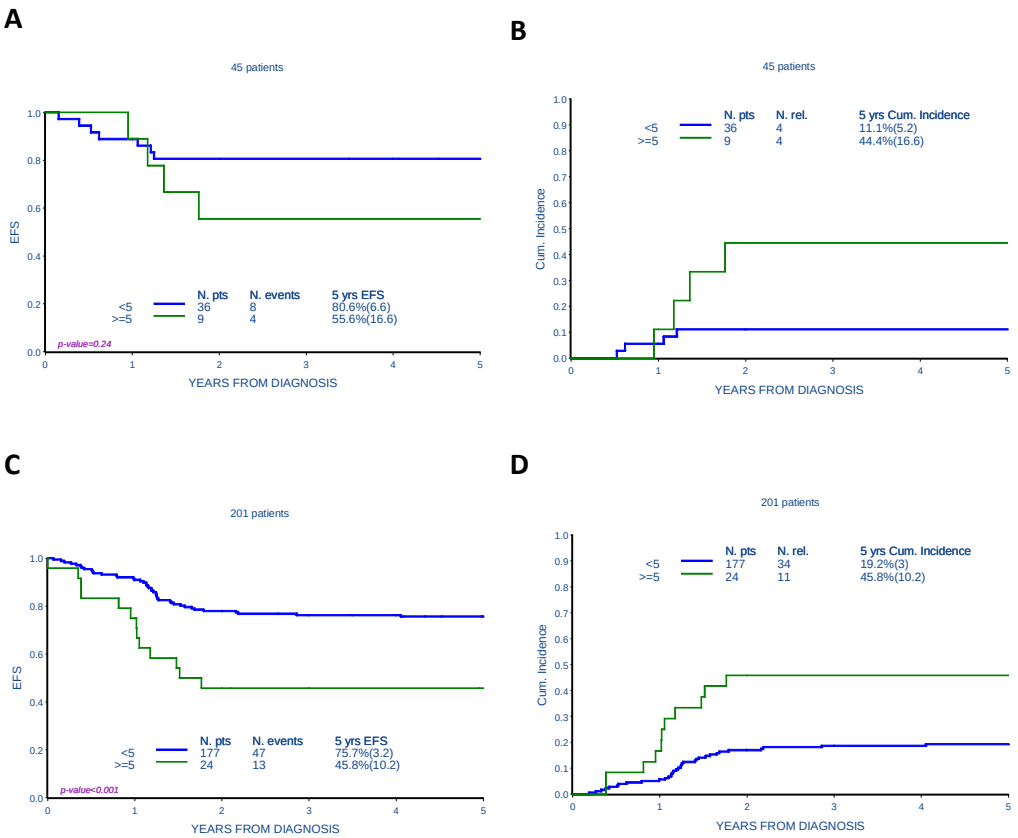

Supplementary Figure 4. Association of *CRLF2* over-expression to treatment outcome in the HR subgroup "PPR-only" and excluding patients with ETP immunophenotype.
(A) EFS and (B) CIR of HR "PPR-only" AIEOP/BFM-G patients according to *CRLF2* expression: *CRLF2-low* and *CRLF2-high*. (C) EFS and (D) CIR of AIEOP/BFM-G patients according to *CRLF2* expression: *CRLF2-low* and *CRLF2-high* when patients with ETP immunophenotype were excluded from the analysis.

CRLF2 surface expression and TSLP-induced pSTAT5 response

Based on available cryopreserved cells, 21 patients were analyzed for CRLF2 surface expression by flow cytometry: 10 patients had been classified as *CRLF2-low* for *CRLF2*-transcript expression and 11 patients as *CRLF2-high*. Unexpectedly, all analyzed patients showed a low percentage of CRLF2-positive blasts (mean=12.6%, range= 0.1-41.8%), with a slight, non-significant increase (p-value=0.17) in the *CRLF2-high* patients (*CRLF2-low:* mean=9.6%, range=0.1-20.3%; *CRLF2-high*: mean=15.3%, range=4.7-41.8%) (Supplementary Figure 5A).

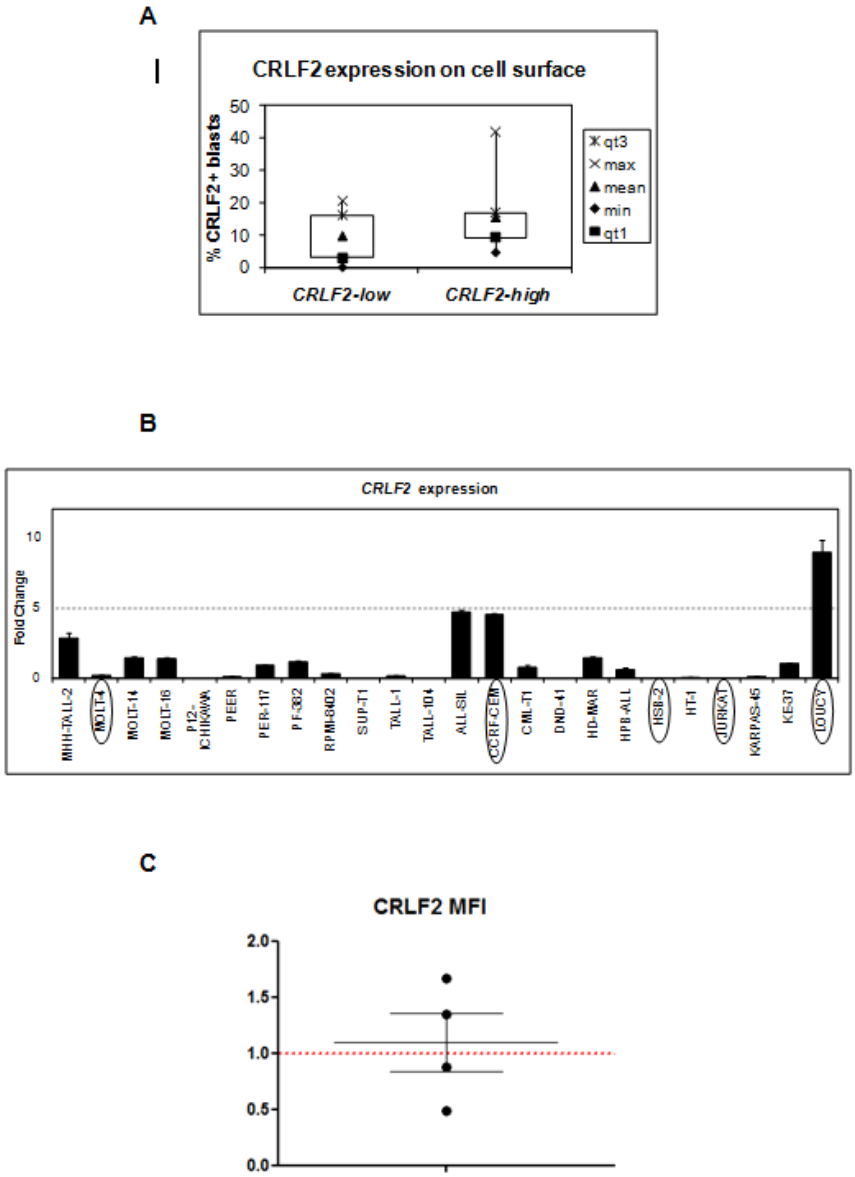

Supplementary Figure 5. CRLF2 expression on T-ALL patients and cell lines.

(A) Analysis of CRLF2 expression on cell surface in 21 T-ALL patients according to their CRLF2 status: 10 *CRLF2-low* and 11 *CRLF2-high* samples. Distribution of % positive blast cells for CRLF2 are represented as scatter plot of 25th and 75th percentile with mean,

minimum and maximum. Leukemic blasts were gated as CD45 intermediate /CD7+/CD19. (B) RQ-PCR analysis of *CRLF2* expression in 24 T-ALL cell lines. Results are reported as fold changes on the median expression value of all the 24 tested cell lines. The 5 cell lines analyzed furthermore for CRLF2 expression on surface and pSTAT5 are circled. (C) Distribution (with indicated 5^{th} and 95^{th} percentiles and mean) of CRLF2 expression on cell surface in T-ALL cell lines measured as MFI levels by FACS. The CRLF2 MFI levels of the cell lines: MOLT4, CCRF-CEM, HSB-2 and JURKAT are showed relative to LOUCY cell line (red line).

Fourteen out of these 21 patients were also selected for phosphoflow cytometric analysis. Interestingly, we observed a tendency (p=0.12) towards a stronger TSLP-induced pSTAT5 response in *CRLF2-high* samples as compared to *CRLF2-low*, showing a mean of 7.6% (range 1.3%-15.1%) and 2.6% (range 0%-6.7%) of pSTAT5 positive cells, respectively (Figure 4A).

In order to experimentally model these results, in collaboration with DSMZ (German Collection of Microorganisms and Cell Cultures GmbH), we tested 24 T-ALL cell lines for the level of *CRLF2* expression. The T-ALL cell line LOUCY presented the highest *CRLF2* expression (Supplementary Figure 5B). As described in the patient cohort, we did not observe a difference in the surface expression of CRLF2 in the *CRLF2-high* LOUCY cells compared to the "*CRLF2*-low" cell lines MOLT4, CCRF-CEM, HSB-2 and JURKAT (Supplementary Figure 5C). Instead, in phosphoflow assays, the *CRLF2-high* LOUCY cells were the only cell line showing STAT5 phosphorylation after TSLP stimulation, and, interestingly, the pSTAT5 response was completely inhibited by the JAK inhibitor Ruxolitinib (Figure 4B).

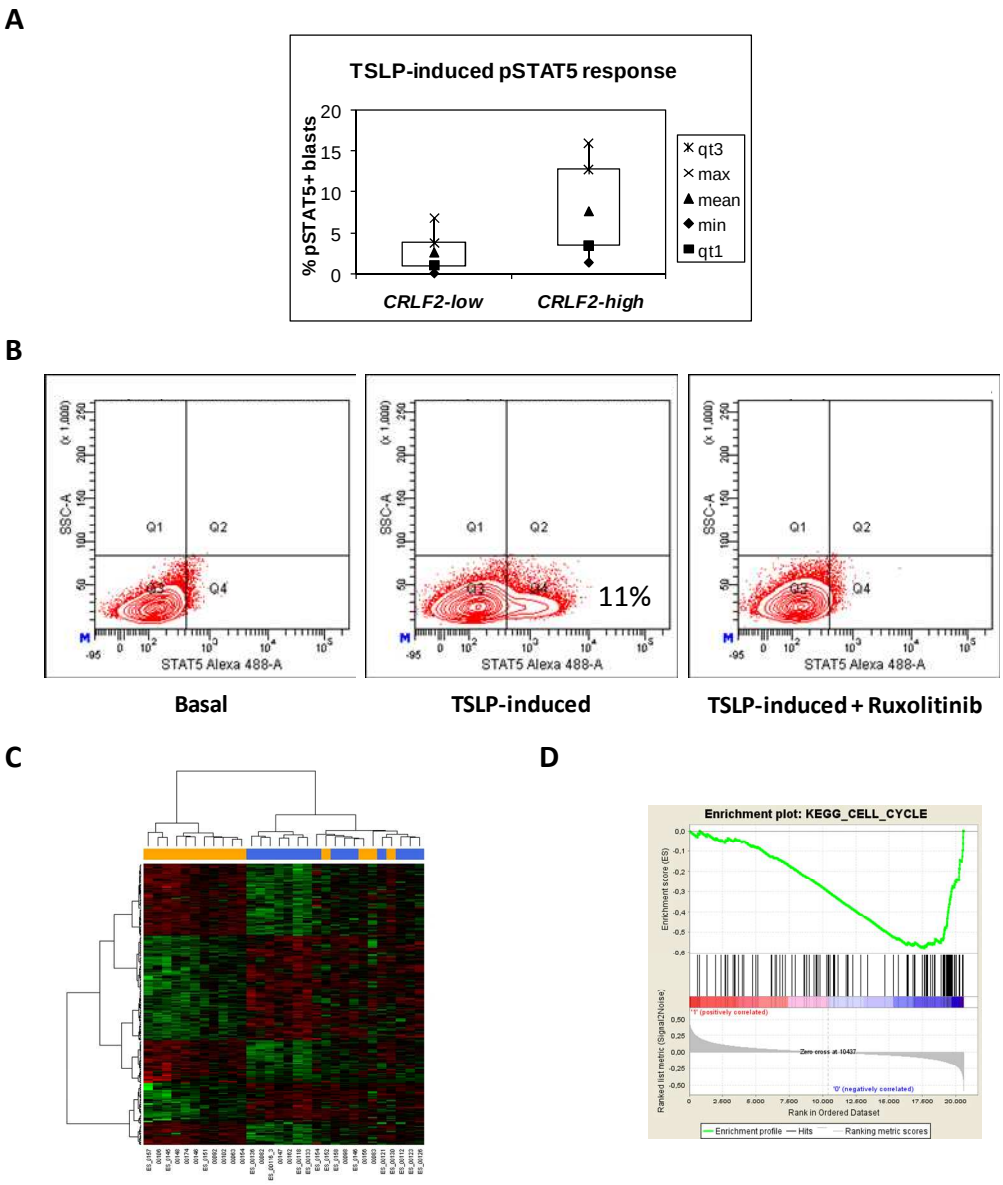

Figure 4. TSLP-induced pSTAT5 response and gene expression profiling associated with *CRLF2* over-expression

(A) Analysis of TSLP-induced pSTAT5 signaling in 14 T-ALL patients according to their CRLF2 status: 8 *CRLF2-low* and 6 *CRLF2-high* samples. Distribution of % positive cells for pSTAT5 are represented as scatter plot of 25th and 75th percentile with mean, minimum and maximum. Data were normalized to the basal STAT5 phosphorylation

status. (B) Phosphoflow analysis of pSTAT5 in LOUCY cell line. The plots show the % positive cells for pSTAT5 in basal condition and after stimulation with TSLP in absence and in presence of the JAK inhibitor Ruxolitinib. (C) Since GEP data were not available from patients of this study cohort, T-ALL cases treated according to the same protocol with available GEP data were analyzed. Consistent with the 15% *CRLF2-high*, identified in the patient cohort, among 100 T-ALL arrayed cases, the top 15 specimens with higher *CRLF2* probe values (orange) were compared to the 15 lowest expressing *CRLF2* specimens (blue). The heat map shows the unsupervised clustering of 290 differentially regulated genes. Red colour depicts overexpressed genes, while downregulated genes are labelled green. (D) Gene set enrichment analysis (GSEA) showing an inverse correlation between the expression of *CRLF2* and cell cycle regulators (enrichment score= -0.6, P=0.018). Enrichment plots depict enrichment scores (green lines) reflecting the appearance of members of the annotated gene sets (black vertical lines) along the gene list ranked from *CRLF2-low* (red) to *CRLF2-high* (blue).

Gene expression profiling associated with CRLF2 over-expression

To identify possible transcriptional patterns associated with *CRLF2* over-expression in T-ALL, a gene expression analysis was performed. Gene expression profiling (GEP) data were not available for patients in this study cohort. Instead, we analyzed T-ALL cases from the same protocol study for whom GEP data were available. Consistent with the 15% *CRLF2-high* cut point, we identified, among 100 GEP arrayed cases, the top 15 with higher *CRLF2* probe values and compared these to the 15 specimens with the lowest expression of *CRLF2*.

As shown in Figure 4C, *CRLF2* over-expression was associated with different regulation of 290 genes. Notably, gene set enrichment analysis (GSEA) showed an inverse correlation between the expression of *CRLF2* and cell cycle regulators,

especially positive regulators (enrichment score= -0.6, P=0.018) (Figure 4D). The list of genes is available upon request.

DISCUSSION

In a subset of BCP-ALL patients without recurrent chromosomal aberrations, new genomic abnormalities leading to the over-expression of *CRLF2* have been found and reported to be associated with poor outcome.[10-16] Deregulation of *CRLF2* expression was further frequently associated with other mutations, such as *JAK2*, *IL7Rα*, *CRLF2* point mutations and *IKZF1* deletions.[14,20,28]

In T-ALL, alterations of *CRLF2* were not reported yet, but recently, mutations in its partner *IL7Rα* have been identified in about 10% of T-ALL patients.[20,21] This prompted us to investigate *CRLF2* expression and associated mutations in T-ALL.

Here, for the first time we report the incidence and prognostic relevance of *CRLF2* over-expression in a cohort of 212 T-ALL patients, consecutively enrolled in the AIEOP-BFM ALL 2000 protocol in Italian and German centers.

Heterogeneous expression of *CRLF2* was observed among T-ALL patients, a distribution comparable to the one found in the BCP-ALL cohort.[15]

The lowest threshold for *CRLF2* expression showing a significant difference in CIR between two groups was 5 times the median, and this value was then adopted as cut-point. By applying this cut-point, high *CRLF2* expression was found in

about 15% of AIEOP and BFM-G T-ALL patients. Notably, this threshold was much lower that the cut-point adopted for AIEOP BCP-ALL patients (20 times the median value),[15] indicating that T-ALL blast cells might be more sensitive to variation of *CRLF2* expression.

Differently from BCP-ALL, the molecular mechanisms responsible for *CRLF2* over-expression in T-ALL remains to be determined, since none of the *CRLF2-high* cases resulted to be positive for *P2RY8-CRLF2* fusion or *IGH@-CRLF2* translocation, and only one showed a supernumerary X chromosome (although only few cases have been screened for these last two alterations). Indeed, only about 50% of BCP-ALL cases with *high-CRLF2* expression lacked known *CRLF2* genomic lesions.[16] Moreover, while in BCP-ALL *CRLF2* over-expression was frequently associated with mutations in *JAK*, *IL7Rα* and in the same *CRLF2* gene,[10,11,20,28,29] *JAK2* and *CRLF2* mutations were absent in all T-ALL analyzed cases. By contrast, *IL7Rα* mutations were detected in 5/107 T-ALL patients (4.7%). They were all insertions or deletions in the transmembrane domain of the receptor and they were not associated with *CRLF2* over-expression. This last observation is consistent with the results reported in literature, namely that, although IL7Rα mutations were more frequently identified in BCP-ALL with aberrant expression of *CRLF2*, the IL7Rα mutant protein with insertions did not require CRLF2 for its activation.[20]

We show here that *CRLF2* over-expression has a prognostic impact in T-ALL, with *CRLF2-high* patients having a significantly

inferior 5-years EFS and a higher CIR compared to *CRLF2-low* patients. The prognostic value of *CRLF2* over-expression, initially identified in the AIEOP cohort, was then confirmed in the BFM-G cohort.

Cox model analysis of the two cohorts analyzed together, adjusted by risk group, showed that *CRLF2-high* expression is an independent prognostic factor in T-ALL, associated to a 2.5-fold increased risk of relapse.

Interestingly, on the contrary to what we observed in BCP-ALL,[15] *CRLF2-high* T-ALL relapsed early, within 2 years from diagnosis. Moreover, this time in concert with BCP-ALL data,[15] samples at relapse showed a median value of *CRLF2* expression higher than the respective samples at diagnosis, this indicating that a high level of *CRLF2* expression could be associated with a higher resistance to therapy.

In order to understand how the prognostic impact of this *CRLF2* alteration can be transferred into clinical practice, *CRLF2* expression was analyzed separately in the different risk subgroups. *CRLF2-high* patients fell more frequently in the HR subgroup (20.9% in HR vs. 8.3% in no-HR), and only in this subgroup, *CRLF2* over-expression was significantly associated with inferior EFS and higher CIR. Therefore, *CRLF2* over-expression identified a subset of HR T-ALL patients with dismal outcome.

Among HR cases, most *CRLF2-high* patients were PPR. In detail, among the subgroup of PPR cases lacking other HR features (“PPR-only”), *CRLF2* expression tend to distinguish a

different incidence of relapse: 4/9 (44%) in *CRLF2-high* compared to 4/36 (11%) in *CRLF2-low*. Although low numbers require caution in drawing conclusions, if this observation was confirmed in a large series, *CRLF2-high* could represent a useful marker to identify cases with poor outcome in the still undefined PPR-only subgroup.

The poor outcome of *CRLF2-high* patients is independent of other known prognostic factors, like ETP immunophenotype or STAT5B mutation.

The contribution of *CRLF2* over-expression to T-ALL is still unclear. Unexpectedly, CRLF2 surface expression by flow cytometry showed a low percentage of CRLF2 positive blasts both in *CRLF2-low* and in *CRLF2-high* patients and in cell lines. Interestingly, we observed a tendency to stronger TSLP-induced pSTAT5 response in patients expressing high levels of *CRLF2* transcript and this finding was confirmed in T-ALL cell lines. Concordantly, we observed STAT5 phosphorylation after TSLP stimulation only in LOUCY cells, the T-ALL cell line with the highest level of *CRLF2* transcript expression. Notably, the pSTAT5 response was completely inhibited by the JAK inhibitor Ruxolitinib.

Finally, by GEP analysis, we found an inverse correlation between the expression of *CRLF2* and that of positive cell cycle regulators, this suggesting that *CRLF2-high* blasts could have a *low proliferating* activity and therefore be less sensitive to conventional chemotherapy; further studies are necessary to test this assumption.

We suggest that the unfavorable prognostic role found for *CRLF2* over-expression in T-ALL may be due to gene expression alteration and associated with a higher TSLP-induced pSTAT5 response. Future studies on the identification of the mechanism of *CRLF2* over-expression in T-ALL are warranted and should provide insight in underlying mechanisms.

In conclusion, we show here that *CRLF2* over-expression is a poor prognostic marker in T-ALL, identifying a subset of HR T-ALL patients that could be eligible for alternative therapies that interfere with the activation of JAK/STAT5 signaling pathway may be considered for treatment of these patients.

REFERENCES

1. Schrappe M, Valsecchi MG, Bartram CR, et al: Late MRD response determines relapse risk overall and in subsets of childhood T-cell ALL: results of the AIEOP-BFM-ALL 2000 study. Blood 118:2077-84, 2011

2. Conter V, Bartram CR, Valsecchi MG, et al: Molecular response to treatment redefines all prognostic factors in children and adolescents with B-cell precursor acute lymphoblastic leukemia: results in 3184 patients of the AIEOP-BFM ALL 2000 study. Blood 115:3206-14, 2010

3. Schultz KR, Bowman WP, Aledo A, et al: Improved early event-free survival with imatinib in Philadelphia chromosome-positive acute lymphoblastic leukemia: a children's oncology group study. J Clin Oncol 27:5175-81, 2009

4. Izraeli S: Application of genomics for risk stratification of childhood acute lymphoblastic leukaemia: from bench to bedside? Br J Haematol 151:119-31, 2010

5. Ferrando AA, Neuberg DS, Staunton J, et al: Gene expression signatures define novel oncogenic pathways in T cell acute lymphoblastic leukemia. Cancer Cell 1:75-87, 2002

6. Kox C, Zimmermann M, Stanulla M, et al: The favorable effect of activating NOTCH1 receptor mutations on long-term outcome in T-ALL patients treated on the ALL-BFM 2000 protocol can be separated from FBXW7 loss of function. Leukemia 24:2005-13, 2010

7. La Starza R, Lettieri A, Pierini V, et al: Linking genomic lesions with minimal residual disease improves prognostic stratification in children with T-cell acute lymphoblastic leukaemia. Leuk Res 37:928-35, 2013

8. Fogelstrand L, Staffas A, Wasslavik C, et al: Prognostic implications of mutations in NOTCH1 and FBXW7 in childhood T-ALL treated according to the NOPHO ALL-1992 and ALL-2000 protocols. Pediatr Blood Cancer 61:424-30, 2014

9. Milani G, Rebora P, Accordi B, et al: Low PKCalpha expression within the MRD-HR stratum defines a new subgroup of childhood T-ALL with very poor outcome. Oncotarget 5:5234-45, 2014

10. Russell LJ, Capasso M, Vater I, et al: Deregulated expression of cytokine receptor gene, CRLF2, is involved in lymphoid transformation in B-cell precursor acute lymphoblastic leukemia. Blood 114:2688-98, 2009

11. Mullighan CG, Collins-Underwood JR, Phillips LA, et al: Rearrangement of CRLF2 in B-progenitor- and Down syndrome-associated acute lymphoblastic leukemia. Nat Genet 41:1243-6, 2009

12. Cario G, Zimmermann M, Romey R, et al: Presence of the P2RY8-CRLF2 rearrangement is associated with a poor prognosis in non-high-risk precursor B-cell acute lymphoblastic leukemia in children treated according to the ALL-BFM 2000 protocol. Blood 115:5393-7, 2010

13. Ensor HM, Schwab C, Russell LJ, et al: Demographic, clinical and outcome features of children with acute lymphoblastic leukemia and CRLF2 deregulation: results from the MRC ALL97 clinical trial. Blood, 117(7):2129-36, 2011

14. Harvey RC, Mullighan CG, Chen IM, et al: Rearrangement of CRLF2 is associated with mutation of JAK kinases, alteration of IKZF1, Hispanic/Latino ethnicity, and a poor outcome in pediatric B-progenitor acute lymphoblastic leukemia. Blood 115:5312-21, 2010

15. Palmi C, Vendramini E, Silvestri D, et al: Poor prognosis for P2RY8-CRLF2 fusion but not for CRLF2 over-expression in children with intermediate risk B-cell precursor acute lymphoblastic leukemia. Leukemia 26:2245-53, 2012

16. Chen IM, Harvey RC, Mullighan CG, et al: Outcome modeling with CRLF2, IKZF1, JAK, and minimal residual disease in pediatric acute lymphoblastic leukemia: a Children's Oncology Group study. Blood 119:3512-22, 2012

17. Liu YJ, Soumelis V, Watanabe N, et al: TSLP: an epithelial cell cytokine that regulates T cell differentiation by conditioning dendritic cell maturation. Annu Rev Immunol 25:193-219, 2007

18. Rochman Y, Kashyap M, Robinson GW, et al: Thymic stromal lymphopoietin-mediated STAT5 phosphorylation via kinases JAK1 and JAK2 reveals a key difference from IL-7-induced signaling. Proc Natl Acad Sci U S A 107:19455-60, 2010

19. Bugarin C, Sarno J, Palmi C, et al: Fine Tuning of Surface CRLF2 Expression and Its Associated Signaling Profile in Childhood B Cell Precursor Acute Lymphoblastic Leukemia. Haematologica, 100(6):e229-32, 2015

20. Shochat C, Tal N, Bandapalli OR, et al: Gain-of-function mutations in interleukin-7 receptor-alpha (IL7R) in childhood acute lymphoblastic leukemias. J Exp Med 208:901-8, 2011

21. Zenatti PP, Ribeiro D, Li W, et al: Oncogenic IL7R gain-of-function mutations in childhood T-cell acute lymphoblastic leukemia. Nat Genet 43:932-9, 2011

22. Livak KJ, Schmittgen TD: Analysis of relative gene expression data using real-time quantitative PCR and the 2(-Delta Delta C(T)) Method. Methods 25:402-8, 2001

23. Coustan-Smith E, Mullighan CG, Onciu M, et al: Early T-cell precursor leukaemia: a subtype of very high-risk acute lymphoblastic leukaemia. Lancet Oncol 10:147-56, 2009

24. Patrick K, Wade R, Goulden N, et al: Outcome for children and young people with Early T-cell precursor acute lymphoblastic leukaemia treated on a contemporary protocol, UKALL 2003. Br J Haematol 166:421-4, 2014

25. Wood BL, Winter SS, Dunsmore KP, et al: T-Lymphoblastic Leukemia (T-ALL) Shows Excellent Outcome, Lack of Significance of the Early Thymic Precursor (ETP) Immunophenotype, and Validation of the Prognostic Value of End-Induction Minimal Residual Disease (MRD) in Children's Oncology Group (COG) Study AALL0434. Presented at the 56th American Society of Hematology Annual Meeting and Exposition. San Francisco, CA, December 6-9, 2014

26. Conter V, Valsecchi MG, Buldini B, et al: Outcome of Early T-Cell Precursor Acute Lymphoblastic Leukemia in AIEOP Patients Treated with the AIEOP-BFM ALL 2000 Study. Presented at the 56th American Society of Hematology Annual Meeting and Exposition. San Francisco, CA, December 6-9, 2014

27. Bandapalli OR, Schuessele S, Kunz JB, et al: The activating STAT5B N642H mutation is a common abnormality in pediatric T-cell acute lymphoblastic leukemia and confers a higher risk of relapse. Haematologica 99:e188-92, 2014

28. Hertzberg L, Vendramini E, Ganmore I, et al: Down syndrome acute lymphoblastic leukemia, a highly heterogeneous disease in which aberrant expression of CRLF2 is associated with mutated JAK2: a report from the International BFM Study Group. Blood 115:1006-17, 2010

29. Yoda A, Yoda Y, Chiaretti S, et al: Functional screening identifies CRLF2 in precursor B-cell acute lymphoblastic leukemia. Proc Natl Acad Sci U S A 107:252-7, 2010

Supplementary Patients and Methods

Patients

T-ALL diagnosis was performed according to standard cytomorphology, cytochemistry and immunophenotypic criteria. DNA and RNA were isolated from mononuclear cells and cDNA was synthesized according to standard methods.[1]

CRLF2 expression was analyzed in the Italian cohort of 120 patients at diagnosis and *P2RY8-CRLF2* rearrangement was tested in 106 patients for which RNA was available. *IGH@-CRLF2* translocation was screened in 5 out of 17 patients positive for *CRLF2* over-expression (≥5 times higher than overall median, see the Results section). DNA was available from 115 patients and the following were analyzed: *CRLF2* mutations (in 84 patients), *IL7Rα* mutations (in 107 patients), *JAK2* mutations (in 90 patients), SIL-TAL (DB1) fusion (in 115 patients), NOTCH1 mutations (in 81 patients) and FBXW7 mutations (in 91 patients). *CRLF2* expression was also analyzed in 10/34 paired diagnosis and relapse samples for which material was available.

CRLF2 expression was analyzed in the BFM-G cohort of 92 patients at diagnosis, and *P2RY8-CRLF2* rearrangement was tested in 90 patients for which RNA was available. *IL7Rα*, NOTCH1 and FBXW7 mutations were analyzed in 49 patients from whom DNA was available.

Protocol stratification

Patient risk groups were defined as follows. The High Risk (HR) group included patients with prednisone poor response (≥ 1,000 blasts/µL on day 8 peripheral blood after 7 days of prednisone and one dose of intrathecal methotrexate on day 1) or inability to achieve clinical remission after Induction Phase IA; high burden (≥ 10^{-3}) of PCR-Minimal Residual Disease (MRD) at day 78. The no-HR group consisting of Standard Risk (SR) and Medium Risk (MR). The SR group included patients who lacked high-risk criteria and tested negative to PCR-MRD for two sensitive markers (≥ 1×10^{-4}) at both day 33 and day 78. The MR group included the remaining patients, and those not evaluated by PCR-MRD.

PCR-MRD was detected by RQ-PCR of Immunoglobulin and/or T-cell receptor gene rearrangements in bone marrow samples collected at the end of the IA (TP1, day 33), and IB (TP2, day 78) induction phases;[2] data were interpreted according to EuroMRD guidelines.[3]

Quantitative expression of CRLF2

CRLF2 transcript levels on AIEOP and BFM-G samples were centrally analyzed by RQ-PCR using the TaqMan Gene Expression Assay Hs00913509_s1 (Applied Biosystems, Foster City, CA, US),[4] the housekeeping *GUS* gene transcript was tested as an internal control by using the Universal Probe Library (UPL) system (Roche Diagnostics, Basel, Switzerland), following the manufacturers' instructions. Optimal primers and

probe for *GUS* amplification were selected using the Roche ProbeFinder software (https://www.roche-appliedscience.com/sis/rtpcr/upl). Each cDNA sample (20ng RNA equivalent) was tested in duplicate (Ct range between replicates <1.5). The amplification reaction was performed on the *7900HT FAST Real Time PCR System* instrument (Applied Biosystems) with the following protocol: initial step at 95°C for 10min, then 50 cycles at 95°C for 15s and at 60°C for 1min.
Relative gene expression (indicated as *fold change*) was quantified by the 2^{-DDCt} method.[5] The DDCt for AIEOP and BFM-G samples was referred to the median DCt of their respective cohort.

CRLF2 rearrangements
The presence of the *P2RY8-CRLF2* fusion transcript in the AIEOP and BFM-G cohort was investigated by RQ-PCR. In particular, the UPL System was used, with primers designed in the first exon of *P2RY8* (5'-GCTACTTCTGCCGCTGCTT-3') and in the first exon of *CRLF2* (5'-GCAGAAAGACGGCAGCTC-3') with the UPL probe n. 28 (Roche UPL cat. n. 04687604001).

IGH@-CRLF2 translocation was searched in *CRLF2* over-expressed AIEOP patient, for which fixed cells from BM at diagnosis were available, by Fluorescence in situ hybridization (FISH) on interphase nuclei using CRLF2 Breakapart Probe (Cytocell Ltd, Cambridge, UK). Analyses were carried out using Zeiss Axio Imager Z2 fluorescent microscope (Carl Zeiss AG

Corporate, Oberkochen, Germany) and ISIS software (MetaSystems GmbH, Altlussheim, Germany). For each case 150/200 interphase nuclei were scored.

Other genetic aberrations

High Resolution Melting (HRM) analysis was performed to identify *JAK2* mutations in exon 16, as previously described.[4] Sequencing of *NOTCH1*, *FBXW7* and *CRLF2* was performed by PCR amplification and direct sequencing. Whole genome was DNA amplified using the GenomePhi V2 DNA Amplification Kit (GE Heathcare Life Science). The following primers were designed for *CRLF2*: *CRLF2-F* (5'-GTGGGCATTGTATGGAAACTGA-3') and *CRLF2-R* (5'-GAGACTGGTTAGGGATGAGATGT-3'); while previously reported primers were used for *NOTCH1* and *FBXW7*.[6 7]

Cell culture

The human T-ALL cell lines LOUCY (a kind gift of DSMZ, Germany), MOLT-4, CCRF-CEM and Jurkat were cultured in RPMI medium with 10-20% bovine calf serum.

CRLF2 expression on cell surface

To assess CRLF2 expression on the surface of T-ALL blasts the following combination of antibodies was used: CRLF2PE (Clone 1B4, Biolegend, London, UK),[8] CD45PerCP (BD Biosciences, Franklin Lakes, NJ, USA), CD19APC (BD Biosciences) and CD7ECD (Beckman Coulter, Brea, California,

USA). Leukemic blasts were gated as CD45 intermediate /CD7+/CD19. The T-ALL cell lines were stained only with the CRLF2PE antibody.

Phosphoflow cytometry assay

Thawed mononuclear cells from primary ALL samples and T-ALL cell lines were starved in X-vivo medium for 2 hours, then cells were stimulated with rh-TSLP (100 ng/mL, ImmunoTools, Friesoythe, Germany) or IL-7 (100 ng/mL,) for 30 minutes at 37°C to allow signal transduction. To test for sensitivity, the LOUCY cell line, after starvation, was incubated for 24h with Ruxolitinib (Selleck Chemicals, Huston, USA) at 0.5 uM. Cells were fixed with 1.5% paraformaldehyde and permeabilized with 90% ice-cold methanol and then incubated with surface antigen-directed antibodies and with the anti-phospho-protein-directed antibody p-STAT5 (Y694) AlexaFluor488 (BD Biosciences) or isotype matched IgG (Cell Signaling, Danvers, MA, USA). Cells were examined on a FACSaria™ flow cytometer (BD) and data were collected and analyzed using DIVA™ software (BD). Basal levels of each phosphoprotein was calculated as proportion (%) of phosphoprotein positive (p-positive) cells in basal conditions. Response to each cytokine (rhTSLP or IL-7) was calculated as a difference between the percentage of p-positive cells after exposure to cytokine and the percentage of p-positive cells in the basal state. IL-7 inducible pSTAT5 signaling in residual normal T and B cells contained

within the primary leukemia samples was considered as positive control of functional signaling (data not shown).[9]

Gene-expression and gene set enrichment analysis

An independent cohort was used to perform Gene expression profiling (GEP) analysis. RNA samples of 100 T-ALL (AIEOP ALL study cohort, diagnosed from 2000 to 2006) were processed according to Affymetrix protocols as previously described.[10] GeneChip Human Genome U133 Plus 2.0 array were used and microarray data (.CEL files) were generated from raw signals using integrated microarray Affymetrix software. Microarray data, normalized by the justRMA algorithm, were analyzed by R-Bioconductor (Version 2.15.3). The expression values of *CRLF2* probe 208303_s_t were analyzed in the 100 T-ALL specimens using the same cut-off values as previously established for *CRLF2* RQ-PCR expression values. Using all gene expression data of .CEL files the 15% of patients with highest *CRLF2* expression were compared with the 15% of patients with lowest *CRLF2* expression. Differentially expressed probes between the two groups (*CRLF2-high* vs. *CRLF2-low*) groups were obtained using Wilcoxon T-test and local false discovery rate (lfdr) was used to correct the p-value. A lfdr <0.05 was considered significant for probe sets differentially expressed between compared groups.

Gene set enrichment analysis (GSEA) was run on the differentially expressed genes resulting from the Wilcoxon test in order to explore presence of specific pathways and

oncogenic signature defined directly from microarray gene expression data.

Supplementary References

1. van Dongen JJ, Macintyre EA, Gabert JA, et al: Standardized RT-PCR analysis of fusion gene transcripts from chromosome aberrations in acute leukemia for detection of minimal residual disease. Report of the BIOMED-1 Concerted Action: investigation of minimal residual disease in acute leukemia. Leukemia 13:1901-28, 1999

2. Schrappe M, Valsecchi MG, Bartram CR, et al: Late MRD response determines relapse risk overall and in subsets of childhood T-cell ALL: results of the AIEOP-BFM-ALL 2000 study. Blood 118:2077-84, 2011

3. van der Velden VH, Cazzaniga G, Schrauder A, et al: Analysis of minimal residual disease by Ig/TCR gene rearrangements: guidelines for interpretation of real-time quantitative PCR data. Leukemia 21:604-11, 2007

4. Cario G, Zimmermann M, Romey R, et al: Presence of the P2RY8-CRLF2 rearrangement is associated with a poor prognosis in non-high-risk precursor B-cell acute lymphoblastic leukemia in children treated according to the ALL-BFM 2000 protocol. Blood 115:5393-7, 2010

5. Livak KJ, Schmittgen TD: Analysis of relative gene expression data using real-time quantitative PCR and the 2(-Delta Delta C(T)) Method. Methods 25:402-8, 2001

6. Sulis ML, Williams O, Palomero T, et al: NOTCH1 extracellular juxtamembrane expansion mutations in T-ALL. Blood 112:733-40, 2008

7. Thompson BJ, Buonamici S, Sulis ML, et al: The SCFFBW7 ubiquitin ligase complex as a tumor suppressor in T cell leukemia. J Exp Med 204:1825-35, 2007

8. Shochat C, Tal N, Bandapalli OR, et al: Gain-of-function mutations in interleukin-7 receptor-alpha (IL7R) in childhood acute lymphoblastic leukemias. J Exp Med 208:901-8, 2011

9. Bugarin C, Sarno J, Palmi C, et al: Fine Tuning of Surface CRLF2 Expression and Its Associated Signaling Profile in Childhood B Cell Precursor Acute Lymphoblastic Leukemia. Haematologica, 2015

10. Haferlach T, Kohlmann A, Wieczorek L, et al: Clinical utility of microarray-based gene expression profiling in the diagnosis and subclassification of leukemia: report from the International Microarray Innovations in Leukemia Study Group. J Clin Oncol 28:2529-37, 2010

Chapter 5

Conclusions and future perspectives

Conclusions and future perspectives

In this thesis we focused on dissecting the role of CRLF2 alterations in different subset of ALL. Overall, we can conclude that *CRLF2* alterations leading to its overexpression represent poor prognostic markers in BCP and T-ALL, easily identified with FCM techniques. Moreover, this genetic abnormality identifies a new high-risk subgroup of patients that could benefit of the introduction of HDAC inhibitors in current chemotherapeutic regimen. In the future, our goal is to introduce the HDAC inhibitor Givinostat in the current chemotherapy in clinic, in order to provide a valid alternative for *CRLF2* rearranged patients, especially DS-ALL patients, to achieve a better cure rate. To reach this goal further studies need to be accomplished to fully demonstrate the efficacy and safety of this drug in this particular subgroup of patients. In particular, to confirm the data obtained *ex vivo, in vivo* experiments of Givinostat in combination with low doses of chemiotherapeutics will be performed on xenograft models of DS-ALL patients. Furthermore, to fully improve therapies for DS-ALL patients, it would be important to dissect the reason why they have a 10-20 fold increased risk of developing ALL and have particularly poor prognosis. This high fatality rate is not due only to enhanced toxicity of chemotherapy, but primarily because of intrinsic resistant of DS-ALL to therapy. Hence, moving backwords to basic research studies aiming to deciphering biology of DS-ALL is urgently needed for rational effective therapy. In particular, we aim to perform exome

sequencing analyses comparing paired diagnosis, remission and relapse samples of DS-ALL patients to uncover the timeline of the appearance of *CRLF2* alterations relative to other mutations co-expressed in leukemia. We expect relatively limited and manageable number of mutations from exome sequencing analysis as we consider that *CRLF2* alteration could have a significant role in the development of the disease (although it is not an initiating event). We hypothesize that additional mutations activating growth and survival pathway cooperating with CRLF2 will be identified.

Moving to the other subset of ALL analyzed in this work, the T-ALL, Cox model analysis showed that *CRLF2*-high expression is an independent prognostic factor also for these patients, associated to a 2.5-fold increased risk of relapse. Thus, *CRLF2*-overexpression proved to be a new marker of poor prognosis also for T-ALL, identifying a subset of High Risk T-ALL patients that could be eligible for alternative therapy. In particular, due to a more intense response of *CRLF2*-high patients to TSLP stimulation, therapies that interfere with the activation of the JAK/STAT5 signaling pathway may be considered for treatment of these patients. A strong candidate could be the HDAC inhibitor Givinostat. Further analyses will be necessary to confirm the efficacy of this drug in this T-ALL subset.

Other publications

Cytoskeletal regulatory gene expression and migratory properties of B-cell progenitors are affected by the ETV6-RUNX1 rearrangement. Palmi C, Fazio G, **Savino AM**, Procter J, Howell L, Cazzaniga V, Vieri M, Longinotti G, Brunati I, Andrè V, Della Mina P, Villa A, Greaves M, Biondi A, D'Amico G, Ford A, Cazzaniga G.*Mol Cancer Res*. 2014 Dec;12(12):1796-806

Impact of IKZF1 deletions on IKZF1 expression and outcome in Philadelphia chromosome negative childhood BCP-ALL. Reply to "incidence and biological significance of IKZF1/Ikaros gene deletions in pediatric Philadelphia chromosome negative and Philadelphia chromosome positive B-cell precursor acute lymphoblastic leukemia". Palmi C, Lana T, Silvestri D, **Savino A**, Kronnie GT, Conter V, Basso G, Biondi A, Valsecchi MG, Cazzaniga G *Haematologica*. 2013 Dec;98(12):e164-5.